



Search for massive, long-lived particles in events with displaced vertices and displaced muons in pp collisions at $\sqrt{s} = 13.6$ TeV with the ATLAS experiment

The ATLAS Collaboration

A search is presented for massive long-lived particles in events featuring at least one displaced vertex and at least one displaced muon, using proton–proton collision data collected by the ATLAS detector at the Large Hadron Collider from 2022 to 2024 at a centre-of-mass energy of 13.6 TeV. The data sample corresponds to an integrated luminosity of 164 fb^{-1} . The analysis targets scenarios in which long-lived particles decay inside the ATLAS inner detector, resulting in a topology of at least one massive, displaced vertex (DV) with multiple associated tracks, and at least one muon with a large transverse impact parameter relative to the primary interaction point. The muon is not required to be associated with the DV. Two signal regions are defined by the transverse distance of the reconstructed DV from the interaction point. Background contributions are estimated by using fully data-driven techniques. No significant excess above the expected background is observed. Upper limits at 95% confidence level are set on the visible cross-section and on the production cross-sections of several benchmark models of R -parity-violating supersymmetry.

1 Introduction

The Standard Model (SM) of particle physics is a remarkably successful framework, yet it leaves several fundamental questions unanswered. It does not provide an explanation for the nature of dark matter, the observed matter–antimatter asymmetry in the Universe, or the origin of neutrino masses. These and other shortcomings strongly motivate the existence of beyond-SM (BSM) physics. The Large Hadron Collider (LHC) [1] at CERN is a powerful tool to probe BSM scenarios through high-energy proton–proton (pp) collisions, enabling searches for new particles and interactions. While most BSM searches at the LHC have targeted promptly decaying particles, many extensions of the SM predict long-lived particles (LLPs) that travel measurable distances before decaying, giving rise to distinctive signatures such as a displaced vertex (DV) [2]. This Letter presents a search for LLPs using pp collision data in events with a DV and a displaced muon. BSM models resulting in DVs include various supersymmetry (SUSY) models addressing the hierarchy problem like minisplit SUSY [3, 4], gauge-mediated SUSY breaking [5], R -parity-violating (RPV) SUSY [6–14], Stealth SUSY [15, 16], and neutral naturalness [17–20], as well as hidden valley models [21, 22] and others addressing dark matter [23–27] and the matter–antimatter asymmetry of the Universe [28–30]. Many such models predict final states with displaced muons, which facilitate efficient triggering and provide powerful background suppression.

The results are presented with a model-independent interpretation on the visible cross-section for events with a DV and a displaced muon, and with interpretations in the context of SUSY models with RPV interactions. Under the RPV assumption, the lightest supersymmetric particle (LSP) is no longer stable and may decay into SM particles via lepton-number-violating (L -violating) or baryon-number-violating (B -violating) interactions. If the corresponding couplings are small, the decays can be significantly suppressed, leading to displaced signatures. Higgsinos and top squarks (\tilde{t}) are common candidates for an unstable LSP, usually produced in pairs at the LHC, and can decay into final states containing muons and quarks in various RPV scenarios. If the LSP is a higgsino, its RPV decay proceeds via a virtual sfermion mediator. If the sfermion mass is assumed to be much heavier than the higgsino mass, this leads to three-body decays in which the virtual sfermion is far off-shell and effectively decouples from the decay kinematics. In this regime, the higgsino lifetime depends only on the higgsino mass and the RPV coupling strength divided by the square of the mediator sfermion mass. If the LSP is the top squark, it decays directly into SM particles via the RPV coupling. This two-body decay results in a lifetime that depends on the top-squark mass and the RPV coupling strength.

Both the ATLAS and CMS Collaborations have conducted searches for long-lived higgsinos and top squarks in RPV SUSY [31–37]. Using Run-1 data at $\sqrt{s} = 8$ TeV, ATLAS searched for higgsino-like neutralinos ($\tilde{\chi}_1^0$) produced via heavier squarks and decaying through $\tilde{\chi}_1^0 \rightarrow \mu^- u \bar{d}$ (and charge conjugate (c.c.)), excluding neutralino masses under this production assumption between 100 and 500 GeV for mean proper lifetimes, τ , between 3 ps and 10 ns [32]. Using Run-2 data at $\sqrt{s} = 13$ TeV, CMS searched for higgsino-like neutralinos with $\tilde{\chi}_1^0 \rightarrow t b s$ (and c.c.) decays in events with two DVs, excluding neutralino masses up to 1100 GeV for lifetimes between 2 ps and 230 ps [36]. For $\tilde{t}\tilde{t}$ production, ATLAS placed limits on $\tilde{t} \rightarrow b\mu$ decays in topologies with a DV and a displaced muon track using Run-2 data at $\sqrt{s} = 13$ TeV [35]. Top-squark masses up to 1.7 TeV were excluded for $\tau = 0.1$ ns, and masses below 1.3 TeV were excluded for lifetimes between 0.01 ns and 30 ns. Most recently, CMS searched for $\tilde{t}\tilde{t}$ production in RPV $\tilde{t} \rightarrow d\ell$ and $\tilde{t} \rightarrow b\ell$ decays, where ℓ denotes an electron or a muon, using Run-2 data at $\sqrt{s} = 13$ TeV [37]. This excluded top-squark masses between 100 GeV and at least 460 GeV for $0.3 \text{ ps} < \tau < 30 \text{ ns}$, with a maximum exclusion of 1500 GeV at $\tau = 70 \text{ ps}$.

Data from pp collisions at $\sqrt{s} = 13.6$ TeV collected by the ATLAS detector between 2022 and 2024 of the LHC Run 3 are used. The selected data sample corresponds to an integrated luminosity of 164 fb^{-1} [38]. Several techniques novel to Run 3 are employed, including a dedicated displaced-muon trigger [39] extending sensitivity to muon transverse momenta as low as 20 GeV, thereby improving the reach for lower-mass LLPs, and specialised tracking and vertexing algorithms [40] for reconstructing displaced decay signatures across a broad lifetime range. The background contributions are estimated by using fully data-driven techniques, and the results are extracted via a profile likelihood fit in a binned observable distribution that separates signal and background. The results are expressed as model-independent upper limits on the visible cross-section for processes yielding a DV and a displaced muon, and are further interpreted in three representative RPV SUSY scenarios involving higgsino pair production and $\tilde{t}\tilde{t}^*$ production.

2 ATLAS detector

The ATLAS experiment [41, 42] at the LHC is a multipurpose particle detector with a forward–backward symmetric cylindrical geometry and a near 4π coverage in solid angle.¹ It consists of an inner tracking detector (ID) surrounded by a thin superconducting solenoid providing a 2 T axial magnetic field, electromagnetic (EM) and hadronic calorimeters, and a muon spectrometer (MS). The ID covers the pseudorapidity range $|\eta| < 2.5$. It consists of silicon pixel, silicon microstrip (SCT), and transition radiation tracking (TRT) detectors. Lead/liquid-argon (LAr) sampling calorimeters provide EM energy measurements with high granularity within the region $|\eta| < 3.2$. A steel/scintillator-tile hadronic calorimeter covers the central pseudorapidity range ($|\eta| < 1.7$). The endcap and forward regions are instrumented with LAr calorimeters for EM and hadronic energy measurements up to $|\eta| = 4.9$. The MS surrounds the calorimeters and is based on three large superconducting air-core toroidal magnets with eight coils each. The field integral of the toroids ranges between 2.0 and 6.0 T m across most of the detector. The MS includes three precision layers, each consisting of layers of monitored drift tubes, covering the region $|\eta| < 2.7$, except in the innermost layer of the endcap region, where layers of small thin-gap and Micromegas chambers provide both precision tracking in the region $1.3 < |\eta| < 1.7$. The muon trigger system, covering $|\eta| < 2.4$, uses various detectors including resistive-plate chambers in the barrel region, thin-gap chambers in the endcaps, and small-strip thin-gap chambers together with Micromegas detectors in the innermost endcap layer. The luminosity is measured mainly by the LUCID–2 detector [43], which is located close to the beampipe. A two-level trigger system was used to select events [39]. The first-level trigger is implemented in hardware and uses a subset of the detector information to accept events at a rate close to 100 kHz. This is followed by a software-based high level trigger (HLT) that reduces the accepted rate of complete events to 3 kHz on average, depending on the data-taking conditions. A software suite [44] is used in data simulation, in the reconstruction and analysis of real and simulated data, in detector operations, and in the trigger and data acquisition systems of the experiment.

¹ ATLAS uses a right-handed coordinate system with its origin at the nominal interaction point (IP) in the centre of the detector and the z -axis along the beam pipe. The x -axis points from the IP to the centre of the LHC ring, and the y -axis points upwards. Polar coordinates (r, ϕ) are used in the transverse plane, ϕ being the azimuthal angle around the z -axis. The pseudorapidity is defined in terms of the polar angle θ as $\eta = -\ln \tan(\theta/2)$ and is equal to the rapidity $y = \frac{1}{2} \ln \left(\frac{E+p_z}{E-p_z} \right)$ in the relativistic limit. Angular distance is measured in units of $\Delta R \equiv \sqrt{(\Delta y)^2 + (\Delta \phi)^2}$.

3 Samples of simulated events

Monte Carlo (MC) simulation samples are used to study the event selection acceptance and the reconstruction efficiency for benchmark signals. The effect of multiple interactions in the same and neighbouring bunch crossings (pile-up) is modelled by overlaying [45] the simulated hard-scattering event with inelastic $p\bar{p}$ events generated from a mix of EPOS 2.0.1.4 [46] and PYTHIA 8.308 [47, 48]. The detector response to each simulated event was modelled using GEANT4 [49]. Correction factors are applied to account for differences between data and simulation in the pile-up, the trigger, reconstruction, and identification efficiencies of muons [39, 50], and for the track reconstruction efficiency [40].

Samples of simulated long-lived higgsino pairs are used as benchmarks to set limits on the visible cross-section for higgsino pair production. The following production modes are considered: $\tilde{\chi}_1^0\tilde{\chi}_2^0$, $\tilde{\chi}_1^0\tilde{\chi}_1^\pm$, $\tilde{\chi}_2^0\tilde{\chi}_1^\pm$, and $\tilde{\chi}_1^\pm\tilde{\chi}_1^\mp$, where $\tilde{\chi}_1^0$ is the LSP, and $\tilde{\chi}_2^0$ and $\tilde{\chi}_1^\pm$ are the next-to-lightest neutralino and the lightest chargino, respectively. A nearly mass-degenerate spectrum is assumed, with mass splittings of 1 GeV between $\tilde{\chi}_1^0$ and $\tilde{\chi}_1^\pm$, and $\tilde{\chi}_1^0$ and $\tilde{\chi}_2^0$ [51, 52]. All other supersymmetric particles are assumed to be heavy and decoupled.

Two RPV decay scenarios are considered, where the higgsinos are assumed to decay through interactions that are either L -violating or B -violating [13]. These interactions arise from additional terms in the supersymmetric superpotential of the form $\lambda'_{ijk}L_iQ_jD_k^c$ and $\lambda''_{ijk}U_i^cD_j^cD_k^c$, where λ'_{ijk} and λ''_{ijk} are the coupling strengths and i, j , and k are generation indices. Here, L and Q denote the lepton and quark $SU(2)$ doublet superfields, while U^c and D^c are the up- and down-type quark $SU(2)$ singlet superfields. Under the decoupling assumption, the masses of the sfermions that mediate the higgsino decays are much larger than the higgsino masses. Thus, the higgsino decays are modelled as effective three-body decays via a contact interaction, with the higgsino mass and decay width treated as independent simulation parameters, without resolving the underlying dependence on the RPV coupling strength and mediator sfermion mass. The following two higgsino benchmark scenarios were simulated, both assuming that all other RPV terms are zero:

- L -violating: λ'_{211} , leading to decays $\tilde{\chi}_1^0, \tilde{\chi}_2^0 \rightarrow \mu^- u \bar{d}$ (+ c.c.), and $\tilde{\chi}_1^\pm \rightarrow \mu^\pm d \bar{d}$.
- B -violating: λ''_{323} , leading to decays $\tilde{\chi}_1^0, \tilde{\chi}_2^0 \rightarrow t s b$ (+ c.c.), and $\tilde{\chi}_1^+ \rightarrow \bar{b} s \bar{b}$, $\tilde{\chi}_1^- \rightarrow b s b$. Sensitivity for this scenario depends on neutralino production and the subsequent semileptonic decay of the resulting top quark, leading to a lower muon multiplicity and reduced signal acceptance with respect to the L -violating benchmark.

The decay modes are illustrated in Figures 1(a) and 1(b). The hard interaction was generated with up to two additional partons with the MADGRAPH5_AMC@NLO 3.5.7 [53] generator at leading order (LO) in perturbative quantum chromodynamics (QCD), using the NNPDF3.0_{NLO} parton distribution function (PDF) set [54]. The parton shower and hadronisation were simulated with PYTHIA 8.308 using the A14 set of tuned parameters [55] and the NNPDF2.3_{LO} PDF set [56]. The decays of bottom and charm hadrons were simulated by EVTGEN 1.6.0 [57]. The L -violating (B -violating) decay mode was generated for higgsino lifetimes between 3 ps and 100 ns for a range of mass values of 100–1900 GeV (200–1500 GeV). The generated sets of events were scaled to cross-sections at approximate next-to-next-to-leading order (NNLO) accuracy in QCD with threshold resummation of the next-to-next-to-leading logarithms (NNLLs) [58], as computed with the RESUMMINO package [59, 60]. The resulting production cross-sections decrease rapidly with increasing higgsino mass, from 19.5 pb at $m = 100$ GeV to $O(10^{-2})$ fb at $m = 1900$ GeV, with scale uncertainties of a few percent and PDF uncertainties increasing from a few percent at low masses to

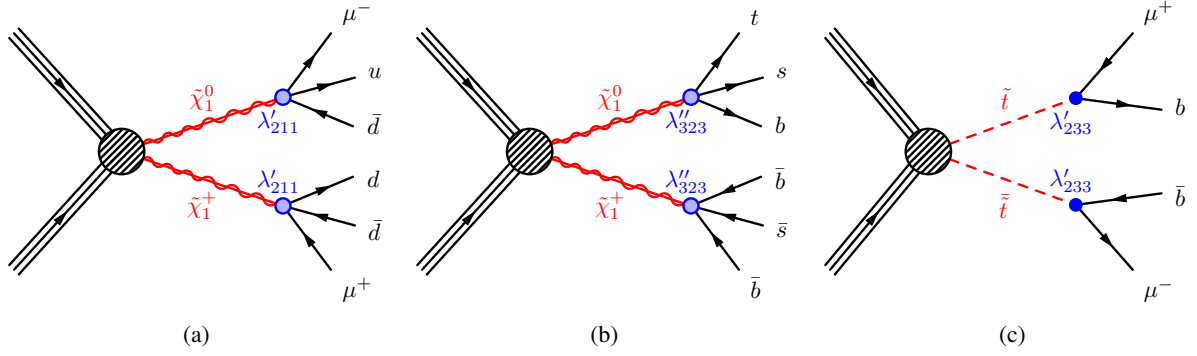


Figure 1: Illustrative diagrams for the three considered R -parity-violating (RPV) SUSY simplified benchmark models, each assuming a single non-zero RPV term: (a) higgsino pair production with λ'_{211} decays, (b) higgsino production with λ''_{323} decays, and (c) top-squark–anti-squark pair production with λ'_{233} decays. Equivalent diagrams with charge-conjugate processes are also considered.

$O(50\text{--}100\%)$ at the largest masses considered. Interactions of charginos with the detector material were found to have a negligible impact on the signal yields and were not simulated in the MC samples.

Using the same MADGRAPH5_AMC@NLO+PYTHIA generator, $\tilde{t}\tilde{t}^*$ production samples were generated at LO QCD with up to two additional partons. The other top-squark mass eigenstate and all other supersymmetric particles are assumed to be heavy and decoupled. The squarks are assumed to decay exclusively via L -violating couplings to a muon and a b -quark, $\tilde{t} \rightarrow \mu b$, given by a non-zero λ'_{233} coupling term. The diagram for this process is illustrated in Figure 1(c). Different samples were generated with $3\text{ ps} < \tau < 100\text{ ns}$ for a range of mass values between 700 GeV and 2100 GeV. The generated sets of events were scaled to cross-sections computed at approximate NNLO accuracy in QCD. The production cross-section decreases rapidly with increasing top-squark mass, from about 0.1 pb at $m_{\tilde{t}} = 700\text{ GeV}$ to about 10^{-2} fb at $m_{\tilde{t}} = 2100\text{ GeV}$, with associated theoretical uncertainties increasing from roughly 6% to about 36%. Since the top squarks carry colour charge and all simulated proper lifetimes are far longer than the hadronisation timescale in QCD, they were hadronised in PYTHIA to form colour-singlet states with SM quarks, called R -hadrons. The top squarks primarily form meson-like states ($\tilde{t}\bar{q}$), but approximately 10% of them form baryon-like states ($\tilde{t}qq$). About half of the R -hadrons carry non-zero electric charge. Interactions of the R -hadrons with the detector material were not simulated in the MC samples.

4 Reconstruction

Charged-particle trajectories (tracks) are reconstructed in two passes using *hits* (individual detector measurement points) found in the ID. The primary pass reconstructs tracks with transverse impact parameter (d_0) relative to the interaction point (IP) of $|d_0| < 5\text{ mm}$ and a minimum transverse momentum (p_T) of 500 MeV [61]. A large-impact-parameter pass uses left-over hits from the primary pass to increase the acceptance up to $|d_0| < 300\text{ mm}$ and a minimum p_T of 1 GeV [40]. All tracks are passed through an ambiguity resolution step to resolve overlaps and remove fake tracks before being re-fit using a global χ^2 method [40]. The tracks from the silicon pixel and SCT sub-detectors may then be extended into the TRT [61]. The pp vertex with the highest sum of squared transverse momenta of associated tracks is taken as the primary interaction vertex (PV).

Muons are reconstructed by combining both primary and large-impact-parameter ID tracks with track segments reconstructed in the MS within $|\eta| < 2.5$. If an MS track segment is matched to both a primary and large-impact-parameter track, the combined track with the best combined fit quality for the given MS track is retained. If they have the same quality, the muon with the smallest $\Delta\eta$ between the MS and ID tracks is kept [61]. Muons must satisfy a modified version of the *Medium* identification criteria as defined in Ref. [50], where the requirements on the number of pixel and TRT hits are omitted if reconstructed from large-impact-parameter tracks. Only muons with $p_T > 25$ GeV, $2 \text{ mm} < |d_0| < 300$ mm, a transverse-displacement significance $|d_0|/\sigma_{d_0} > 150$, and a longitudinal displacement relative to the PV of $|z_0| < 500$ mm are considered.

To reconstruct the vertex of the LLP decay, primary and large-impact-parameter tracks are passed to a modified version of the DV reconstruction algorithm described in Ref. [62]. The vertex reconstruction first forms two-track vertices from a set of *seed tracks*. These seed tracks are selected following the criteria in Ref. [62], but with the requirement for at least one track in the seed pair to have $|d_0| > 2$ mm relaxed to $|d_0| > 1$ mm, improving efficiency for LLP decays whose decay products – particularly in models with short lifetimes – tend to point back towards the PV and have small $|d_0|$. Two-track vertices are combined to form multi-track vertices and tracks not initially preselected for vertex seeding are attached to compatible vertices.

Candidate DVs are required to be within the fiducial volume of the ID, with a transverse distance from the beamline of $R_{xy} < 300$ mm and a longitudinal position of $|z| < 300$ mm, but with a minimum transverse distance from the PV of $d_T(\text{PV}, \text{DV}) > 1$ mm. They are further required to fulfil a vertex quality requirement of $\chi_{\text{red}}^2 < 5$, where ‘red’ in the subscript indicates division by the number of degrees of freedom of the vertex fit, to suppress vertices formed from random track crossings. Additional background rejection is achieved using two angular requirements that exploit the expected topology of displaced decays. These requirements suppress backgrounds in which tracks are misassociated with the DV or arise from random crossings or back-to-back configurations. First, a minimum azimuthal angle between the DV displacement vector and any of its associated tracks is required, $\cos_{\min} \phi(\text{DV}, \text{track}) > -0.995$, rejecting vertices containing tracks that point nearly opposite to the DV displacement direction. Second, among all tracks forming an acute angle with the DV displacement direction, at least one must have a sufficiently large angle, $\cos_{\min} \phi(\text{DV}, \text{acute-angle track}) < 0.97$. This requirement suppresses backgrounds where tracks are nearly collinear with the displacement direction, while retaining signal-like decays with a broader angular spread.

5 Event selection

Events are selected using two MS-only triggers and a novel displaced-muon trigger introduced in Run 3 [39]. The MS-only triggers accept events based on muon tracks reconstructed in the MS without requiring a matching ID track. The first MS-only trigger selects muon track segments with transverse momentum of $p_T > 60$ GeV for $|\eta| < 1.05$, while the second requires $p_T > 80$ GeV over the full pseudorapidity range in the muon trigger system of $|\eta| < 2.4$, with an additional requirement of three hits in precision tracking layers for $|\eta| > 1.05$. The displaced-muon trigger selects events containing at least one muon candidate reconstructed in the HLT with $p_T > 20$ GeV, $|\eta| < 2.4$, and $|d_0| > 2$ mm. It exploits the dedicated large-impact-parameter track reconstruction introduced in the HLT in Run 3, which is designed to suppress incorrectly reconstructed displaced tracks and enables lower p_T thresholds than in Run 2. Figure 2 shows the trigger efficiency as a function of the highest muon p_T in the event and of its transverse

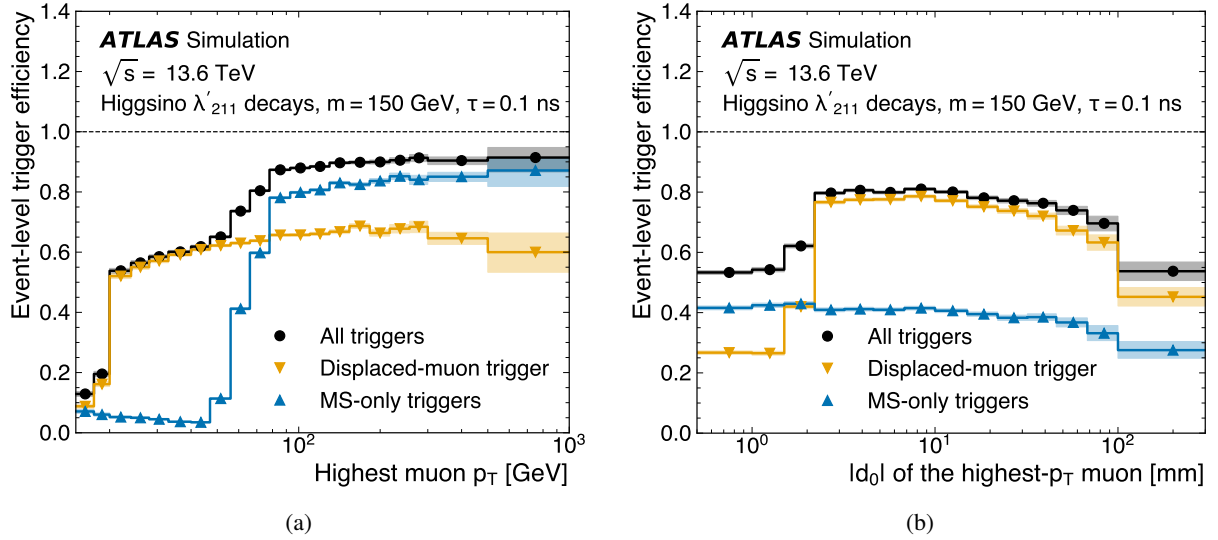


Figure 2: Event-level trigger efficiency for the triggers used in this analysis. The plots show separate curves for the MS-only triggers and the displaced-muon trigger, which exploits the dedicated large-impact-parameter track reconstruction introduced in the HLT in Run 3, and their combination. The efficiencies are evaluated as a function of (a) the highest muon p_T in the event, and (b) the transverse impact parameter, $|d_0|$, of that muon. The benchmark sample used here consists of higgsino pair-production events with L -violating λ'_{211} decays ($m = 150$ GeV, $\tau = 0.1$ ns). For the MS-only triggers, the trigger plateau criteria are applied to the highest- p_T muon in the event (63 GeV for the $p_T > 60$ GeV, $|\eta| < 1.05$ trigger and 84 GeV for the $p_T > 80$ GeV, $|\eta| < 2.4$ trigger with additional requirement of three hits in precision tracking layers for $|\eta| > 1.05$). The muon p_T plot shows the combined trigger efficiency turn-on behaviour.

impact parameter, $|d_0|$, evaluated using simulated higgsino pair-production events with L -violating λ'_{211} decays, $m = 150$ GeV and $\tau = 0.1$ ns. The combination of these triggers achieves high efficiency across a broad range of muon p_T and $|d_0|$ values.

Events selected in the analysis must contain at least one muon candidate that either is spatially matched to the HLT muon that fired the displaced-muon trigger, or has p_T at least 5% above the relevant MS-only trigger threshold (63 GeV and 84 GeV) to operate on the trigger-efficiency plateau [63].

If present, DVs are categorised as ‘far’ or ‘near’ by their transverse distance from the PV, $d_T(\text{PV}, \text{DV})$. Far DVs have $d_T(\text{PV}, \text{DV}) \geq 4$ mm and near DVs have $1 \text{ mm} < d_T(\text{PV}, \text{DV}) < 4$ mm. A DV is considered *signal-like* if it has at least four associated tracks ($n_{\text{track}} \geq 4$) and if the invariant mass of all DV-associated tracks fulfils $m_{\text{DV}} \geq 20$ GeV for far DVs and $m_{\text{DV}} \geq 40$ GeV for near DVs. Signal-like DVs are also required to be outside the material layers defined by a map described in Ref. [64] to veto potential hadronic interactions between particles and the detector material. This material-map veto removes 42% of the fiducial volume. The presence of far or near signal-like DVs is used to categorise events as detailed in Section 6.

Three primary muon background sources are considered: muons from heavy-flavour decays, cosmic-ray muons, and algorithmic fakes. Heavy-flavour backgrounds are suppressed by requiring candidates to satisfy the *Tight_VarRad* isolation criteria described in Ref. [50], hereafter referred to as the *heavy-flavour veto*. This requirement eliminates approximately 98.9% of heavy-flavour muons and provides an optimal balance between background rejection and signal efficiency. Cosmic-ray rejection is performed by requiring $|\eta_\mu + \eta_{\text{MS}}| > 0.014$ and $|\phi_\mu - \phi_{\text{MS}}| - \pi > 0.25$, where the μ (MS) subscripts refer to the reconstructed

muon (MS track segment). This rejects muon candidates with an MS track segment on the opposite side of the detector. A geometric correction is applied so that the muon direction is expressed in the detector reference frame for comparison with the MS track segment. The η and ϕ requirements are optimised using a dedicated cosmic-ray data sample recorded in 2023. Additionally, a muon-material-map veto described in Ref. [63] is applied to account for detector inefficiencies in regions where MS track segment reconstruction is not possible. The combined *cosmic-ray veto* achieves a rejection of approximately 97.5% for cosmic-ray muons. Algorithmic fakes – reconstructed muon candidates that do not originate from real muons – are suppressed by requiring a high-quality match between the ID and MS tracks: the combined fit must satisfy $\chi_{\text{red}}^2 < 3$ and have at least three precision layer hits, achieving rejection rates of approximately 97.4% and 99.7% in the barrel and endcap regions, respectively. The combination of these matching requirements is referred to as the *algorithmic-fake veto*.

Events are considered to contain a signal-like muon if the muon with the highest p_T in the event passes the heavy-flavour, cosmic-ray, and algorithmic-fake vetoes. No association between the signal-like muon and the DV is required to preserve model independence. Two signal regions, denoted SR_{far} and SR_{near} , are defined and correspond to events with a signal-like muon and at least one far or near signal-like DV, respectively. Only a single DV is required to retain sensitivity for long lifetimes, including cases where one decay occurs outside the ID, while preserving a model-independent interpretation. Events in which either the muon or the vertex is not signal-like are placed in validation regions for the background estimate.

6 Background estimate

Background contributions arise from events with displaced muons from heavy-flavour decays, cosmic rays, or algorithmic fakes, and from DVs produced by hadronic interactions or random crossings of tracks in the detector. These backgrounds are efficiently suppressed by the muon-veto requirements and by the requirements on m_{DV} and n_{track} in the signal regions. To predict the event yields from these sources in the signal regions, a fully data-driven transfer factor method is employed. In this approach, the muon-veto requirements and the DV selection criteria are used to define exclusive regions in data: region A, where both the muon-veto and DV selection are applied (the signal region); regions B_i and C, where exactly one criterion is inverted; and region D_i , where both criteria are inverted. Here, i denotes the specific muon background type. The background estimate relies on the fact that the variables used to reject displaced muons from background sources are uncorrelated with the variables used to reject DVs from background. The event yields in region A for source i can then be estimated from the observed yields in region B_i and the ratio of yields in regions C and D_i via $N_{A,i} = N_{B_i} \cdot N_C/N_{D_i}$. The ratio $f_i = N_C/N_{D_i}$ is referred to as the transfer factor (TF) for background source i . For background events, the probabilities to satisfy the DV and muon selection criteria were validated to be independent in data by confirming that the shapes of the muon observables are unchanged under varying DV selections. Any residual correlations are measured and treated as a systematic uncertainty in the background prediction, as described in Section 6.2.

TFs are derived separately for each muon background source i , with algorithmic fakes further split into barrel and endcap categories with a transition at $|\eta| = 1.2$ to account for different fake rates in the two MS regions, yielding four muon background sources in total. Events are categorised based on the highest- p_T muon: if this muon fails exactly one of the three vetoes (heavy-flavour, cosmic-ray, or algorithmic-fake), it is considered to be of that background type and the event enters region B_i or D_i ; for algorithmic fakes, the $|\eta|$ of the muon is used to determine the barrel/endcap category. Regions A or C consist of events where

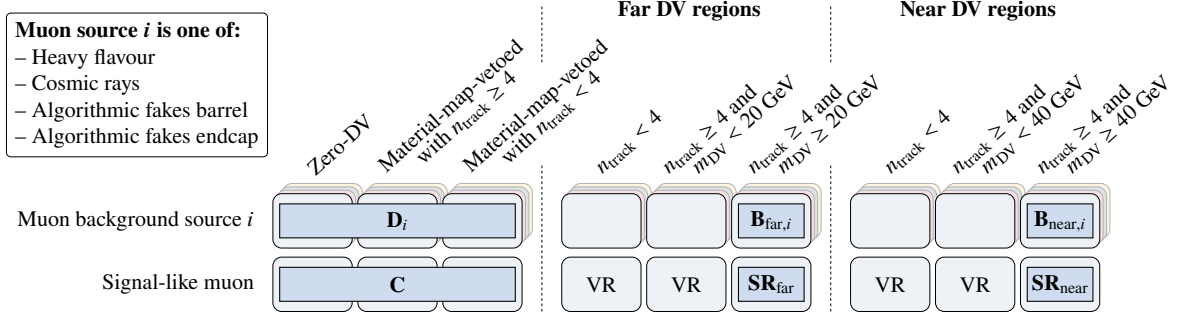


Figure 3: Categorisation of events based on the presence and quality of displaced vertices (DVs) (horizontal axis) and the background source i of the highest- p_T muon (vertical axis). The schematic is compressed vertically for simplicity. If a muon fails the veto for a specific muon background source, it is assigned that background category; if it passes all muon requirements, it is considered signal-like. The signal regions, SR_{far} and SR_{near} , require at least one signal-like muon and at least one signal-like far or near DV, respectively. Additional validation regions are defined by dropping or inverting the n_{track} and m_{DV} requirements for signal-like DVs. The regions C and D_i consist of the zero-DV and material-map-vetoed DV classes; the transfer factors (TFs) are derived from subsets of these regions by applying additional muon selections to enhance the purity for each source. The background predictions for SR_{far} and SR_{near} are then obtained by applying the TFs to the $B_{\text{far},i}$ and $B_{\text{near},i}$ regions, respectively.

the highest- p_T muon passes all vetoes. Events where the highest- p_T muon fails two or more vetoes are discarded. A schematic overview of the constructed regions is shown in Figure 3.

For the DV selection criterion, events are assigned to categories following a fixed sequence: events with no reconstructed DV enter the zero-DV category; if a DV is present, those failing to meet the m_{DV} requirement are considered first, followed by those obtained by dropping the m_{DV} requirement and selecting $n_{\text{track}} < 4$, with far DVs given precedence over near ones at both steps; events with DVs rejected by the material-layer map, referred to as *material-map-vetoed* DVs, are further divided into those with $n_{\text{track}} \geq 4$ and $n_{\text{track}} < 4$.

While material-map-vetoed DVs originate from hadronic interactions and differ from signal-like DVs, the efficiency of the muon vetoes in these events is expected to be uncorrelated with whether a DV occurs in the detector material or in the fiducial volume. Consequently, events with material-map-vetoed DVs and those with no DVs are used to populate the regions C and D_i , providing high-statistics samples. These regions contain an admixture of the muon background sources, thus, the TFs are derived from subsets of these regions, with additional muon requirements to enhance the purity for specific backgrounds, as detailed in Section 6.1. The remaining DV categories are used to define validation regions and the signal regions SR_{far} and SR_{near} . The total predicted background yield in SR_{far} (SR_{near}) is obtained as $N_A^{\text{pred}} = \sum_{i=1}^4 f_i N_{B_{\text{far},i}}$ ($N_{B_{\text{near},i}}$), where the sum runs over the four muon background sources i . To obtain a prediction in SR_{far} and SR_{near} for a binned observable, the TFs are multiplied by the corresponding binned yields in $B_{\text{far},i}$ and $B_{\text{near},i}$, respectively.

6.1 Transfer-factor derivation

Zero-DV events and those with material-map-vetoed DVs are highly enriched in background muons, but the TF derivation requires sets of events dominated by a single source of muon background. Thus, additional muon selection criteria are applied to the highest- p_T muon in the event when defining regions C and D_i for the TF calculation:

1. Muons from heavy-flavour decays dominate at small displacement, so a requirement of $|d_0(\mu)| < 3$ mm is imposed when deriving the heavy-flavour TF; for the other three background TFs, $|d_0(\mu)| > 15$ mm is required to remove heavy-flavour contributions. These requirements are applied in addition to the overall muon selection criterion of $2 \text{ mm} < |d_0(\mu)| < 300 \text{ mm}$.
2. Cosmic-ray muons predominantly occur in the central detector and enter from one side in azimuth; therefore, $|\eta| < 1.05$ and $\phi < 0$ are required to isolate a pure sample for the cosmic-ray TF derivation.
3. Muons from algorithmic fakes are treated separately in the barrel ($|\eta| \leq 1.2$) and endcap ($|\eta| > 1.2$) regions; to avoid cosmic-ray contamination, an additional $\phi > 0$ requirement is applied for the barrel.

The derived TFs are of the order of $O(10^{-2})$, reflecting the strong suppression of the background muon sources by the muon-veto requirements. Statistical uncertainties from the finite event yields in the TF derivation regions range between 2% and 6%.

6.2 Systematic uncertainties in the transfer factors

Multiple uncertainties are assigned to the TFs to account for potential residual correlations in the probabilities for background events to satisfy the muon and DV selection criteria, for residual correlations between the TFs and the muon properties, and for possible contamination of the TF derivation regions by other muon background sources.

Potential residual correlations between the DV and muon selection criteria are assessed by recomputing the TFs individually for zero-DV events and for events with DVs rejected by the material-map veto. As the latter are enriched in background DVs from hadronic interactions with detector material, comparing these TFs provides a test of whether the probabilities to satisfy the muon and DV selection criteria are independent for background events. The largest relative difference between the nominal and recomputed TFs is assigned as a systematic uncertainty for each muon background class. These uncertainties range between 8% and 35% and are largest for the heavy-flavour and the algorithmic fake barrel TFs.

To account for residual dependencies of the TF values on the muon $|d_0|$, the chosen $|d_0|$ ranges are split into two subregions at midpoint values that balance the statistical uncertainties on either side. The TFs are recomputed independently in these subregions and compared with the nominal values. This comparison provides a check for unmodelled $|d_0|$ dependencies given the available data, without attempting to model a detailed functional dependence. The largest relative differences between the nominal and recomputed TFs are assigned as a systematic uncertainty for each background class. The computed midpoints are $|d_0| = 2.3$ mm for muons from heavy-flavour decays, $|d_0| = 85$ mm for cosmic-ray muons, $|d_0| = 130$ mm for algorithmic fakes in the barrel, and $|d_0| = 102.5$ mm for algorithmic fakes in the endcap. The d_0 uncertainties range between 3% for cosmic-ray muons and 21% for algorithmic fakes in the endcap.

Additional sources of systematic uncertainty are considered for the cosmic-ray, algorithmic-fake barrel and algorithmic-fake endcap TFs to account for residual dependencies of the TF values on the muon η and ϕ coordinates, and for possible contamination of the TF derivation regions by other muon background sources. For all three TFs, the ϕ regions are split in half to compute separate TFs, and the largest relative differences between the original and recomputed TFs are taken as systematic uncertainties. For the cosmic-ray and algorithmic-fake barrel TFs, the midpoint is picked so that the statistical uncertainty is minimal on either side, while for the algorithmic-fake endcap TF, a split at $\phi = 0$ is used to account for possible residual cosmic-ray contamination in the negative- ϕ region. The cosmic-ray and algorithmic-fake barrel ϕ uncertainties amount to approximately 4%, while the algorithmic-fake endcap ϕ uncertainty is

Table 1: Predicted event yields for each background category in the two signal regions. The uncertainties include the statistical and systematic uncertainties in the transfer factors (TFs), and statistical uncertainties reflecting the finite event yields in the regions to which the TFs are applied. An additional uncertainty is included for SR_{far} , derived from an observed discrepancy between predicted and observed event yields in the $m_{\text{DV}} < 20$ GeV validation region (see Section 6.3).

Category	SR_{far}	SR_{near}
Heavy flavour	1.2 ± 1.0	2.3 ± 0.8
Cosmic rays	0.18 ± 0.10	0.23 ± 0.13
Algorithmic fakes barrel	0.31 ± 0.15	0.31 ± 0.15
Algorithmic fakes endcap	0.11 ± 0.06	0.06 ± 0.04
Total predicted	1.8 ± 1.1	2.9 ± 0.8

as high as 49%. For the cosmic-ray TF, an additional midpoint split in $|\eta|$ that minimises the statistical uncertainties on either side is performed, yielding an additional $|\eta|$ uncertainty of 42%.

Table 1 lists the predicted event yields for each background category in SR_{far} and SR_{near} , including all uncertainties in the TFs. In both regions, muons from heavy-flavour decays dominate the background estimate.

6.3 Validation

The TFs are validated in the zero-DV and material-map-vetoed DV selections, but without applying the restrictive muon selection criteria used for the TF derivation in Section 6.1. This provides a direct check that these criteria do not bias the TFs, and that the systematic uncertainties cover potential residual correlations between the muon-veto requirements and the DV selection criteria, and residual background contamination of the TF derivation regions. Good agreement is observed, with all data yields within 1σ uncertainty of the predictions, demonstrating the robustness of the background estimate. The agreement between predicted and observed event yields in these validation regions is shown in Figure 4.

Further validation is performed by applying the TFs to the other validation regions outlined in Figure 3, namely events with DVs that fail to meet one or multiple signal DV criteria: events with a far DV with $n_{\text{track}} < 4$, events with a far DV with $m_{\text{DV}} < 20$ GeV, events with a near DV with $n_{\text{track}} < 4$, and events with a near DV with $m_{\text{DV}} < 40$ GeV. Good agreement is observed for all but the far $m_{\text{DV}} < 20$ GeV region: while the TF method predicts 16 ± 4 events, only six are observed. Although no physical source for a systematic bias was identified, as supported by the good agreement observed in the corresponding near DV region with $m_{\text{DV}} < 40$ GeV, a conservative approach is adopted and a non-closure uncertainty is derived for the heavy-flavour background, which dominates this selection. This uncertainty of approximately 77% is then applied to the heavy-flavour estimate in this region and propagated to SR_{far} . Figure 4 also shows the agreement between predicted and observed event yields in these validation regions, with the non-closure uncertainty included where applicable. Figure 5 shows the distributions of the predicted background yields and the observed data for events with a far DV with $n_{\text{track}} < 4$ and a near DV with $n_{\text{track}} < 4$ as a function of the $|d_0|$ of the highest- p_{T} muon and the p_{T} of the highest- p_{T} muon, respectively.

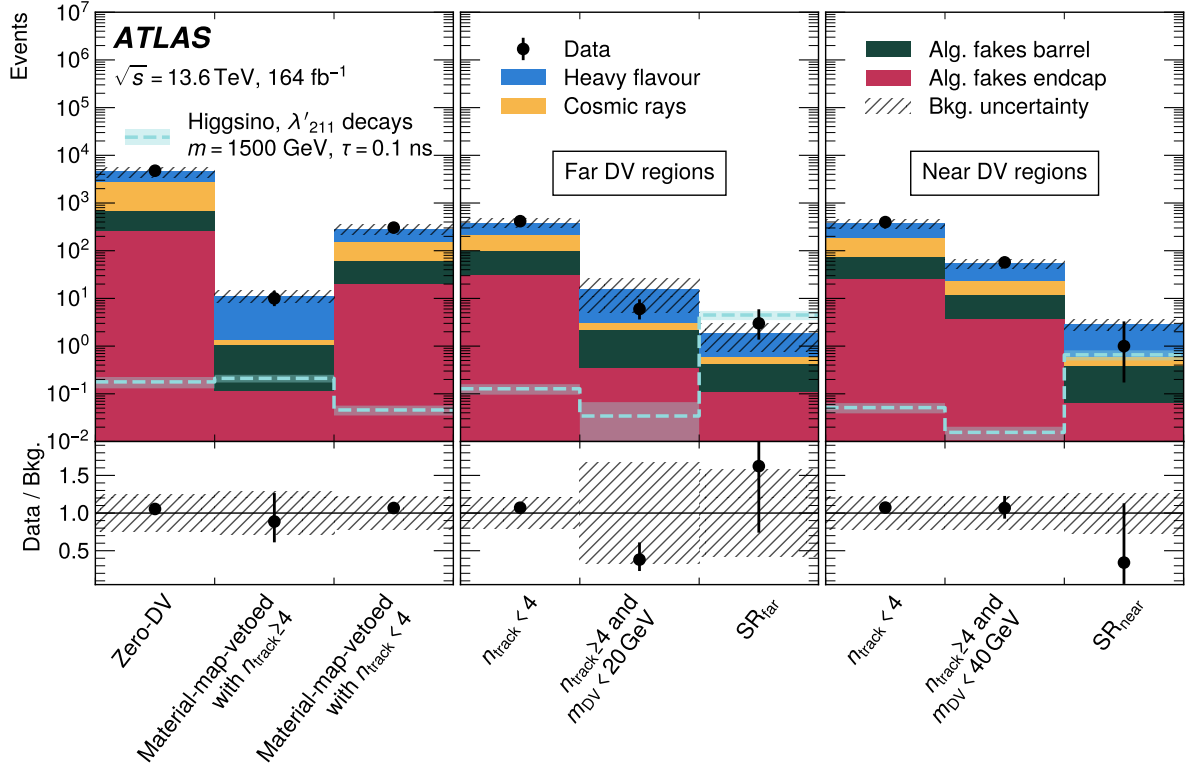


Figure 4: Overview of the analysis regions with varying displaced vertex (DV) selection criteria. The predicted background yields are obtained via the transfer factor method from the zero-DV and material-map-vetoed DV selections, with additional muon selection criteria to enhance the purity for each background. Good agreement is observed in all validation regions, except the far $n_{\text{track}} \geq 4, m_{\text{DV}} < 20$ GeV region. An additional non-closure uncertainty is applied to the heavy-flavour estimate in that region and in SR_{far} . The hatched band represents the total uncertainty in the prediction. The predictions are overlaid with one representative higgsino pair production benchmark model, with $m = 1500$ GeV and $\tau = 0.1$ ns, and lepton-number-violating decays via the λ'_{211} coupling. The uncertainty in the signal prediction includes statistical and systematic uncertainties.

7 Signal Systematic Uncertainties

Several sources of systematic uncertainty are evaluated for the predicted yields from the signal benchmark models. These include modelling and instrumental uncertainties, affecting both overall event yields and shapes of distributions used in the statistical analysis described in Section 8.

For all considered signal modelling uncertainties, differences between the overall signal normalisation are removed, such that the quoted uncertainties reflect only acceptance effects. Uncertainties from missing higher orders in QCD in the simulation are evaluated by varying the renormalisation and factorisation scale by factors 0.5 and 2. The variations are done both simultaneously and independently, and the largest deviation from the nominal prediction in each direction is taken as the uncertainty. The average variation over the considered signal samples is 3% for SR_{near} and 2% for SR_{far} . The maximal variations are 13% and 9%, respectively. Uncertainties owing to the choice of the PDF set are evaluated following Ref. [65] by reweighting the simulated events to the 100 replica sets of the NNPDF PDF set and taking the standard deviation of the resulting event yields as the uncertainty. The average effect on the signal predictions is observed to be 3% and 5% in SR_{near} and SR_{far} , respectively.

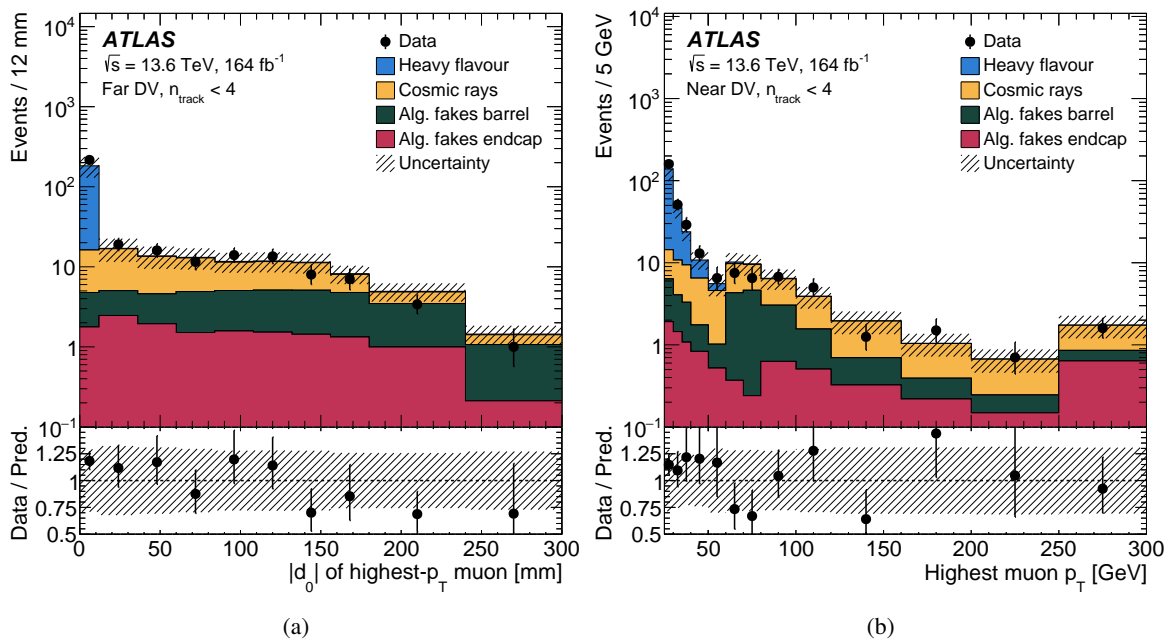


Figure 5: Distributions of the predicted background yields and the observed data for events with (a) a far displaced vertex (DV) with a transverse distance from the primary vertex larger than 4 mm and $n_{\text{track}} < 4$ as a function of the $|d_0|$ of the highest- p_T muon, and (b) a near DV with a transverse distance from the primary vertex between 1 mm and 4 mm and $n_{\text{track}} < 4$ as a function of the p_T of the highest- p_T muon. The hatched band represents the total uncertainty in the prediction. Overflow events are included in the last bins. Good agreement is observed in both regions.

The uncertainty in the efficiency for the reconstruction of primary and large-impact-parameter tracks is derived and propagated to the vertexing efficiency, following the methods described in Ref. [66]. The average effect on the event yields for the different benchmark models is around 2% and 3% in SR_{near} and SR_{far} , respectively.

Uncertainties in the muon reconstruction, isolation and identification efficiencies are computed following the method described in Ref. [50]; additional uncertainties in the background veto efficiencies are evaluated. A dedicated efficiency correction is applied for the identification of displaced muons. Uncertainties are derived combining two terms: one associated with the reconstruction of the ID track, and one associated with the reconstruction in the MS segments. Overall, these correspond to a signal uncertainty between 0.1% and 2%. Uncertainties in the simulation-to-data trigger scale factors are considered for standard prompt muons, and the impact varies between 0.2% and 8%; an additional 3% uncertainty accounts for the displaced-muon trigger efficiency, computed by comparing the trigger tracking efficiency relative to offline tracks in data and MC simulation, as done in Ref. [39].

The uncertainty associated with the pile-up reweighting procedure [67], averaged over the signal simulations considered, is 3% and 2% for SR_{near} and SR_{far} , respectively.

Furthermore, the expected number of signal events depends on the total integrated luminosity of the data sample. The combined integrated 2022–2024 luminosity has an uncertainty of 1.9%, determined using the LUCID–2 detector [43], which provides the primary luminosity measurement, complemented by measurements using the ID and the calorimeters.

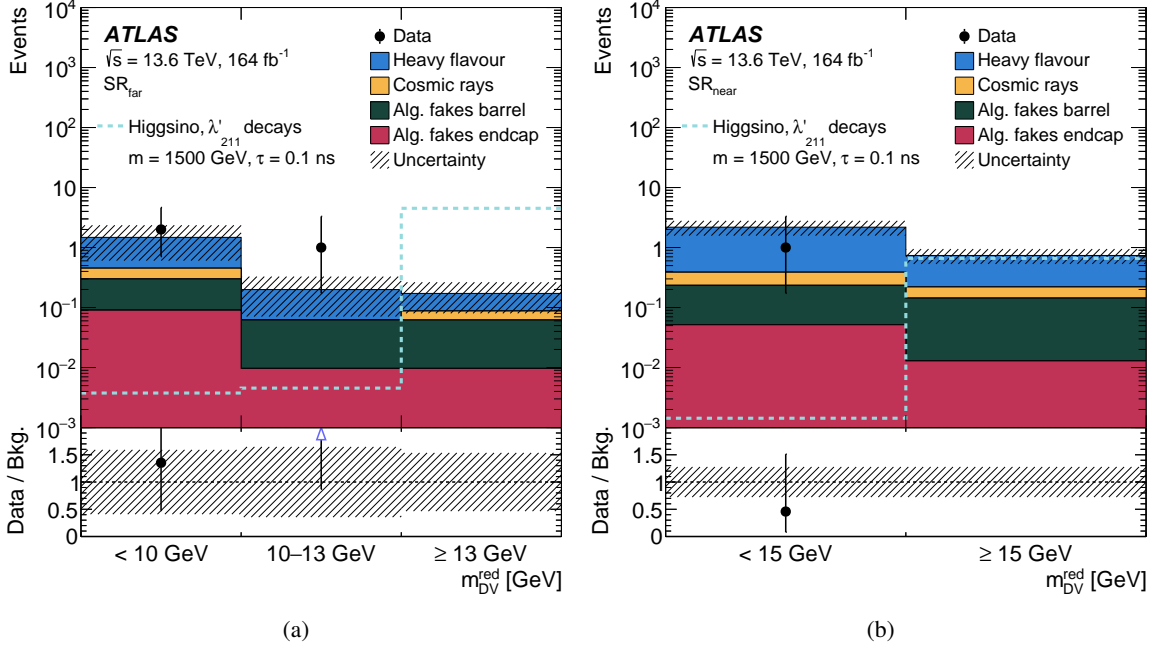


Figure 6: Distributions of the largest reduced invariant mass of any displaced vertex, m_{DV}^{red} , in the two signal regions: (a) SR_{far} and (b) SR_{near} . In both signal regions, no events are observed in data in the two highest m_{DV}^{red} bins. The background predictions derived using the data-driven transfer factor method are shown, along with an example signal benchmark (higgsino pair production with λ'_{211} decays, $m = 1500$ GeV and $\tau = 0.1$ ns) overlaid for illustration. The lower panels show the ratio of observed data to the total background prediction.

8 Results

Three events are observed in SR_{far} and one event is observed in SR_{near} , fully consistent with the combined background predictions, as summarised in Table 2.

A statistical analysis is performed to derive upper limits on the visible cross-section of final states with DVs and displaced muons, and to interpret the results in terms of upper limits on the production cross-sections of the benchmark models described in Section 3. The reduced invariant mass of the DV, $m_{DV}^{\text{red}} = m_{DV} / \Delta R_{\text{max}}$, where ΔR_{max} is the largest angular separation between any pair of DV-associated tracks, is used as the fitting observable. The average angular separation is typically smaller for signal than for background events, providing additional discrimination over m_{DV} alone. In events with more than one signal-like DV, only the vertex with the highest m_{DV}^{red} value is considered. The best sensitivity to a broad range of signal benchmark models is achieved with three bins in SR_{far} , with boundaries at $m_{DV}^{\text{red}} = 10$ GeV and $m_{DV}^{\text{red}} = 13$ GeV, and two bins in SR_{near} , with a boundary at $m_{DV}^{\text{red}} = 15$ GeV. The m_{DV}^{red} distributions with this binning in the two signal regions are shown in Figure 6, overlaid with one example signal benchmark.

The limit extraction is done with the profile likelihood method as implemented in the RooFIT, HistFACTORY and TREXFITTER frameworks [68–71]. The signal strength serves as the parameter of interest, while nuisance parameters account for systematic uncertainties in the signal and background predictions and are constrained by Gaussian priors. The likelihood combines Poisson terms for the event yields in the signal regions and in the regions used to derive the background estimates, to which the TFs are applied. Upper limits at 95% confidence level (CL) are derived using the CL_s method [72, 73], profiling the

Table 2: Model-independent upper limits at 95% confidence level on the visible cross-section, $\langle\sigma A\epsilon\rangle_{\text{obs}}^{95}$, in the two signal regions. The limits are derived using the CL_s method [72, 73] and include the effect of systematic uncertainties as nuisance parameters in the statistical analysis. The limits are given for three different minimum requirements on the reduced invariant mass of the displaced vertex, $m_{\text{DV}}^{\text{red}}$, in SR_{far} and two different minimum requirements in SR_{near} . *Total predicted* lists the total background prediction in each selection, with uncertainties including both statistical and systematic components. *Observed* lists the number of events observed in data for each selection. The $\langle\sigma A\epsilon\rangle_{\text{obs}}^{95}$ column lists the observed upper limits on the visible cross-section; the S_{obs}^{95} and S_{exp}^{95} columns list the observed and expected upper limits on the number of signal events, respectively.

	Total predicted	Observed	$\langle\sigma A\epsilon\rangle_{\text{obs}}^{95}$ [fb]	S_{obs}^{95}	S_{exp}^{95}
$\text{SR}_{\text{far}}, m_{\text{DV}}^{\text{red}}$ inclusive	1.8 \pm 1.1	3	0.038	6.2	4.9
$\text{SR}_{\text{far}}, m_{\text{DV}}^{\text{red}} \geq 10$ GeV	0.37 \pm 0.20	1	0.023	3.8	3.1
$\text{SR}_{\text{far}}, m_{\text{DV}}^{\text{red}} \geq 13$ GeV	0.17 \pm 0.09	0	0.018	3.0	3.0
$\text{SR}_{\text{near}}, m_{\text{DV}}^{\text{red}}$ inclusive	2.9 \pm 0.8	1	0.021	3.5	4.7
$\text{SR}_{\text{near}}, m_{\text{DV}}^{\text{red}} \geq 15$ GeV	0.73 \pm 0.20	0	0.018	3.0	3.0

nuisance parameters to obtain limits on the signal strength. For the RPV interpretations, the likelihood fit incorporates the binned distributions of the discriminating variable, $m_{\text{DV}}^{\text{red}}$, to enhance sensitivity across the benchmark models.

Model-independent 95% CL upper limits on the visible cross-section, $\langle\sigma A\epsilon\rangle$, for final states containing at least one DV and at least one displaced muon are obtained from counting experiments performed separately in SR_{far} and SR_{near} . In each region, progressively tighter selections are formed by increasing the minimum $m_{\text{DV}}^{\text{red}}$ threshold through the exclusion of one bin at a time. Limits are derived from ensembles of pseudo-experiments using the CL_s method. Table 2 summarises the total background predictions, observed yields, and the resulting $\langle\sigma A\epsilon\rangle_{\text{obs}}^{95}$ for each selection, and the corresponding observed and expected upper limits on the number of signal events. The most stringent cross-section limits are obtained when only the highest- $m_{\text{DV}}^{\text{red}}$ bin of SR_{far} or SR_{near} is considered. The limits on the visible cross-section are of the same order of magnitude as those obtained in the ATLAS Run-2 search for DVs and displaced muon tracks [35], but derived in a different fiducial volume.

Model-dependent 95% CL upper limits on the production cross-sections of the benchmark models described in Section 3 are obtained from ensembles of pseudo-experiments following a simultaneous fit to SR_{far} and SR_{near} , using a one-sided profile-likelihood ratio test statistic [74] within the CL_s framework. The signal acceptance times efficiency ($A \times \epsilon$) reaches peak values of approximately 38% (31%) for the L -violating higgsino (top-squark) model for a proper lifetime of 0.1 ns, while being about one order of magnitude lower for the B -violating higgsino model where muons only arise from top-quark decays. Figure 7 shows the expected and observed exclusion contours in the plane of the LLP mass and proper lifetime for the three considered benchmark models: higgsino pair production with (a) L -violating λ'_{211} and (b) B -violating λ'_{323} couplings, and (c) $\tilde{t}\bar{\tilde{t}}$ production with L -violating λ'_{233} couplings. The contours are overlaid with isocontours of the RPV SUSY coupling strength for each model. For the top-squark model, these isocontours correspond to the coupling strength $\lambda'_{233} \cos \theta_t$, where θ_t is the mixing angle between left- and right-handed top squarks, calculated following the expression provided in Ref. [75]. In the higgsino models, the values are given for the coupling strengths $\lambda/m_{\tilde{f}}^2$, where $m_{\tilde{f}}$ is the mass of the virtual sfermion mediating the RPV decay, following the parameterisation in Ref. [76]. Upper limits on the production cross-sections are also derived for four representative lifetime values, shown as a function of the LLP mass in Figure 8.

Limits on higgsino masses up to 1600 GeV (1150 GeV) are placed for proper lifetimes of 0.1 ns for λ'_{211} (λ''_{323}) decays, and higgsino masses between 100 GeV and at least 450 GeV are excluded for proper lifetimes between 1 ps and 100 ns for λ'_{211} decays. Compared with the λ'_{211} limits set by the ATLAS Run-1 search for higgsino-like neutralinos [32], the reach is significantly extended in both mass and proper lifetime while placing fewer assumptions on the production mechanism. On average, the limits on the production cross-sections for higgsino-like neutralinos with λ'_{211} decays are improved by approximately two orders of magnitude. For λ''_{323} decays, the proper lifetime reach is extended up to 100 ns, providing complementary coverage to the CMS Run-2 search for hadronic DV pairs [36]. Optimised for vertex pairs within the beam pipe radius of 22 mm, the CMS search sets tighter limits at proper lifetimes below 0.1 ns, whereas this result provides unique sensitivity at larger displacements.

Top-squark masses of up to 1850 GeV are excluded for proper lifetimes of 0.1 ns, and any values between 700 GeV and 1500 GeV are excluded for proper lifetimes between 10 ps and 5 ns. This improves upon the limits set by the previous ATLAS search for DVs and displaced muon tracks using Run-2 data [35], particularly for proper lifetimes below 5 ns, highlighting the enhanced sensitivity provided by the new dedicated muon triggers and improved reconstruction techniques employed. For longer lifetimes, the Run-2 search retains more stringent limits due to the usage of missing transverse momentum triggers, which were not considered in this Letter.

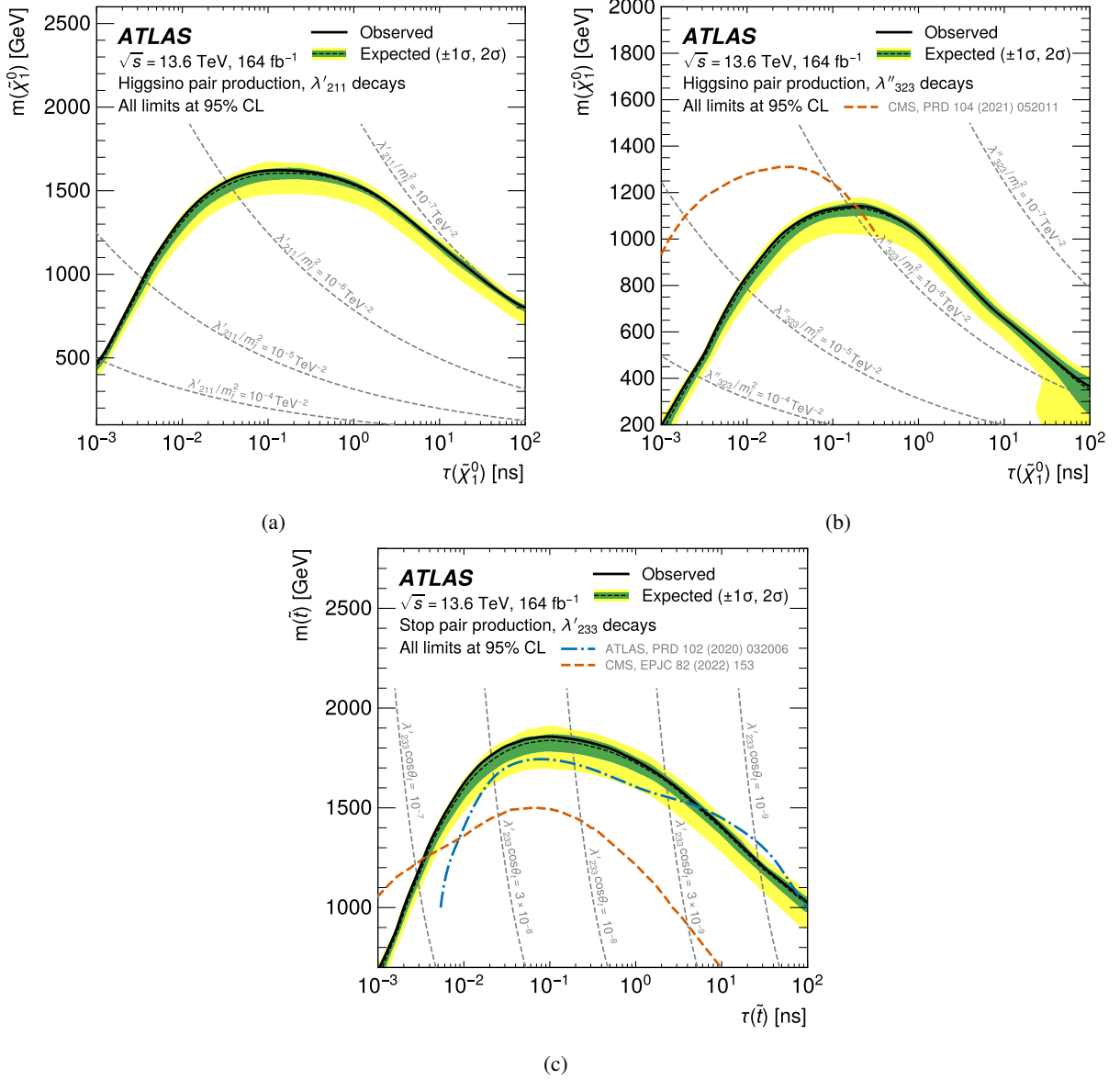


Figure 7: Expected and observed exclusion contours at 95% confidence level in the plane of the long-lived particle’s mass and proper lifetime, for the three considered benchmark models: higgsino pair production with (a) L -violating λ'_{211} and (b) B -violating λ''_{323} decays, and (c) $t\bar{t}$ pair production with L -violating λ'_{233} decays. A triangular interpolation scheme between simulated and lifetime-reweighted points is used to obtain a smooth contour. The triangulation is done linearly in mass, and logarithmically in lifetime and signal strength. Additional smoothing using a Gaussian kernel is applied to the observed limit contour to reduce artifacts from the interpolation. The contours are overlaid with isocontours of the R -parity-violating (RPV) SUSY coupling strength. In the top-squark model, these isocontours correspond to the coupling strength $\lambda'_{233} \cos \theta_t$, where θ_t is the mixing angle between left- and right-handed top squarks. In the higgsino models, the values are given for the coupling strengths $\lambda/m_{\tilde{f}}$, where $m_{\tilde{f}}$ is the mass of the virtual sfermion mediating the RPV decay (with the assumption that $m_{\tilde{f}} \gg m_{\tilde{\chi}_1^0}$). The contours in (b) and (c) are overlaid with results from previous searches for similar models [35–37].

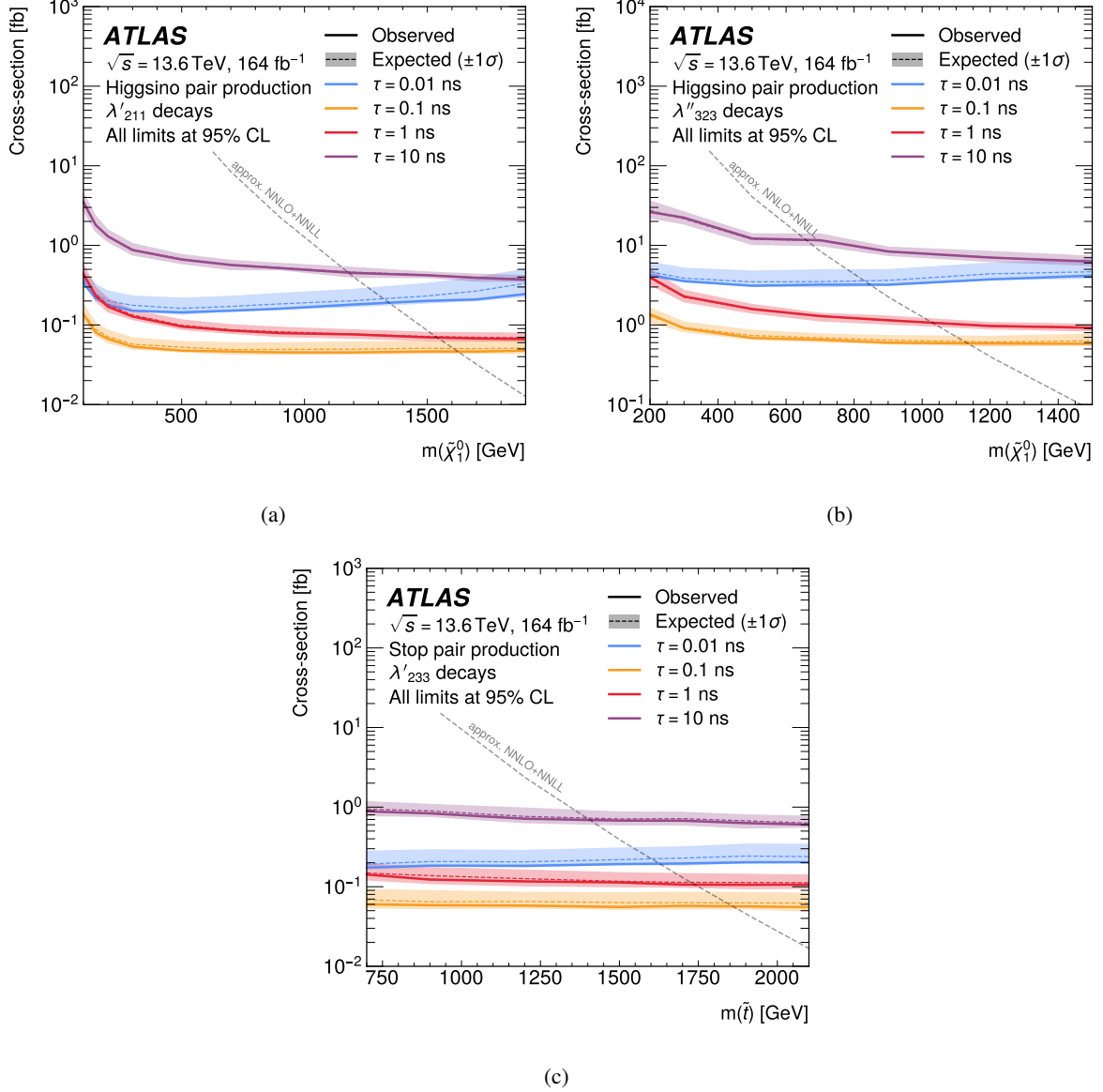


Figure 8: Expected and observed 95% confidence level upper limits on the production cross-section for four representative lifetime values, shown as a function of the long-lived particle mass in the higgsino pair production benchmark model with decays via (a) the λ'_{211} coupling and (b) the λ''_{323} coupling, and (c) the top-squark mass in the top-squark model with decays via the λ'_{233} coupling. The expected limits are shown with their one standard deviation uncertainty bands. The plots are overlaid with the approximate NNLO+NNLL cross-section curves for higgsino and top-squark pair production [58–60]. Good sensitivity is achieved across the entire mass ranges, with the best sensitivity for lifetimes of 0.1 ns.

9 Conclusion

A search for LLPs decaying into a DV and a muon is presented, using 164 fb^{-1} of $\sqrt{s} = 13.6 \text{ TeV}$ pp collision data collected by the ATLAS detector at the LHC between 2022 and 2024. The search targets events with a DV with at least four associated tracks and an invariant mass above 20 GeV, along with at least one muon with a transverse impact parameter $|d_0| > 2 \text{ mm}$. A data-driven TF method is employed to estimate the background contributions from heavy-flavour decays, cosmic-ray muons, and algorithmic fakes. Two signal regions are defined based on the transverse distance between the DV and the primary interaction vertex; in both regions, the background is dominated by muons from heavy-flavour decays. No significant excess above the expected background is observed. The results are interpreted in terms of upper limits on the visible cross-section for final states with at least one DV and at least one displaced muon, and as upper limits on the production cross-sections of benchmark models involving LLPs from RPV SUSY. The sensitivity is significantly enhanced over previous searches: cross-section limits for higgsino-like neutralinos with L -violating λ'_{211} decays are improved by approximately two orders of magnitude relative to Run-1 measurements, and the reach for B -violating λ''_{323} decays is extended to proper lifetimes of 100 ns. For top squarks, the dedicated Run-3 muon triggers and refined reconstruction techniques lead to better sensitivity to $\lambda'_{233} \cos \theta_t$ for proper lifetimes below 5 ns than achieved in prior ATLAS results.

Acknowledgements

We thank CERN for the very successful operation of the LHC and its injectors, as well as the support staff at CERN and at our institutions worldwide without whom ATLAS could not be operated efficiently.

The crucial computing support from all WLCG partners is acknowledged gratefully, in particular from CERN, the ATLAS Tier-1 facilities at TRIUMF/SFU (Canada), NDGF (Denmark, Norway, Sweden), CC-IN2P3 (France), KIT/GridKA (Germany), INFN-CNAF (Italy), NL-T1 (Netherlands), PIC (Spain), RAL (UK) and BNL (USA), the Tier-2 facilities worldwide and large non-WLCG resource providers. Major contributors of computing resources are listed in Ref. [77].

We gratefully acknowledge the support of ANPCyT, Argentina; YerPhI, Armenia; ARC, Australia; BMWFW and FWF, Austria; ANAS, Azerbaijan; CNPq and FAPESP, Brazil; NSERC, NRC and CFI, Canada; CERN; ANID, Chile; CAS, MOST and NSFC, China; Minciencias, Colombia; MEYS CR, Czech Republic; DNRF and DNSRC, Denmark; IN2P3-CNRS and CEA-DRF/IRFU, France; SRNSFG, Georgia; BMFTR, HGF and MPG, Germany; GSRI, Greece; RGC and Hong Kong SAR, China; ICHEP and Academy of Sciences and Humanities, Israel; INFN, Italy; MEXT and JSPS, Japan; CNRST, Morocco; NWO, Netherlands; RCN, Norway; MNiSW, Poland; FCT, Portugal; MNE/IFA, Romania; MSTDI, Serbia; MSSR, Slovakia; ARIS and MVZI, Slovenia; DSI/NRF, South Africa; MICIU/AEI, Spain; SRC and Wallenberg Foundation, Sweden; SERI, SNSF and Cantons of Bern and Geneva, Switzerland; NSTC, Taipei; TENMAK, Türkiye; STFC/UKRI, United Kingdom; DOE and NSF, United States of America.

Individual groups and members have received support from BCKDF, CANARIE, CRC and DRAC, Canada; CERN-CZ, FORTE and PRIMUS, Czech Republic; COST, ERC, ERDF, Horizon 2020 and Marie Skłodowska-Curie Actions, European Union; Investissements d’Avenir Labex, Investissements d’Avenir IDEX and ANR, France; DFG and AvH Foundation, Germany; Herakleitos, Thales and Aristeia programmes co-financed by EU-ESF and the Greek NSRF, Greece; BSF-NSF and MINERVA, Israel; NCN and NAWA, Poland; La Caixa Banking Foundation, CERCA Programme Generalitat de Catalunya and PROMETEO

and GenT Programmes Generalitat Valenciana, Spain; Göran Gustafssons Stiftelse, Sweden; The Royal Society and Leverhulme Trust, United Kingdom; United States of America.

In addition, individual members wish to acknowledge support from Chile: Agencia Nacional de Investigación y Desarrollo (ANID FONDECYT reg. 1230987, FONDECYT 1230812, FONDECYT 1240864, Fondecyt 3240661, Fondecyt Regular 1240721); China: Chinese Ministry of Science and Technology (MOST-2023YFA1605700, MOST-2023YFA1609300), National Natural Science Foundation of China (NSFC 12275265, NSFC-W2543005); Czech Republic: Czech Science Foundation (GACR - 24-11373S), Ministry of Education Youth and Sports (ERC-CZ-LL2327, FORTE CZ.02.01.01/00/22_008/0004632), PRIMUS Research Programme (PRIMUS/21/SCI/017); EU: H2020 European Research Council (ERC - 101002463); European Union: European Research Council (BARD No. 101116429, ERC - 948254, ERC 101089007), European Regional Development Fund (HE COFUND GA No.101081355, ERDF), Marie Skłodowska-Curie Actions (GAP-101168829); France: Agence Nationale de la Recherche (ANR-21-CE31-0013, ANR-22-EDIR-0002, ANR-24-CE31-0504-01); Germany: Deutsche Forschungsgemeinschaft (DFG - 469666862); China: Research Grants Council (GRF); Italy: Ministero dell'Università e della Ricerca (NextGenEU 153D23001490006 M4C2.1.1, NextGenEU I53D23000820006 M4C2.1.1, NextGenEU I53D23001490006 M4C2.1.1, SOE2024_0000023); Japan: Japan Society for the Promotion of Science (JSPS KAKENHI JP22H01227, JSPS KAKENHI JP22H04944, JSPS KAKENHI JP22KK0227, JSPS KAKENHI JP24K23939, JSPS KAKENHI JP24KK0251, JSPS KAKENHI JP25H00650, JSPS KAKENHI JP25H01291, JSPS KAKENHI JP25K01023); Norway: Research Council of Norway (RCN-314472); Poland: Polish National Science Centre (NCN 2021/42/E/ST2/00350, NCN OPUS 2023/51/B/ST2/02507, NCN OPUS nr 2022/47/B/ST2/03059, NCN UMO-2019/34/E/ST2/00393, UMO-2022/47/O/ST2/00148, UMO-2023/49/B/ST2/04085, UMO-2023/51/B/ST2/00920, UMO-2024/53/N/ST2/00869); Spain: Agencia de Gestión de Ayudas Universitarias y de Investigación (AGAUR - 2023 BP 00141), Ministry of Science and Innovation (RYC2019-028510-I, RYC2020-030254-I, RYC2021-031273-I, RYC2022-038164-I), Ministerio de Ciencia, Innovación y Universidades/Agencia Estatal de Investigación (PID2022-142604OB-C22); Sweden: Carl Trygger Foundation (Carl Trygger Foundation CTS 22:2312), Swedish Research Council (Swedish Research Council 2023-04654, VR 2021-03651, VR 2022-03845, VR 2022-04683, VR 2023-03403, VR 2024-05451, VR 2025-05940), Knut and Alice Wallenberg Foundation (KAW 2023.0366); Switzerland: Swiss National Science Foundation (SNSF - PCEFP2_194658); United Kingdom: The Binks Trust, Royal Society (NIF-R1-231091); United States of America: U.S. Department of Energy (ECA DE-AC02-76SF00515), John Templeton Foundation (John Templeton Foundation 63206), Neubauer Family Foundation.

References

- [1] L. Evans and P. Bryant, *LHC Machine*, [JINST 3 \(2008\) S08001](#).
- [2] J. Alimena et al., *Searching for long-lived particles beyond the Standard Model at the Large Hadron Collider*, [J. Phys. G 47 \(2020\) 090501](#), arXiv: [1903.04497 \[hep-ex\]](#).
- [3] A. Arvanitaki, N. Craig, S. Dimopoulos and G. Villadoro, *Mini-Split*, [JHEP 02 \(2013\) 126](#), arXiv: [1210.0555 \[hep-ph\]](#).
- [4] N. Arkani-Hamed, A. Gupta, D. E. Kaplan, N. Weiner and T. Zorawski, *Simply Unnatural Supersymmetry*, arXiv: [1212.6971 \[hep-ph\]](#).

- [5] G. F. Giudice and R. Rattazzi, *Theories with gauge-mediated supersymmetry breaking*, [Phys. Rept. **322** \(1999\) 419](#), arXiv: [hep-ph/9801271 \[hep-ph\]](#).
- [6] G. R. Farrar and P. Fayet, *Phenomenology of the production, decay, and detection of new hadronic states associated with supersymmetry*, [Phys. Lett. B **76** \(1978\) 575](#).
- [7] Yu. A. Gol'fand and E. P. Likhtman, *Extension of the Algebra of Poincare Group Generators and Violation of P Invariance*, [JETP Lett. **13** \(1971\) 20](#), [*Pisma Zh. Eksp. Teor. Fiz.* **13** (1971) 452].
- [8] D. V. Volkov and V. P. Akulov, *Is the neutrino a goldstone particle?*, [Phys. Lett. B **46** \(1973\) 109](#).
- [9] J. Wess and B. Zumino, *Supergauge transformations in four dimensions*, [Nucl. Phys. B **70** \(1974\) 39](#).
- [10] J. Wess and B. Zumino, *Supergauge invariant extension of quantum electrodynamics*, [Nucl. Phys. B **78** \(1974\) 1](#).
- [11] S. Ferrara and B. Zumino, *Supergauge invariant Yang-Mills theories*, [Nucl. Phys. B **79** \(1974\) 413](#).
- [12] A. Salam and J. Strathdee, *Super-symmetry and non-Abelian gauges*, [Phys. Lett. B **51** \(1974\) 353](#).
- [13] R. Barbier et al., *R-Parity-violating supersymmetry*, [Phys. Rept. **420** \(2005\) 1](#), arXiv: [hep-ph/0406039 \[hep-ph\]](#).
- [14] B. C. Allanach, M. A. Bernhardt, H. K. Dreiner, C. H. Kom and P. Richardson, *Mass spectrum in R-parity violating minimal supergravity and benchmark points*, [Phys. Rev. D **75** \(2007\)](#).
- [15] J. Fan, M. Reece and J. T. Ruderman, *Stealth supersymmetry*, [JHEP **11** \(2011\) 012](#), arXiv: [1105.5135 \[hep-ph\]](#).
- [16] J. Fan, M. Reece and J. T. Ruderman, *A stealth supersymmetry sampler*, [JHEP **07** \(2012\) 196](#), arXiv: [1201.4875 \[hep-ph\]](#).
- [17] Z. Chacko, D. Curtin and C. B. Verhaaren, *A quirky probe of neutral naturalness*, [Phys. Rev. D **94** \(2016\) 011504](#), arXiv: [1512.05782 \[hep-ph\]](#).
- [18] G. Burdman, Z. Chacko, H.-S. Goh and R. Harnik, *Folded supersymmetry and the LEP paradox*, [JHEP **0702** \(2007\) 009](#), arXiv: [hep-ph/0609152 \[hep-ph\]](#).
- [19] H. Cai, H.-C. Cheng and J. Terning, *A quirky little Higgs model*, [JHEP **05** \(2009\) 045](#), arXiv: [0812.0843 \[hep-ph\]](#).
- [20] Z. Chacko, H.-S. Goh and R. Harnik, *Natural Electroweak Breaking from a Mirror Symmetry*, [Phys. Rev. Lett. **96** \(2006\) 231802](#), arXiv: [hep-ph/0506256 \[hep-ph\]](#).
- [21] M. J. Strassler and K. M. Zurek, *Echoes of a hidden valley at hadron colliders*, [Phys. Lett. B **651** \(2007\) 374](#), arXiv: [hep-ph/0604261 \[hep-ph\]](#).
- [22] M. J. Strassler and K. M. Zurek, *Discovering the Higgs through highly-displaced vertices*, [Phys. Lett. B **661** \(2008\) 263](#), arXiv: [hep-ph/0605193 \[hep-ph\]](#).
- [23] M. Baumgart, C. Cheung, J. T. Ruderman, L.-T. Wang and I. Yavin, *Non-abelian dark sectors and their collider signatures*, [JHEP **04** \(2009\) 014](#), arXiv: [0901.0283 \[hep-ph\]](#).
- [24] D. E. Kaplan, M. A. Luty and K. M. Zurek, *Asymmetric dark matter*, [Phys. Rev. D **79** \(2009\) 115016](#), arXiv: [0901.4117 \[hep-ph\]](#).

- [25] Y. F. Chan, M. Low, D. E. Morrissey and A. P. Spray, *LHC signatures of a minimal supersymmetric hidden valley*, *JHEP* **05** (2012) 155, arXiv: [1112.2705 \[hep-ph\]](#).
- [26] K. R. Dienes and B. Thomas, *Dynamical dark matter. I. Theoretical overview*, *Phys. Rev. D* **85** (2012) 083523, arXiv: [1106.4546 \[hep-ph\]](#).
- [27] K. R. Dienes, S. Su and B. Thomas, *Distinguishing dynamical dark matter at the LHC*, *Phys. Rev. D* **86** (2012) 054008, arXiv: [1204.4183 \[hep-ph\]](#).
- [28] Y. Cui and R. Sundrum, *Baryogenesis for weakly interacting massive particles*, *Phys. Rev. D* **87** (2013) 116013, arXiv: [1212.2973 \[hep-ph\]](#).
- [29] Y. Cui, *Natural baryogenesis from unnatural supersymmetry*, *JHEP* **12** (2013) 067, arXiv: [1309.2952 \[hep-ph\]](#).
- [30] Y. Cui and B. Shuve, *Probing baryogenesis with displaced vertices at the LHC*, *JHEP* **02** (2015) 049, arXiv: [1409.6729 \[hep-ph\]](#).
- [31] ATLAS Collaboration, *Search for displaced vertices arising from decays of new heavy particles in 7 TeV pp collisions at ATLAS*, *Phys. Lett. B* **707** (2012) 478, arXiv: [1109.2242 \[hep-ex\]](#).
- [32] ATLAS Collaboration, *Search for long-lived, heavy particles in final states with a muon and multi-track displaced vertex in proton–proton collisions at $\sqrt{s} = 7$ TeV with the ATLAS detector*, *Phys. Lett. B* **719** (2013) 280, arXiv: [1210.7451 \[hep-ex\]](#).
- [33] CMS Collaboration, *Search for Displaced Supersymmetry in Events with an Electron and a Muon with Large Impact Parameters*, *Phys. Rev. Lett.* **114** (2015) 061801, arXiv: [1409.4789 \[hep-ex\]](#).
- [34] CMS Collaboration, *Search for new long-lived particles at $\sqrt{s} = 13$ TeV*, *Phys. Lett. B* **780** (2018) 432, arXiv: [1711.09120 \[hep-ex\]](#).
- [35] ATLAS Collaboration, *Search for long-lived, massive particles in events with a displaced vertex and a muon with large impact parameter in pp collisions at $\sqrt{s} = 13$ TeV with the ATLAS detector*, *Phys. Rev. D* **102** (2020) 032006, arXiv: [2003.11956 \[hep-ex\]](#).
- [36] CMS Collaboration, *Search for long-lived particles decaying to jets with displaced vertices in proton–proton collisions at $\sqrt{s} = 13$ TeV*, *Phys. Rev. D* **104** (2021) 052011, arXiv: [2104.13474 \[hep-ex\]](#).
- [37] CMS Collaboration, *Search for long-lived particles decaying to leptons with large impact parameter in proton–proton collisions at $\sqrt{s} = 13$ TeV*, *Eur. Phys. J. C* **82** (2022) 153, arXiv: [2110.04809 \[hep-ex\]](#).
- [38] ATLAS Collaboration, *Preliminary luminosity calibration of the ATLAS 13.6 TeV data recorded in 2024 and combination with the 2022 and 2023 measurements*, ATL-DAPR-PUB-2025-001, 2025, URL: <https://cds.cern.ch/record/2948582>.
- [39] ATLAS Collaboration, *The ATLAS trigger system for LHC Run 3 and trigger performance in 2022*, *JINST* **19** (2024) P06029, arXiv: [2401.06630 \[hep-ex\]](#).
- [40] ATLAS Collaboration, *Performance of the reconstruction of large impact parameter tracks in the inner detector of ATLAS*, *Eur. Phys. J. C* **83** (2023) 1081, arXiv: [2304.12867 \[hep-ex\]](#).
- [41] ATLAS Collaboration, *The ATLAS Experiment at the CERN Large Hadron Collider*, *JINST* **3** (2008) S08003.

- [42] ATLAS Collaboration, *The ATLAS experiment at the CERN Large Hadron Collider: a description of the detector configuration for Run 3*, *JINST* **19** (2024) P05063, arXiv: [2305.16623 \[physics.ins-det\]](#).
- [43] G. Avoni et al., *The new LUCID-2 detector for luminosity measurement and monitoring in ATLAS*, *JINST* **13** (2018) P07017.
- [44] ATLAS Collaboration, *Software and computing for Run 3 of the ATLAS experiment at the LHC*, *Eur. Phys. J. C* **85** (2025) 234, arXiv: [2404.06335 \[hep-ex\]](#), Erratum: *Eur. Phys. J. C* **85** (2025) 907.
- [45] ATLAS Collaboration, *Emulating the impact of additional proton–proton interactions in the ATLAS simulation by presampling sets of inelastic Monte Carlo events*, *Comput. Softw. Big Sci.* **6** (2022) 3, arXiv: [2102.09495 \[hep-ex\]](#).
- [46] K. Werner, F.-M. Liu and T. Pierog, *Parton ladder splitting and the rapidity dependence of transverse momentum spectra in deuteron–gold collisions at the BNL Relativistic Heavy Ion Collider*, *Phys. Rev. C* **74** (2006) 044902, arXiv: [hep-ph/0506232](#).
- [47] T. Sjöstrand et al., *An introduction to PYTHIA 8.2*, *Comput. Phys. Commun.* **191** (2015) 159, arXiv: [1410.3012 \[hep-ph\]](#).
- [48] C. Bierlich et al., *A comprehensive guide to the physics and usage of PYTHIA 8.3*, *SciPost Phys. Codebases* (2022) 8, arXiv: [2203.11601 \[hep-ph\]](#).
- [49] S. Agostinelli et al., *GEANT4 – a simulation toolkit*, *Nucl. Instrum. Meth. A* **506** (2003) 250.
- [50] ATLAS Collaboration, *Muon reconstruction and identification efficiency in ATLAS using the full Run 2 pp collision data set at $\sqrt{s} = 13$ TeV*, *Eur. Phys. J. C* **81** (2021) 578, arXiv: [2012.00578 \[hep-ex\]](#).
- [51] M. Ibe, S. Matsumoto and R. Sato, *Mass Splitting between Charged and Neutral Winos at Two-Loop Level*, *Phys. Lett. B* **721** (2013) 252, arXiv: [1212.5989 \[hep-ph\]](#).
- [52] N. Nagata and S. Shirai, *Higgsino Dark Matter in High-Scale Supersymmetry*, *JHEP* **01** (2015) 029, arXiv: [1410.4549 \[hep-ph\]](#).
- [53] J. Alwall et al., *The automated computation of tree-level and next-to-leading order differential cross sections, and their matching to parton shower simulations*, *JHEP* **07** (2014) 079, arXiv: [1405.0301 \[hep-ph\]](#).
- [54] NNPDF Collaboration, R. D. Ball et al., *Parton distributions for the LHC run II*, *JHEP* **04** (2015) 040, arXiv: [1410.8849 \[hep-ph\]](#).
- [55] ATLAS Collaboration, *ATLAS Pythia 8 tunes to 7 TeV data*, ATL-PHYS-PUB-2014-021, 2014, URL: <https://cds.cern.ch/record/1966419>.
- [56] NNPDF Collaboration, R. D. Ball et al., *Parton distributions with LHC data*, *Nucl. Phys. B* **867** (2013) 244, arXiv: [1207.1303 \[hep-ph\]](#).
- [57] D. J. Lange, *The EvtGen particle decay simulation package*, *Nucl. Instrum. Meth. A* **462** (2001) 152.
- [58] J. Fiaschi and M. Klasen, *Higgsino and gaugino pair production at the LHC with aNNLO+NNLL precision*, *Phys. Rev. D* **102** (2020) 095021, arXiv: [2006.02294 \[hep-ph\]](#).

- [59] B. Fuks, M. Klasen, D. R. Lamprea and M. Rothering, *Precision predictions for electroweak superpartner production at hadron colliders with RESUMMINO*, *Eur. Phys. J. C* **73** (2013) 2480, arXiv: [1304.0790 \[hep-ph\]](#).
- [60] J. Fiaschi, B. Fuks, M. Klasen and A. Neuwirth, *Electroweak superpartner production at 13.6 TeV with Resummino*, *Eur. Phys. J. C* **83** (2023) 707, arXiv: [2304.11915 \[hep-ph\]](#).
- [61] ATLAS Collaboration, *Software Performance of the ATLAS Track Reconstruction for LHC Run 3*, *Comput. Softw. Big Sci.* **8** (2024) 9, arXiv: [2308.09471 \[hep-ex\]](#).
- [62] ATLAS Collaboration, *Performance of vertex reconstruction algorithms for detection of new long-lived particle decays within the ATLAS inner detector*, ATL-PHYS-PUB-2019-013, 2019, URL: <https://cds.cern.ch/record/2669425>.
- [63] ATLAS Collaboration, *Search for displaced leptons in $\sqrt{s} = 13$ TeV and 13.6 TeV pp collisions with the ATLAS detector*, *Phys. Rev. D* **112** (2025) 012016, arXiv: [2410.16835 \[hep-ex\]](#).
- [64] ATLAS Collaboration, *Search for long-lived, massive particles in events with displaced vertices and multiple jets in pp collisions at $\sqrt{s} = 13$ TeV with the ATLAS detector*, *JHEP* **06** (2023) 200, arXiv: [2301.13866 \[hep-ex\]](#).
- [65] J. Butterworth et al., *PDF4LHC recommendations for LHC Run II*, *J. Phys. G* **43** (2016) 023001, arXiv: [1510.03865 \[hep-ph\]](#).
- [66] ATLAS Collaboration, *Search for exotic decays of the Higgs boson into long-lived particles in pp collisions at $\sqrt{s} = 13$ TeV using displaced vertices in the ATLAS inner detector*, *JHEP* **11** (2021) 229, arXiv: [2107.06092 \[hep-ex\]](#).
- [67] ATLAS Collaboration, *Measurement of the Inelastic Proton–Proton Cross Section at $\sqrt{s} = 13$ TeV with the ATLAS Detector at the LHC*, *Phys. Rev. Lett.* **117** (2016) 182002, arXiv: [1606.02625 \[hep-ex\]](#).
- [68] W. A. Rolke, A. M. López and J. Conrad, *Limits and confidence intervals in the presence of nuisance parameters*, *Nucl. Instrum. Meth. A* **551** (2005) 493, ed. by L. Lyons and M. Karagoz, arXiv: [physics/0403059](#).
- [69] W. Verkerke and D. Kirkby, *The RooFit toolkit for data modeling*, 2003, arXiv: [physics/0306116 \[physics.data-an\]](#).
- [70] ROOT Collaboration, *HistFactory: A tool for creating statistical models for use with RooFit and RooStats*, CERN-OPEN-2012-016, 2012, URL: <https://cds.cern.ch/record/1456844>.
- [71] M. Aly et al., *TRExFitter*, version 1.4.0, 2025, URL: <https://doi.org/10.5281/zenodo.16684099>.
- [72] A. L. Read, *Presentation of search results: the CL_s technique*, *J. Phys. G* **28** (2002) 2693.
- [73] T. Junk, *Confidence level computation for combining searches with small statistics*, *Nucl. Instrum. Meth. A* **434** (1999) 435, arXiv: [hep-ex/9902006](#).
- [74] G. Cowan, K. Cranmer, E. Gross and O. Vitells, *Asymptotic formulae for likelihood-based tests of new physics*, *Eur. Phys. J. C* **71** (2011) 1554, arXiv: [1007.1727 \[physics.data-an\]](#), Erratum: *Eur. Phys. J. C* **73** (2013) 2501.

- [75] T. Kon, T. Kobayashi and S. Kitamura,
Signatures of scalar top with R-parity breaking coupling at HERA, *Phys. Lett. B* **333** (1994) 263,
arXiv: [hep-ph/9403288](https://arxiv.org/abs/hep-ph/9403288).
- [76] H. K. Dreiner and G. G. Ross, *R-parity violation at hadron colliders*, *Nucl. Phys. B* **365** (1991) 597.
- [77] ATLAS Collaboration, *ATLAS Computing Acknowledgements*, ATL-SOFT-PUB-2026-001, 2026,
URL: <https://cds.cern.ch/record/2952666>.

The ATLAS Collaboration

G. Aad ¹⁰², E. Aakvaag ¹⁷, B. Abbott ¹²², S. Abdelhameed ^{118a}, K. Abeling ⁵⁴, N.J. Abicht ⁴⁸, S.H. Abidi ³⁰, M. Aboeela ⁴⁴, A. Aboulhorma ^{36e}, H. Abramowicz ¹⁵⁵, B.S. Acharya ^{68a,68b,m}, A. Ackermann ^{62a}, C. Adam Bourdarios ⁴, L. Adamczyk ^{85a}, S.V. Addepalli ¹⁴⁷, M.J. Addison ¹⁰¹, J. Adelman ¹¹⁷, A. Adiguzel ^{22c}, T. Adye ¹³⁶, A.A. Affolder ¹³⁸, Y. Afik ³⁹, M.N. Agaras ¹³, A. Aggarwal ¹⁰⁰, C. Agheorghiesei ^{28c}, A. Ahmad ^{83a}, F. Ahmadov ^{38,ad}, S. Ahuja ⁹⁵, S. Ahuja ¹⁶⁶, X. Ai ^{113c}, G. Aielli ^{75a,75b}, A. Aikot ¹⁶⁶, M. Ait Tamlihat ^{36e}, T.P.A. Åkesson ⁹⁸, D. Akiyama ¹⁷¹, N.N. Akolkar ²⁵, S. Aktas ¹⁶⁹, G.L. Alberghi ^{24b}, J. Albert ¹⁶⁸, U. Alberti ²⁰, P. Albicocco ⁵², S. Alderweireldt ⁵¹, Z.L. Alegria ¹²³, M. Aleksa ³⁷, I.N. Aleksandrov ³⁸, C. Alexa ^{28b}, T. Alexopoulos ¹⁰, F. Alfonsi ^{24b}, M. Algren ⁵⁵, M. Alhroob ¹⁷⁰, B. Ali ¹³⁴, H.M.J. Ali ^{91,v}, S. Ali ³², S.W. Alibocus ⁹², M. Aliev ^{34c}, G. Alimonti ^{70a}, C. Allaire ⁶⁵, B.M.M. Allbrooke ¹⁵⁰, D.R. Allen ¹²³, J.S. Allen ¹⁰¹, J.F. Allen ⁵¹, C.S. Alley ¹, E.R. Almazan ¹³⁸, A. Aloisio ^{71a,71b}, F. Alonso ⁹⁰, C. Alpigliani ¹⁴¹, A. Alvarez Fernandez ¹⁰⁰, M. Alves Cardoso ⁵⁵, M.G. Alviggi ^{71a,71b}, M. Aly ¹⁰¹, Y. Amaral Coutinho ^{81b}, A. Ambler ¹⁰⁴, C. Amelung ³⁷, M. Amerl ¹⁰¹, T. Amezza ¹²⁹, B. Amini ⁵³, K. Amirie ¹⁵⁹, A. Amirkhanov ³⁸, D. Amperiadou ¹⁵⁶, S. An ⁸², C. Anastopoulos ¹⁴³, T. Andeen ¹¹, J.K. Anders ⁹², A.C. Anderson ⁵⁸, A. Andreazza ^{70a,70b}, S. Angelidakis ⁹, A. Angerami ⁴¹, A.V. Anisenkov ³⁸, A. Annovi ^{73a}, C. Antel ³⁷, E. Antipov ¹⁴⁹, M. Antonelli ⁵², F. Anulli ^{74a}, M. Aoki ⁸², T. Aoki ¹⁵⁷, M.A. Aparo ¹³, L. Aperio Bella ⁴⁷, M. Apicella ³¹, C. Appelt ¹⁵⁵, A. Apyan ²⁷, M. Arampatzi ¹⁰, S.J. Arbiol Val ⁸⁶, C. Arcangeletti ⁵², A.T.H. Arce ⁵⁰, J-F. Arguin ¹⁰⁸, S. Argyropoulos ¹⁵⁶, J.-H. Arling ⁴⁷, O. Arnaez ⁴, H. Arnold ¹⁴⁹, G. Artoni ^{74a,74b}, H. Asada ¹¹¹, S. Asatryan ¹⁷⁶, N.A. Asbah ³⁷, R.A. Ashby Pickering ¹⁷⁰, A.M. Aslam ⁹⁵, J. Assahsah ^{36d}, K. Assamagan ³⁰, R. Astalos ^{29a}, K.S.V. Astrand ⁹⁸, S. Atashi ¹⁶³, R.J. Atkin ^{34a}, H. Atmani ^{36f}, P.A. Atmasiddha ¹³⁰, K. Augsten ¹³⁴, A.D. Auriol ⁴⁰, V.A. Austrup ¹⁰¹, A.S. Avad ⁹⁴, G. Avolio ³⁷, K. Axiotis ⁵⁵, A. Azzam ¹³, D. Babal ^{29b}, H. Bachacou ¹³⁷, K. Bachas ^{156,p}, A. Bachiu ³⁵, E. Bachmann ⁴⁹, M.J. Backes ^{62a}, A. Badea ³⁹, T.M. Baer ¹⁰⁶, M. Bahmani ¹⁹, D. Bahner ⁵³, K. Bai ¹²⁵, L. Baines ⁹⁴, O.K. Baker ¹⁷⁵, D. Bakshi Gupta ⁸, L.E. Balabram Filho ^{81b}, V. Balakrishnan ¹²², R. Balasubramanian ⁴, P. Balek ^{85a}, E. Ballabene ^{24b,24a}, F. Balli ¹³⁷, L.M. Baltes ^{62a}, W.K. Balunas ¹²⁸, I. Bamwidhi ^{118b}, E. Banas ⁸⁶, M. Bandieramonte ¹³¹, A. Bandyopadhyay ²⁵, S. Bansal ²⁵, L. Barak ¹⁵⁵, M. Barakat ⁴⁷, E.L. Barberio ¹⁰⁵, D. Barberis ^{18b}, M. Barbero ¹⁰², M.Z. Barel ¹¹⁶, T. Barillari ¹¹⁰, M-S. Barisits ³⁷, T. Barklow ¹⁴⁷, P. Baron ¹³⁵, D.A. Baron Moreno ¹⁰¹, A. Baroncelli ⁶¹, A.J. Barr ¹²⁸, J.D. Barr ⁹⁶, F. Barreiro ⁹⁹, J. Barreiro Guimarães da Costa ¹⁴, M.G. Barros Teixeira ^{132a}, F. Bartels ^{62a}, R. Bartoldus ¹⁴⁷, A.E. Barton ⁹¹, P. Bartos ^{29a}, M. Baselga ⁴⁸, S. Bashiri ⁸⁶, A. Bassalat ^{65,b}, M.J. Basso ^{160a}, S. Bataju ⁴⁴, R. Bate ¹⁶⁷, R.L. Bates ⁵⁸, S. Batlamous ⁹⁹, M. Battaglia ¹³⁸, D. Battulga ¹⁹, M. Baucé ^{74a,74b}, L. Bauckhage ⁴⁷, P. Bauer ²⁵, L.T. Bayer ⁴⁷, L.T. Bazzano Hurrell ³¹, T. Beau ¹²⁹, J.Y. Beaucamp ⁹⁰, S. Beauceron ¹²⁹, P.H. Beauchemin ¹⁶², P. Bechtel ²⁵, H.P. Beck ^{20,o}, K. Becker ¹⁷⁰, A.J. Beddall ⁸⁰, V.A. Bednyakov ³⁸, C.P. Bee ¹⁴⁹, L.J. Beemster ¹⁶, M. Begalli ^{81d}, M. Begel ³⁰, J.K. Behr ⁴⁷, J.F. Beirer ³⁷, F. Beisiegel ²⁵, M. Belfkir ^{118b}, G. Bella ¹⁵⁵, L. Bellagamba ^{24b}, A. Bellerive ³⁵, C.D. Bellgraph ⁶⁷, P. Bellos ²¹, I. Benaoumeur ²¹, D. Benckekroun ^{36a}, F. Bendebba ^{36a}, Y. Benhammou ¹⁵⁵, K.C. Benkendorfer ¹⁶⁸, L. Beresford ⁴⁷, M. Beretta ⁵², E. Bergeas Kuutmann ¹⁶⁴, N. Berger ⁴, B. Bergmann ¹³⁴, J. Beringer ^{18a}, M. Berkat ¹³⁷, G. Bernardi ⁵, C. Bernius ¹⁴⁷, F.U. Bernlochner ²⁵, A. Berrocal Guardia ¹³, T. Berry ⁹⁵, P. Berta ¹³⁵, A. Berti ^{132a},

R. Bertrand ¹⁰², S. Bethke ¹¹⁰, A. Betti ^{74a,74b}, T.F. Beumker ¹⁷⁴, A.J. Bevan ⁹⁴, L. Bezio ⁵⁵, N.K. Bhalla ⁵³, S. Bharthuar ¹¹⁰, S. Bhatta ¹⁴⁹, P. Bhattacharai ¹⁴⁷, Z.M. Bhatti ¹¹⁹, K.D. Bhide ⁵³, V.S. Bhopatkar ¹²³, R.M. Bianchi ¹³¹, G. Bianco ^{24b,24a}, O. Biebel ¹⁰⁹, M. Biglietti ^{76a}, P. Bijl ⁵³, C.S. Billingsley ⁴⁴, Y. Bimondi ^{36f}, M. Bindi ⁵⁴, A. Bingham ¹⁷⁴, A. Bingul ^{22b}, C. Bini ^{74a,74b}, G.A. Bird ³³, M. Biro ¹³⁵, S. Biryukov ¹⁵⁰, T. Bisanz ⁴⁸, E. Bisceglie ^{24b,24a}, J.P. Biswal ¹³⁶, D. Biswas ¹⁴⁵, M. Biyabi ¹⁴, I. Bloch ⁴⁷, A. Blue ⁵⁸, U. Blumenschein ⁹⁴, V.S. Bobrovnikov ³⁸, L. Boccardo ^{56b,56a}, M. Boehler ⁵³, B. Boehm ¹⁶⁹, D. Bogavac ¹³, L.S. Boggia ¹²⁹, V. Boisvert ⁹⁵, P. Bokan ¹⁶⁴, T. Bold ^{85a}, M. Bomben ⁵, M. Bona ⁹⁴, M. Boonekamp ¹³⁷, A.G. Borbély ⁵⁸, G. Borissov ⁹¹, A. Borkar ¹⁶⁹, D. Bortoletto ¹²⁸, D. Boscherini ^{24b}, M. Bosman ¹³, K. Bouaouda ^{36a}, L. Boudet ⁴, J. Boudreau ¹³¹, E.V. Bouhova-Thacker ⁹¹, D. Boumediene ⁴⁰, R. Bouquet ^{56b,56a}, A. Boveia ¹²¹, J. Boyd ³⁷, D. Boye ³⁰, I.R. Boyko ³⁸, L. Bozianu ⁵⁵, J. Bracik ²¹, N. Brahimi ⁴, G. Brandt ¹⁷⁴, O. Brandt ³³, B. Brau ¹⁰³, R. Brenner ¹⁷², L. Brenner ¹¹⁶, R. Brenner ¹⁶⁴, S. Bressler ¹⁷², M. Brettell ⁹⁶, G. Brianti ¹¹⁶, D. Britton ⁵⁸, D. Britzger ¹¹⁰, I. Brock ²⁵, R. Brock ¹⁰⁷, H. Bronson ¹³⁰, G. Brooijmans ⁴¹, A.J. Brooks ⁶⁷, E.M. Brooks ^{160b}, E. Brost ³⁰, L.M. Brown ^{168,160a}, L.E. Bruce ⁶⁰, T.L. Bruckler ¹²⁸, P.A. Bruckman de Renstrom ⁸⁶, B. Brüers ⁴⁷, A. Bruni ^{24b}, G. Bruni ^{24b}, D. Brunner ^{46a,46b}, M. Bruschi ^{24b}, N. Brusino ^{74a,74b}, T. Buanes ¹⁷, Q. Buat ¹⁴¹, D. Buchin ¹¹⁰, A.G. Buckley ⁵⁸, J. Bucko ¹³⁵, M. Bühring ⁴⁹, O. Bulekov ⁸⁰, B.A. Bullard ¹⁴⁷, T.O. Buratovich ⁹⁰, S. Burdin ⁹², C.D. Burgard ⁴⁸, A.M. Burger ⁸⁹, B. Burghgrave ⁸, O. Burlayenko ⁵³, J. Burleson ¹⁶⁵, J.C. Burzynski ¹²², V. Büscher ¹⁰⁰, P.J. Bussey ⁵⁸, O. But ²⁵, J.M. Butler ²⁶, C.M. Buttar ⁵⁸, J.M. Butterworth ⁹⁶, P. Butti ³⁷, W. Buttinger ¹³⁶, C.J. Buxo Vazquez ¹⁰⁷, A.R. Buzykaev ³⁸, S. Cabrera Urbán ¹⁶⁶, L. Cadamuro ⁶⁵, H. Cai ³⁷, Y. Cai ^{24b,112c,24a}, Y. Cai ^{112a}, M.A. Cairo ¹³⁰, V.M.M. Cairo ³⁷, O. Cakir ^{3a}, N. Calace ³⁷, P. Calafiura ^{18a}, G. Calderini ¹²⁹, P. Calfayan ³⁵, L. Calic ⁹⁸, G. Callea ⁵⁸, L.P. Caloba ^{81b}, D. Calvet ⁴⁰, S. Calvet ⁴⁰, R. Camacho Toro ¹²⁹, S. Camarda ³⁷, D. Camarero Munoz ²⁷, P. Camarri ^{75a,75b}, C. Camincher ³⁷, M. Campanelli ⁹⁶, A. Camplani ⁴², V. Canale ^{71a,71b}, A.C. Canbay ^{3a}, E. Canonero ⁹⁵, J. Cantero ¹⁶⁶, F. Capocasa ²⁷, P. Cappelli ²⁷, M. Capua ^{43b,43a}, A. Carbone ^{70a,70b}, R. Cardarelli ^{75a}, J.C.J. Cardenas ⁸, M.P. Cardiff ²⁷, G. Carducci ^{43b,43a}, T. Carli ³⁷, G. Carlino ^{71a}, J.I. Carlotto ¹³, B.T. Carlson ^{131,q}, E.M. Carlson ¹⁶⁸, L. Carminati ^{70a,70b}, A. Carnelli ⁴, M. Carnesale ³⁷, S. Caron ¹¹⁵, E. Carquin ^{139g}, I.B. Carr ¹⁰⁵, S. Carrá ^{72a,72b}, G. Carratta ^{24b,24a}, C. Carrion Martinez ¹⁶⁶, A.M. Carroll ¹²⁵, N. Cartalade ⁴⁰, M.P. Casado ^{13,h}, P. Casolaro ^{71a,71b}, M. Caspar ⁴⁷, F. Cassinese ⁹⁰, W.R. Castiglioni ³⁹, F.L. Castillo ⁴, L. Castillo Garcia ¹³, V. Castillo Gimenez ¹⁶⁶, N.F. Castro ^{132a,132e}, A. Catinaccio ³⁷, J.R. Catmore ¹²⁷, T. Cavaliere ⁴, V. Cavaliere ³⁰, E. Celebi ⁸⁰, S. Cella ³⁰, V. Cepaitis ⁵⁵, K. Cerny ¹²⁴, A.S. Cerqueira ^{81a}, A. Cerri ^{73a,ap}, L. Cerrito ^{75a,75b}, F. Cerutti ^{18a}, B. Cervato ^{70a,70b}, A. Cervelli ^{24b}, G. Cesarini ⁵², S.A. Cetin ⁸⁰, P.M. Chabrilat ¹²⁹, R. Chakkappai ⁶⁵, S. Chakraborty ¹⁷⁰, A. Chambers ⁶⁰, J. Chan ^{18a}, J.D. Chapman ³³, E. Chapon ¹³⁷, B. Chargeishvili ^{153b}, D.G. Charlton ²¹, C. Chauhan ¹³³, Y. Che ^{112a}, S. Chekanov ⁶, G.A. Chelkov ^{38,a}, H. Chen ³⁰, J. Chen ^{142a}, J. Chen ¹⁴⁶, M. Chen ⁵⁹, S. Chen ⁸⁷, S.J. Chen ^{112a}, X. Chen ^{142a}, X. Chen ^{15,ai}, Z. Chen ⁶¹, C.L. Cheng ¹⁷³, H.C. Cheng ^{63a}, S. Cheong ¹⁴⁷, A. Cheplakov ³⁸, E. Cherepanova ¹¹⁶, E. Cheu ⁷, K. Cheung ⁶⁴, L. Chevalier ¹³⁷, G. Chiarelli ^{73a}, G. Chiodini ^{69a}, A.S. Chisholm ²¹, A. Chitan ^{28b}, M. Chitishvili ¹⁶⁶, M.V. Chizhov ^{38,r}, K. Choi ¹¹, Y. Chou ¹⁴¹, E.Y.S. Chow ¹¹⁵, K.L. Chu ¹⁷², M.C. Chu ^{63a}, Z. Chubinidze ⁵², J. Chudoba ¹³³, J.J. Chwastowski ⁸⁶, D. Cieri ¹¹⁰, K.M. Ciesla ^{85a}, V. Cindro ⁹³, A. Ciocio ^{18a}, F. Ciotto ^{71a,71b}, Z.H. Citron ¹⁷², M. Citterio ^{70a}, D.A. Ciubotaru ^{28b}, A. Clark ⁵⁵, P.J. Clark ⁵¹, N. Clarke Hall ⁹⁶, C. Clarry ¹⁵⁹, S.E. Clawson ⁴⁷, C. Clement ^{46a,46b}, L. Clissa ^{24b,24a}, Y. Coadou ¹⁰², M. Cokal ^{68a,68c}, A. Coccaro ^{56b},

M.G. Cochran Branson [id](#)¹⁴¹, R.F. Coelho Barrue [id](#)^{132a}, R. Coelho Lopes De Sa [id](#)¹⁰³, S. Coelli [id](#)^{70a},
M.M. Cohen [id](#)¹³⁰, L.S. Colangeli [id](#)¹⁵⁹, B. Cole [id](#)⁴¹, P. Collado Soto [id](#)⁹⁹, J. Collot [id](#)⁵⁹,
M.R. Coluccia [id](#)^{69a}, I. Combes⁶⁵, P. Conde Muiño [id](#)^{132a,132g}, M.P. Connell [id](#)^{34c}, S.H. Connell [id](#)^{34c},
E.I. Conroy [id](#)¹²⁸, M. Contreras Cossio [id](#)¹¹, F. Conventi [id](#)^{71a,ak}, A.M. Cooper-Sarkar [id](#)¹²⁸,
L. Corazzina [id](#)^{74a,74b}, F.A. Corchia [id](#)^{24b,24a}, A. Cordeiro Oudot Choi [id](#)¹⁴¹, L.D. Corpe [id](#)⁴⁰,
M. Corradi [id](#)^{74a,74b}, F. Corriveau [id](#)^{104,ab}, A. Cortes-Gonzalez [id](#)¹⁵⁷, M.J. Costa [id](#)¹⁶⁶, F. Costanza [id](#)⁴,
D. Costanzo [id](#)¹⁴³, J. Couthures [id](#)⁴, G. Cowan [id](#)⁹⁵, K. Cranmer [id](#)¹⁷³, L. Cremer [id](#)⁴⁸,
D. Cremonini [id](#)^{24b,24a}, S. Crépe-Renaudin [id](#)⁵⁹, F. Crescioli [id](#)¹²⁹, T. Cresta [id](#)^{72a,72b}, M. Cristinziani [id](#)¹⁴⁵,
M. Cristoforetti [id](#)^{77a,77b}, E. Critelli [id](#)⁹⁶, A. Cueto [id](#)⁹⁹, H. Cui [id](#)⁹⁶, Z. Cui [id](#)⁷, B.M. Cunnett [id](#)¹⁵⁰,
W.R. Cunningham [id](#)⁵⁸, E. Cuppini¹¹⁰, F. Curcio [id](#)¹⁶⁶, J.R. Curran [id](#)⁵¹,
M.J. Da Cunha Sargedas De Sousa [id](#)^{56b,56a}, J.V. Da Fonseca Pinto [id](#)^{81b}, C. Da Via [id](#)¹⁰¹,
W. Dabrowski [id](#)^{85a}, T. Dado [id](#)³⁷, S. Dahbi [id](#)¹⁵², T. Dai [id](#)¹⁰⁶, D. Dal Santo [id](#)²⁰, C. Dallapiccola [id](#)¹⁰³,
M. Dam [id](#)⁴², G. D'amen [id](#)³⁰, V. D'Amico [id](#)¹⁰⁹, J.R. Dandoy [id](#)³⁵, M. D'Andrea [id](#)^{56b,56a},
D. Dannheim [id](#)³⁷, G. D'anniballe [id](#)^{73a,73b}, M. Danninger [id](#)¹⁴⁶, V. Dao [id](#)¹⁴⁹, G. Darbo [id](#)^{56b},
F. Dattola [id](#)⁴⁷, S. D'Auria [id](#)^{70a,70b}, A. D'Avanzo [id](#)^{71a,71b}, T. Davidek [id](#)¹³⁵, J. Davidson [id](#)¹⁷⁰,
I. Dawson [id](#)⁹⁴, K. De [id](#)⁸, C. De Almeida Rossi [id](#)¹⁵⁹, N. De Biase [id](#)⁴⁷, S. De Castro [id](#)^{24b,24a},
N. De Groot [id](#)¹¹⁵, P. de Jong [id](#)¹¹⁶, H. De la Torre [id](#)¹¹⁷, A. De Maria [id](#)^{112a}, S. De Miranda Rimes [id](#)^{81d},
A. De Salvo [id](#)^{74a}, U. De Sanctis [id](#)^{75a,75b}, F. De Santis [id](#)^{69a,69b}, A. De Santo [id](#)¹⁵⁰,
J.B. De Vivie De Regie [id](#)⁵⁹, K.G. De Vries [id](#)¹¹⁶, J. Debevc [id](#)⁹³, D.V. Dedovich³⁸, J. Degens [id](#)⁹²,
A.M. Deiana [id](#)⁴⁴, J. Del Peso [id](#)⁹⁹, L. Delagrangé [id](#)²⁷, F. Deliot [id](#)¹³⁷, C.M. Delitzsch [id](#)⁴⁸,
M. Della Pietra [id](#)^{71a,71b}, D. Della Volpe [id](#)⁵⁵, A. Dell'Acqua [id](#)³⁷, L. Dell'Asta [id](#)^{70a,70b}, M. Delmastro [id](#)⁴,
C.C. Delogu [id](#)^{56b,56a}, P.A. Delsart [id](#)⁵⁹, S. Demers [id](#)¹⁷⁵, M. Demichev [id](#)³⁸, H. Denizli [id](#)^{22a,1},
M.G. Depala [id](#)⁹², L. D'Eramo [id](#)⁴⁰, D. Derendarz [id](#)⁸⁶, L. Derin [id](#)^{56b,56a}, F. Derue [id](#)¹²⁹, P. Dervan [id](#)^{92,*},
A.M. Desai [id](#)¹, K. Desch [id](#)²⁵, F.A. Di Bello [id](#)^{73a,73b}, A. Di Ciaccio [id](#)^{75a,75b}, L. Di Ciaccio [id](#)⁴,
D. Di Croce [id](#)³⁷, C. Di Donato [id](#)^{71a,71b}, A. Di Girolamo [id](#)³⁷, G. Di Gregorio [id](#)⁶⁵, A. Di Luca [id](#)^{77a,77b},
B. Di Micco [id](#)^{76a,76b}, R. Di Nardo [id](#)^{76a,76b}, K.F. Di Petrillo [id](#)³⁹, M. Diamantopoulou [id](#)³⁵, F.A. Dias [id](#)¹¹⁶,
M.A. Diaz [id](#)^{139a,139b}, A.R. Didenko [id](#)³⁸, M. Didenko [id](#)¹⁶⁶, S.D. Diefenbacher [id](#)^{18a}, E.B. Diehl [id](#)¹⁰⁶,
S. Díez Cornell [id](#)⁴⁷, C. Diez Pardos [id](#)¹⁴⁵, C. Dimitriadi [id](#)¹⁴⁸, A. Dimitrievska [id](#)²¹, A. Dimri [id](#)¹⁴⁹,
Y. Ding⁶¹, J. Dingfelder [id](#)²⁵, T. Dingley [id](#)¹²⁸, I-M. Dinu [id](#)^{28b}, S.J. Dittmeier [id](#)^{62b}, F. Dittus [id](#)³⁷,
M. Divisek [id](#)¹³⁵, B. Dixit [id](#)⁹², F. Djama [id](#)¹⁰², T. Djobava [id](#)^{153b}, C. Doglioni [id](#)^{101,98}, A. Dohnalova [id](#)^{29a},
Z. Dolezal [id](#)¹³⁵, K. Domijan [id](#)^{85a}, K.M. Dona [id](#)³⁹, M. Donadelli [id](#)^{81d}, B. Dong [id](#)¹⁰⁷, J. Donini [id](#)⁴⁰,
A. D'Onofrio [id](#)^{71a,71b}, M. D'Onofrio [id](#)⁹², J. Dopke [id](#)¹³⁶, A. Doria [id](#)^{71a}, N. Dos Santos Fernandes [id](#)^{132a},
I.A. Dos Santos Luz [id](#)^{81e}, P. Dougan [id](#)⁴⁴, M.T. Dova [id](#)⁹⁰, A.T. Doyle [id](#)⁵⁸, M.P. Drescher [id](#)⁵⁴,
E. Dreyer [id](#)¹⁷², I. Drivas-koulouris [id](#)¹⁰, M. Drnevich [id](#)¹¹⁹, D. Du [id](#)⁶¹, T. Du³⁹, T.A. du Pree [id](#)¹¹⁶,
Z. Duan^{112a}, M. Dubau [id](#)⁴, F. Dubinin [id](#)³⁸, M. Dubovsky [id](#)^{29a}, E. Duchovni [id](#)¹⁷², G. Duckeck [id](#)¹⁰⁹,
P.K. Duckett⁹⁶, O.A. Ducu [id](#)^{28b}, D. Duda [id](#)⁵¹, A. Dudarev [id](#)³⁷, M.M. Dudek [id](#)⁸⁶, E.R. Duden [id](#)²⁷,
M. D'uffizi [id](#)¹⁰¹, L. Dufflot [id](#)⁶⁵, M. Dührssen [id](#)³⁷, I. Duminica [id](#)^{28g}, A.E. Dumitriu [id](#)^{28b},
M. Dunford [id](#)^{62a}, T. Duong⁴, A. Duperrin [id](#)¹⁰², A.F. Duque Bran [id](#)⁴⁰, H. Duran Yildiz [id](#)^{3a},
A. Durglishvili [id](#)^{153b}, G.I. Dyckes [id](#)^{18a}, M. Dyndal [id](#)^{85a}, B.S. Dziedzic [id](#)³⁷, G.H. Eberwein [id](#)¹²⁸,
B. Eckerova [id](#)^{29a}, J.C. Egan [id](#)⁹⁶, S. Eggebrecht [id](#)⁵⁴, E. Egidio Purcino De Souza [id](#)^{81e}, G. Eigen [id](#)¹⁷,
K. Einsweiler [id](#)^{18a}, T. Ekelof [id](#)¹⁶⁴, P.A. Ekman [id](#)⁹⁸, S. El Farkh [id](#)^{36b}, Y. El Ghazali [id](#)⁶¹,
H. El Jarrari [id](#)¹⁰⁴, A. El Moussaouy [id](#)^{36a}, I. Elbaz [id](#)¹⁵⁵, D. Elitez [id](#)³⁷, M. Ellert [id](#)¹⁶⁴, F. Ellinghaus [id](#)¹⁷⁴,
T.A. Elliot [id](#)⁹⁵, J. Elmsheuser [id](#)³⁰, M. Elsayy [id](#)^{118a}, M. Elsing [id](#)³⁷, D. Emeliyanov [id](#)¹³⁶, Y. Enari [id](#)⁸²,
S. Epari [id](#)¹⁰⁸, D. Ernani Martins Neto [id](#)⁸⁶, F. Ernst³⁷, M. Escalier [id](#)⁶⁵, C. Escobar [id](#)¹⁶⁶,
R. Estevam De Paula [id](#)^{81c}, E. Etzion [id](#)¹⁵⁵, G. Evans [id](#)^{132a,132b}, H. Evans [id](#)⁶⁷, L.S. Evans [id](#)⁴⁷,
S. Ezzarqtouni [id](#)^{36a}, F. Fabbri [id](#)^{24b,24a}, L. Fabbri [id](#)^{24b,24a}, G. Facini [id](#)⁹⁶, V. Fadeyev [id](#)¹³⁸,
D. Fakoudis [id](#)¹⁰⁰, S. Falciano [id](#)^{74a}, L.F. Falda Ulhoa Coelho [id](#)²⁷, F. Fallavollita [id](#)¹¹⁰, G. Falsetti [id](#)^{43b,43a},

J. Faltova [ID](#)¹³⁵, C. Fan [ID](#)¹⁶⁵, K.Y. Fan [ID](#)^{63b}, Y. Fan [ID](#)¹⁴, Y. Fang [ID](#)^{14,112c}, M. Fanti [ID](#)^{70a,70b}, M. Faraj [ID](#)^{68a,68c}, Z. Farazpay [ID](#)⁹⁷, A. Farbin [ID](#)⁸, A. Farilla [ID](#)^{76a}, K. Farman [ID](#)¹⁵², J.N. Farr [ID](#)¹⁷⁵, M.S. Farrington [ID](#)⁶⁰, S.M. Farrington [ID](#)^{136,51}, F. Fassi [ID](#)^{36e}, D. Fassouliotis [ID](#)⁹, L. Fayard [ID](#)⁶⁵, P. Federic [ID](#)¹³⁵, P. Federicova [ID](#)¹³³, M. Feickert [ID](#)¹⁷³, L. Feligioni [ID](#)¹⁰², D.E. Fellers [ID](#)^{18a}, C. Feng [ID](#)^{113b}, Y. Feng¹⁴, Z. Feng [ID](#)⁶⁵, B. Fernandez Barbadillo [ID](#)⁹¹, P. Fernandez Martinez [ID](#)⁶⁶, C. Fernandez Ruiz [ID](#)³³, J. Ferrando [ID](#)⁹¹, A. Ferrari [ID](#)¹⁶⁴, P. Ferrari [ID](#)^{116,115}, R. Ferrari [ID](#)^{72a}, D. Ferrere [ID](#)⁵⁵, C. Ferretti [ID](#)¹⁰⁶, M.P. Fewell [ID](#)¹, D. Fiacco [ID](#)^{74a,74b}, F. Fiedler [ID](#)¹⁰⁰, P. Fiedler [ID](#)¹³⁴, S. Filimonov [ID](#)³⁸, M.S. Filip [ID](#)^{28b,s}, A. Filipčič [ID](#)⁹³, E.K. Filmer [ID](#)^{160a}, F. Filthaut [ID](#)¹¹⁵, M.C.N. Fiolhais [ID](#)^{132a,132c,c}, L. Fiorini [ID](#)¹⁶⁶, W.C. Fisher [ID](#)¹⁰⁷, T. Fitschen [ID](#)¹⁰¹, I. Fleck [ID](#)¹⁴⁵, P. Fleischmann [ID](#)¹⁰⁶, T. Flick [ID](#)¹⁷⁴, M. Flores [ID](#)^{34d,ag}, L.R. Flores Castillo [ID](#)^{63a}, M. Foll [ID](#)¹²⁷, F.M. Follega [ID](#)^{77a,77b}, N. Fomin [ID](#)³³, J.H. Foo [ID](#)¹⁵⁹, A. Formica [ID](#)¹³⁷, M. Fornasiero [ID](#)¹⁵⁰, A.C. Forti [ID](#)¹⁰¹, E. Fortin [ID](#)¹⁰², A.W. Fortman [ID](#)^{18a}, L. Foster [ID](#)^{18a}, L. Fountas [ID](#)⁹, H. Fox [ID](#)⁹¹, P. Francavilla [ID](#)^{73a,73b}, S. Francescato [ID](#)⁶⁰, S. Franchellucci [ID](#)²⁰, M. Franchini [ID](#)^{24b,24a}, S. Franchino [ID](#)^{62a}, D. Francis³⁷, L. Franco [ID](#)⁴⁷, L. Franconi [ID](#)⁴⁷, M. Franklin [ID](#)⁶⁰, G. Frattari [ID](#)²⁷, Y.Y. Frid [ID](#)¹⁵⁵, N. Fritzsche [ID](#)³⁷, A. Froch [ID](#)⁵⁵, D. Froidevaux [ID](#)³⁷, J.A. Frost [ID](#)¹³⁶, Y. Fu [ID](#)¹⁰⁷, S. Fuenzalida Garrido [ID](#)^{139g}, Y.C. Fujikake [ID](#)¹³⁸, M. Fujimoto [ID](#)¹⁴⁹, K.Y. Fung [ID](#)^{63a}, E. Furtado De Simas Filho [ID](#)^{81e}, M. Furukawa [ID](#)¹⁵⁷, M. Fuste Costa [ID](#)⁴⁷, J. Fuster [ID](#)¹⁶⁶, A. Gaa [ID](#)⁵⁴, A. Gabrielli [ID](#)^{24b,24a}, A. Gabrielli [ID](#)¹⁵⁹, G. Gagliardi [ID](#)^{56b,56a}, L.G. Gagnon [ID](#)^{18a}, S. Galantzan [ID](#)¹⁵⁵, J. Gallagher [ID](#)¹, E.J. Gallas [ID](#)¹²⁸, A.L. Gallen [ID](#)¹⁶⁴, B.J. Gallop [ID](#)¹³⁶, K.K. Gan [ID](#)¹²¹, Y. Gao [ID](#)⁵¹, Z. Gao [ID](#)^{112a}, A. Garabaglu [ID](#)¹⁴¹, F.M. Garay Walls [ID](#)^{139a,139b}, C. García [ID](#)¹⁶⁶, A. Garcia Alonso [ID](#)¹¹⁶, A.G. Garcia Caffaro [ID](#)¹⁷⁵, J.E. García Navarro [ID](#)¹⁶⁶, M.A. Garcia Ruiz [ID](#)^{23b}, M. Garcia-Sciveres [ID](#)^{18a}, G.L. Gardner [ID](#)¹³⁰, R.W. Gardner [ID](#)³⁹, N. Garelli [ID](#)¹⁶², R.B. Garg [ID](#)¹⁴⁷, J.M. Gargan [ID](#)³³, C.A. Garner¹⁵⁹, C.M. Garvey [ID](#)^{34a}, V.K. Gassmann¹⁶², G. Gaudio [ID](#)^{72a}, A.J. Gavin [ID](#)⁹⁴, J. Gavranovic [ID](#)⁹³, I.L. Gavrilenko [ID](#)^{132a}, C. Gay [ID](#)¹⁶⁷, G. Gaycken [ID](#)¹²⁵, A. Gekow¹²¹, C. Gemme [ID](#)^{56b}, M.H. Genest [ID](#)⁵⁹, A.D. Gentry [ID](#)¹¹⁴, S. George [ID](#)⁹⁵, T. Geralis [ID](#)⁴⁵, A.A. Gerwin [ID](#)¹²², P. Gessinger-Befurt [ID](#)³⁷, M. Ghani [ID](#)¹⁷⁰, K. Ghorbanian [ID](#)⁹⁴, A. Ghosal [ID](#)¹⁴⁵, A. Ghosh [ID](#)¹⁶³, A. Ghosh [ID](#)⁷, B. Giacobbe [ID](#)^{24b}, S. Giagu [ID](#)^{74a,74b}, A. Giannini [ID](#)⁶¹, S.M. Gibson [ID](#)⁹⁵, D.T. Gil [ID](#)^{85b}, A.K. Gilbert [ID](#)^{85a}, B.J. Gilbert [ID](#)⁴¹, D. Gillberg [ID](#)³⁵, G. Gilles [ID](#)¹¹⁶, D.M. Gingrich [ID](#)^{2,aj}, M.P. Giordani [ID](#)^{68a,68c}, P.F. Giraud [ID](#)¹³⁷, G. Giugliarelli [ID](#)^{68a,68c}, D. Giugni [ID](#)^{70a}, F. Giuli [ID](#)^{75a,75b,al}, I. Gkialas [ID](#)^{9,i}, C. Glasman [ID](#)⁹⁹, M. Glazewska [ID](#)²⁰, R.M. Gleason [ID](#)¹⁶³, G. Glemža [ID](#)⁴⁷, I. Gnesi [ID](#)^{24b,24a,am}, Y. Go [ID](#)³⁰, M. Goblirsch-Kolb [ID](#)³⁷, B. Gocke [ID](#)⁴⁸, D. Godin¹⁰⁸, B. Gokturk [ID](#)^{22a}, S. Goldfarb [ID](#)¹⁰⁵, T. Golling [ID](#)⁵⁵, M.G.D. Gololo [ID](#)^{34c}, A. Golub [ID](#)¹⁴¹, J.P. Gombas [ID](#)¹⁰⁷, A. Gomes [ID](#)^{132a,132b}, G. Gomes Da Silva [ID](#)¹⁴⁵, A.J. Gomez Delegido [ID](#)³⁷, R. Gonçalves [ID](#)^{132a}, A. Gongadze [ID](#)^{153c}, F. Gonnella [ID](#)²¹, J.L. Gonski [ID](#)¹⁴⁷, R.Y. González Andana [ID](#)⁵¹, S. González de la Hoz [ID](#)¹⁶⁶, M.V. Gonzalez Rodrigues [ID](#)⁴⁷, R. Gonzalez Suarez [ID](#)¹⁶⁴, S. Gonzalez-Sevilla [ID](#)⁵⁵, L. Goossens [ID](#)³⁷, B. Gorini [ID](#)³⁷, E. Gorini [ID](#)^{69a,69b}, A. Gorišek [ID](#)⁹³, T.C. Gosart [ID](#)¹³⁰, A.T. Goshaw [ID](#)⁵⁰, M.I. Gostkin [ID](#)³⁸, S. Goswami [ID](#)¹²³, C.A. Gottardo [ID](#)³⁷, S.A. Gotz [ID](#)¹⁰⁹, M. Goughri [ID](#)^{36b}, A.G. Goussiou [ID](#)¹⁴¹, N. Govender [ID](#)^{34c}, R.P. Grabarczyk [ID](#)¹²⁸, I. Grabowska-Bold [ID](#)^{85a}, K. Graham [ID](#)³⁵, E. Gramstad [ID](#)¹²⁷, S. Grancagnolo [ID](#)^{69a,69b}, C.M. Grant¹, P.M. Gravila [ID](#)^{28f}, F.G. Gravili [ID](#)^{69a,69b}, H.M. Gray [ID](#)^{18a}, M. Greco [ID](#)¹¹⁰, M.J. Green [ID](#)¹, C. Grefe [ID](#)²⁵, A.S. Grefsrud [ID](#)¹⁷, I.M. Gregor [ID](#)⁴⁷, K.T. Greif [ID](#)¹⁶³, P. Grenier [ID](#)¹⁴⁷, S.G. Grewe¹¹⁰, K. Grimm [ID](#)³², S. Grinstein [ID](#)^{13,x}, E. Gross [ID](#)¹⁷², J. Grosse-Knetter [ID](#)⁵⁴, L.H. Grossman [ID](#)^{18b}, L. Guan [ID](#)¹⁰⁶, G. Guerrieri [ID](#)³⁷, R. Guevara [ID](#)¹²⁷, R. Gugel [ID](#)¹⁰⁰, J.A.M. Guhit [ID](#)¹⁰⁶, A. Guida [ID](#)¹⁹, E. Guilloton [ID](#)¹⁷⁰, S. Guindon [ID](#)³⁷, F. Guo [ID](#)^{14,112c}, J. Guo [ID](#)^{142a}, L. Guo [ID](#)⁴⁷, L. Guo [ID](#)^{112b,u}, Y. Guo [ID](#)¹⁰⁶, Y. Guo [ID](#)⁴¹, A. Gupta [ID](#)⁴⁸, R. Gupta [ID](#)¹³¹, S. Gupta [ID](#)²⁷, S. Gurbuz [ID](#)²⁵, S.S. Gurdasani [ID](#)⁴⁷, G. Gustavino [ID](#)^{74a,74b}, P. Gutierrez [ID](#)¹²², L.F. Gutierrez Zagazeta [ID](#)¹³⁰, M. Gutsche [ID](#)⁴⁹, C. Gutschow [ID](#)⁹⁶, W. Guérin [ID](#)⁸⁹, C. Gwenlan [ID](#)¹²⁸, C.B. Gwilliam [ID](#)⁹², E.S. Haaland [ID](#)¹²⁷, A. Haas [ID](#)¹¹⁹, M. Habedank [ID](#)⁵⁸, C. Haber [ID](#)^{18a}, R.J. Haberle [ID](#)¹⁷², H.K. Hadavand [ID](#)⁸, A. Haddad [ID](#)⁴⁰, A. Hadeef [ID](#)⁴⁹, A.I. Hagan [ID](#)⁹¹, J.J. Hahn [ID](#)¹⁴⁵,

M. Haleem ¹⁶⁹, J. Haley ¹²³, G.D. Hallewell ¹⁰², J.A. Hallford ⁴⁷, K. Hamano ¹⁶⁸,
H. Hamdaoui ¹⁶⁴, M. Hamer ²⁵, S.E.D. Hammoud ⁶⁵, E.J. Hampshire ⁹⁵, L. Han ^{112a},
L. Han ⁶¹, S. Han ¹⁴, K. Hanagaki ⁸², M. Hance ¹³⁸, D.A. Hangal ⁴¹, H. Hanif ¹⁴⁶,
M.D. Hank ¹³⁰, J.B. Hansen ⁴², P.H. Hansen ⁴², T. Harenberg ¹⁷⁴, S. Harkusha ¹⁷⁶,
M.L. Harris ¹⁰³, Y.T. Harris ²⁵, J. Harrison ¹³, P.F. Harrison ¹⁷⁰, M.L.E. Hart ⁹⁶,
N.M. Hartman ¹¹⁰, N.M. Hartmann ¹⁰⁹, R.Z. Hasan ^{95,136}, Y. Hasegawa ¹⁴⁴, D. Hashimoto ¹¹¹,
F. Haslbeck ³⁷, S. Hassan ¹²⁷, R. Hauser ¹⁰⁷, M. Haviernik ¹³⁵, C.M. Hawkes ²¹,
R.J. Hawkings ³⁷, Y. Hayashi ¹⁵⁷, D. Hayden ¹⁰⁷, R.L. Hayes ¹¹⁶, C.P. Hays ¹²⁸, J.M. Hays ⁹⁴,
H.S. Hayward ⁹², M. He ^{14,112c}, Y. He ⁴⁷, Y. He ⁹⁶, N.B. Heatley ⁹⁴, V. Hedberg ⁹⁸,
J. Heilman ³⁵, S. Heim ⁴⁷, T. Heim ^{18a}, J.J. Heinrich ¹²⁵, L. Heinrich ¹¹⁰, J. Hejbal ¹³³,
M. Helbig ⁴⁹, A. Held ¹⁷³, S. Hellesund ¹⁷, C.M. Helling ¹⁶⁷, F.N.E. Henry ⁵⁸, H. Herde ⁹⁸,
Y. Hernández Jiménez ¹⁴⁹, G. Herten ⁵³, R. Hertenberger ¹⁰⁹, L. Hervas ³⁷, M.E. Hesping ¹⁰⁰,
N.P. Hessey ^{160a}, J. Hessler ¹¹⁰, R. Hicks ¹³⁰, M. Hidaoui ^{36b}, N. Hidic ¹³⁵, E. Hill ¹⁵⁹,
T.S. Hillersoy ¹⁷, S.J. Hillier ²¹, J.R. Hinds ¹⁰⁷, F. Hinterkeuser ²⁵, M. Hirose ¹²⁶, S. Hirose ¹⁶¹,
D. Hirschbuehl ¹⁷⁴, B. Hiti ⁹³, J. Hobbs ¹⁴⁹, R. Hobincu ^{28e}, N. Hod ¹⁷², A.M. Hodges ¹⁶⁵,
M.C. Hodgkinson ¹⁴³, B.H. Hodgkinson ¹²⁸, A. Hoecker ³⁷, D.D. Hofer ¹⁰⁶, J. Hofer ¹⁶⁶,
J. Hofner ¹⁰⁰, M. Holzbock ³⁷, L.B.A.H. Hommels ³³, V. Homsak ¹²⁸, J.J. Hong ⁶⁷,
T.M. Hong ¹³¹, B.H. Hooberman ¹⁶⁵, W.H. Hopkins ⁶, M.C. Hoppesch ¹⁶⁵, Y. Horii ¹¹¹,
M.E. Horstmann ¹¹⁰, M.M. Horzela ⁵⁴, S. Hou ¹⁵², M.R. Housenga ¹⁶⁵, J. Howarth ⁵⁸,
J. Hoya ⁶, M. Hrabovsky ¹²⁴, T. Hryn'ova ⁴, P.J. Hsu ⁶⁴, S.-C. Hsu ¹⁴¹, T. Hsu ⁶⁵, M. Hu ^{18a},
P. Hu ^{63b}, Q. Hu ⁶¹, S. Huang ³³, X. Huang ^{14,112c}, Y. Huang ¹³⁵, Y. Huang ^{112b}, Y. Huang ¹⁴,
Z. Huang ⁶⁵, Z. Hubacek ¹³⁴, F. Huegging ²⁵, T.B. Huffman ¹²⁸,
M. Hufnagel Maranha De Faria ^{81a}, C.A. Hugli ⁴⁷, M. Huhtinen ³⁷, S.K. Huiberts ¹⁷,
R. Hulsken ¹⁰⁴, C.E. Hultquist ^{18a}, D.L. Humphreys ¹⁰³, N. Huseynov ¹², J. Huston ¹⁰⁷,
B. Huth ³⁷, J. Huth ⁶⁰, L. Huth ⁴⁷, R. Hyneman ⁷, G. Iacobucci ⁵⁵, G. Iakovidis ³⁰,
L. Iconomidou-Fayard ⁶⁵, J.P. Iddon ³⁷, P. Iengo ^{71a,71b}, Y. Iiyama ¹⁵⁷, T. Iizawa ¹⁵⁷,
Y. Ikegami ⁸², D. Iliadis ¹⁵⁶, N. Ilic ¹⁵⁹, H. Imam ^{36a}, G. Inacio Goncalves ^{81d},
S.A. Infante Cabanas ^{139c}, T. Ingebretsen Carlson ^{46a,46b}, J.M. Inglis ⁹⁴, G. Introzzi ^{72a,72b},
M. Iodice ^{76a}, V. Ippolito ^{74a,74b}, R.K. Irwin ⁹², M. Ishino ¹⁵⁷, W. Islam ¹⁷³, C. Issever ¹⁹,
S. Istin ^{22a,ar}, K. Itabashi ¹²⁶, H. Ito ¹⁷¹, R. Iuppa ^{77a,77b}, A. Ivina ¹⁷², F. Ivone ³⁷,
S. Izumiyama ¹¹¹, V. Izzo ^{71a}, P. Jacka ¹³⁴, P. Jackson ¹, P.R. Jacobson ⁵⁰, P. Jain ⁴⁷,
K. Jakobs ⁵³, J. Jamieson ⁵⁸, W. Jang ¹⁵⁷, S. Jankovych ¹¹⁶, B.K. Jashal ¹³⁶, M. Javurkova ¹⁰³,
P. Jawahar ¹⁰¹, L. Jeanty ¹²⁵, J. Jejelava ^{153a,ae}, P. Jenni ^{53,f}, L. Jerala ⁹³, C.E. Jessiman ³⁵,
H. Jia ¹⁶⁷, J. Jia ¹⁴⁹, X. Jia ^{110,112c}, C. Jiang ⁵¹, Q. Jiang ^{63b}, S. Jiggins ⁴⁷,
M. Jimenez Ortega ¹⁶⁶, J. Jimenez Pena ¹³, S. Jin ^{112a}, A. Jinaru ^{28b}, O. Jinnouchi ¹⁴⁰,
P. Johansson ¹⁴³, K.A. Johns ⁷, J.W. Johnson ¹³⁸, F.A. Jolly ⁴⁷, D.M. Jones ¹⁵⁰, E. Jones ⁴⁷,
K.S. Jones⁸, P. Jones ³³, R.W.L. Jones ⁹¹, T.J. Jones ⁹², H.L. Joos ³⁷, R. Joshi ¹²¹,
J. Jovicevic ¹⁶, X. Ju ^{18a}, J.J. Junggeburth ³⁷, T. Junkermann ^{62a}, A. Juste Rozas ^{13,x},
M.K. Juzek ⁸⁶, S. Kabana ^{139f}, A. Kaczmarska ⁸⁶, S.A. Kadir ¹⁴⁷, M. Kado ¹¹⁰, H. Kagan ¹²¹,
M. Kagan ¹⁴⁷, A. Kahn ¹³⁰, C. Kahra ¹⁰⁰, T. Kaji ¹⁵⁷, E. Kajomovitz ¹⁵⁴, N. Kakati ¹⁷²,
N. Kakoty ¹³, S. Kandel ⁸, N. Kanellos ¹⁰, D. Kar ^{34j,*}, E. Karentzos ²⁵, K. Karki ⁸,
O. Karkout ¹¹⁶, S.N. Karpov ³⁸, Z.M. Karpova ³⁸, V. Kartvelishvili ^{91,153b}, E. Kasimi ¹⁵⁶,
J. Katzy ⁴⁷, S. Kaur ³⁵, R. Kavak ¹⁶⁵, K. Kawade ¹⁴⁴, M.P. Kawale ¹²², C. Kawamoto ⁸⁷,
E.F. Kay ³⁷, S. Kazakos ¹⁰⁷, K. Kazakova ¹⁰², J.M. Keaveney ^{34a}, R. Keeler ¹⁶⁸, G.V. Kehris ⁶⁰,
J.S. Keller ³⁵, J.M. Kelly ¹⁶⁸, J.J. Kempster ¹⁵⁰, O. Kepka ¹³³, J. Kerr ^{160b}, B.P. Kerridge ¹³⁶,
B.P. Kerševan ⁹³, L. Keszeghova ^{29a}, R.A. Khan ¹³¹, A. Khanov ¹²³, M. Kholodenko ^{132a},
T.J. Khoo ¹⁹, G. Khoraiuli ¹⁶⁹, Y. Khoulaki ^{36a}, Y.A.R. Khwaira ¹²⁹, D. Kim ⁶, D.W. Kim ^{18b},

Y.K. Kim ³⁹, N. Kimura ⁹⁶, M.K. Kingston ⁵⁴, F. Kirfel ²⁵, J. Kirk ¹³⁶, A.E. Kiryunin ¹¹⁰,
 S. Kita ¹⁶¹, O. Kivernyk ²⁵, M. Klassen ¹⁶², C. Klein ³⁵, L. Klein ¹⁶⁹, M.H. Klein ⁴⁴,
 S.B. Klein ⁵⁵, U. Klein ⁹², A. Klimentov ³⁰, P. Kluit ¹¹⁶, S. Kluth ¹¹⁰, E. Kneringer ⁷⁸,
 T.M. Knight ¹⁵⁹, A. Knue ⁴⁸, M. Kobel ⁴⁹, D. Kobylanskii ¹⁷², S.F. Koch ³⁷, M. Kocian ¹⁴⁷,
 P. Kodyš ¹³⁵, D.M. Koeck ¹²⁵, T. Koffas ³⁵, K. Kojima ⁸², O. Kolay ⁴⁹, I. Koletsou ⁴,
 T. Komarek ⁸⁶, S. Kondo ¹⁵⁷, K. Köneke ⁵⁴, A.X.Y. Kong ¹, T. Kono ¹²⁰, N. Konstantinidis ⁹⁶,
 P. Kontaxakis ⁵⁵, B. Konya ⁹⁸, R. Kopeliansky ⁴¹, S. Koperny ^{85a}, R. Koppenhofer ⁵³,
 K. Korcyl ⁸⁶, K. Kordas ^{156,d}, A. Korn ⁹⁶, S. Korn ⁵⁴, I. Korolkov ¹³, B. Kortman ¹¹⁶,
 O. Kortner ¹¹⁰, S. Kortner ¹¹⁰, W.H. Kostecka ¹¹⁷, M. Kostov ^{29a}, V.V. Kostyukhin ¹⁴⁵,
 A. Kotskechagia ³⁷, A. Kotwal ⁵⁰, A. Koulouris ³⁷, A. Kourkoumeli-Charalampidi ^{72a,72b},
 O. Kovanda ¹²⁵, R. Kowalewski ¹⁶⁸, W. Kozanecki ¹²⁵, G. Kramberger ⁹³, P. Kramer ²⁵,
 A. Krasznahorkay ¹⁰³, A.C. Kraus ¹¹⁷, J.W. Kraus ¹⁷⁴, J.A. Kremer ⁴⁷, N.B. Krenzel ¹⁴⁵,
 T. Kresse ¹⁵⁹, L. Kretschmann ¹⁷⁴, J. Kretschmar ⁹², P. Krieger ¹⁵⁹, K. Krizka ²¹,
 K. Kroeninger ⁴⁸, H. Kroha ¹¹⁰, J. Kroll ¹³³, J. Kroll ¹³⁰, K.S. Krowpman ¹⁰⁷, U. Kruchonak ³⁸,
 H. Krüger ²⁵, N. Krumnack ⁷⁹, J. Krupa ¹⁴⁷, M.C. Kruse ⁵⁰, O. Kuchinskaia ³⁸, S. Kuday ^{3a},
 S. Kuehn ³⁷, R. Kuesters ⁵³, T. Kuhl ⁴⁷, V. Kukhtin ³⁸, Y. Kulchitsky ³⁸, S. Kuleshov ^{139d,139b},
 J. Kull ¹, E.V. Kumar ¹⁰⁹, M. Kumar ^{34j}, N. Kumari ⁴⁷, P. Kumari ^{160b}, A. Kupco ¹³³,
 O. Kuprash ⁵³, H. Kurashige ⁸⁴, L.L. Kurchaninov ^{160a}, O. Kurdysh ⁴, M. Kuze ¹⁴⁰,
 A.K. Kvam ¹⁰³, J. Kvita ¹²⁴, N.G. Kyriacou ¹⁴¹, M. Laassiri ³⁰, C. Lacasta ¹⁶⁶, H. Lacker ¹⁹,
 D. Lacour ¹²⁹, E. Ladygin ³⁸, A. Lafarge ⁴⁰, B. Laforge ¹²⁹, T. Lagouri ¹⁷⁵, F.Z. Lahbabi ^{36a},
 S. Lai ⁵⁴, W.S. Lai ⁹⁶, I.K. Lakomic ⁵⁴, J.E. Lambert ¹⁶⁸, S. Lammers ⁶⁷, W. Lampl ⁷,
 C. Lampoudis ¹⁵⁶, G. Lamprinoudis ¹⁶⁹, A.N. Lancaster ¹¹⁷, U. Landgraf ⁵³, M.P.J. Landon ⁹⁴,
 V.S. Lang ⁵³, A.J. Lankford ¹⁶³, F. Lanni ³⁷, C.S. Lantz ¹⁶⁵, K. Lantzsch ²⁵, A. Lanza ^{72a},
 M. Lanzac Berrocal ¹⁶⁶, T. Lari ^{70a}, D. Larsen ¹⁷, L. Larson ¹¹, F. Lasagni Manghi ^{24b},
 M. Lassnig ³⁷, H.C. Lau ¹⁶⁸, S.D. Lawlor ¹⁴³, R. Lazaridou ¹⁶³, M. Lazzaroni ^{70a,70b}, E.T.T. Le ¹⁶³,
 H.D.M. Le ¹⁰⁷, E.M. Le Boulicaut ¹⁷⁵, L.T. Le Pottier ^{18a}, B. Leban ^{24b,24a}, F. Ledroit-Guillon ⁵⁹,
 T.F. Lee ^{160b}, L.L. Leeuw ^{34h}, M. Lefebvre ¹⁶⁸, C. Leggett ^{18a}, L.M. Lehmann ¹¹⁶,
 G. Lehmann Miotto ³⁷, M. Leigh ⁵⁵, W.A. Leight ¹⁰³, W. Leinonen ¹¹⁵, A. Leisos ^{156,t},
 M.A.L. Leite ^{81c}, C.E. Leitgeb ¹⁹, R. Leitner ¹³⁵, K.J.C. Leney ⁴⁴, T. Lenz ²⁵, S. Leone ^{73a},
 C. Leonidopoulos ⁵¹, A. Leopold ¹⁴⁸, J. LePage-Bourbonnais ³⁵, R. Les ¹⁰⁷, C.G. Lester ³³,
 J. Levêque ⁴, L.J. Levinson ¹⁷², G. Levrini ^{24b,24a}, M.P. Lewicki ⁸⁶, C. Lewis ¹⁴¹, D.J. Lewis ⁴,
 L. Lewitt ¹⁴³, A. Li ³⁰, B. Li ^{113b}, C. Li ¹⁰⁶, C-Q. Li ¹¹⁰, H. Li ^{113b}, H. Li ¹⁰¹, H. Li ¹⁵, H. Li ⁶¹,
 H. Li ^{113b}, J. Li ^{142a}, L. Li ^{142a}, R. Li ¹⁷⁵, S. Li ^{142b,142a}, T. Li ⁵, Y. Li ¹⁴, Z. Li ^{14,112c},
 Z. Li ⁶¹, S. Liang ^{14,112c}, Z. Liang ¹⁴, M. Liberatore ¹³⁷, B. Liberti ^{75a}, G.B. Libotte ^{81d},
 K. Lie ^{63c}, J. Lieber Marin ^{81e}, H. Lien ⁶⁷, H. Lin ¹⁰⁶, S.F. Lin ¹⁴⁹, L. Linden ¹⁰⁹,
 R.E. Lindley ⁷, J.H. Lindon ³⁷, J. Ling ⁶⁰, E. Lipeles ¹³⁰, A. Lipniacka ¹⁷, A. Lister ¹⁶⁷,
 J.D. Little ⁶⁷, B. Liu ^{113a}, B.X. Liu ^{112b}, D. Liu ¹⁵⁴, D. Liu ¹³⁸, E.H.L. Liu ²¹, H. Liu ^{112b},
 J.K.K. Liu ¹¹⁹, K. Liu ^{142b}, K. Liu ^{142b}, M. Liu ⁶¹, M.Y. Liu ⁶¹, P. Liu ^{113b}, Q. Liu ¹⁴⁷,
 S. Liu ¹⁴⁹, X. Liu ^{113b}, Y. Liu ^{112b,112c}, Y. Liu ¹⁶⁵, Y.L. Liu ^{113b}, Y.W. Liu ⁶¹, Z. Liu ^{65,j},
 S.L. Lloyd ⁹⁴, E.M. Lobodzinska ⁴⁷, P. Loch ⁷, E. Lodhi ¹⁵⁹, K. Lohwasser ¹⁴³, E. Loiacono ¹²³,
 J.D. Lomas ²¹, I. Longarini ¹⁶³, R. Longo ^{24b,24a,am}, A. Lopez Solis ¹³, N.A. Lopez-canelas ⁷,
 N. Lorenzo Martinez ⁴, A.M. Lory ¹⁰⁹, M. Losada ^{118a}, G. Lösckce Centeno ⁴, X. Lou ^{14,112c},
 P.A. Love ⁹¹, M. Lu ⁶⁵, S. Lu ¹³⁰, Y.J. Lu ¹⁵², H.J. Lubatti ¹⁴¹, C. Luci ^{74a,74b},
 F.L. Lucio Alves ^{112a}, F. Luehring ⁶⁷, B.S. Lunday ¹³⁰, O. Lundberg ¹⁴⁸, J. Lunde ³⁷,
 N.A. Luongo ⁶, M.S. Lutz ¹⁵⁹, A.B. Lux ²⁶, D. Lynn ³⁰, R. Lysak ¹³³, V. Lysenko ¹³⁴,
 E. Lytken ⁹⁸, V. Lyubushkin ³⁸, T. Lyubushkina ³⁸, M.M. Lyukova ¹⁴⁹, H. Ma ³⁰, K. Ma ⁶¹,
 L.L. Ma ^{113b}, W. Ma ⁶¹, Y. Ma ^{113b}, J.C. MacDonald ¹⁰⁰, P.C. Machado De Abreu Farias ^{81e},

D. Macina ³⁷, R. Madar ⁴⁰, T. Madula ⁹⁶, J. Maeda ⁸⁴, T. Maeno ³⁰, P.T. Mafa ^{34f},
 H. Maguire ¹⁴³, M. Maheshwari ³³, V. Maiboroda ⁶⁵, A. Maio ^{132a,132b,132d}, K. Maj ^{85a},
 O. Majersky ⁴⁷, S. Majewski ¹²⁵, A. Makita ¹⁵⁷, N. Makovec ⁶⁵, V. Maksimovic ¹⁶,
 B. Malaescu ¹²⁹, J. Malamant ¹²⁷, Pa. Malecki ⁸⁶, F. Malek ^{59,n}, M. Mali ⁹³, D. Malito ⁹⁵,
 A. Maloizel ⁵, A. Malvezzi Lopes ^{81d}, S. Malyukov ³⁸, J. Mamuzic ⁹³, G. Mancini ⁵²,
 M.N. Mancini ²⁷, G. Manco ^{72a,72b}, S.S. Mandarry ¹⁵⁰, I. Mandić ⁹³,
 L. Manhaes de Andrade Filho ^{81a}, I.M. Maniatis ¹⁷², J. Manjarres Ramos ⁸⁹, D.C. Mankad ¹⁷²,
 A. Mann ¹⁰⁹, T. Manoussos ³⁷, M.N. Mantinan ³⁹, S. Manzoni ³⁷, L. Mao ^{142a},
 X. Mapekula ^{34c}, A. Marantis ¹⁵⁶, R.R. Marcelo Gregorio ¹, G. Marchiori ⁵, C. Marcon ^{70a},
 E. Maricic ¹⁶, M. Marinescu ⁴⁷, S. Marium ⁴⁷, M. Marjanovic ¹²², A. Markhoos ⁵³,
 M. Markovitch ⁶⁵, M.K. Maroun ¹⁰³, M.C. Marr ¹⁴⁶, G.T. Marsden ¹⁰¹, Z. Marshall ^{18a},
 S. Marti-Garcia ¹⁶⁶, J. Martin ⁹⁶, T.A. Martin ¹³⁶, V.J. Martin ⁵¹, B. Martin dit Latour ¹⁷,
 L. Martinelli ^{74a,74b}, V.I. Martinez Outschoorn ¹⁰³, P. Martinez Suarez ³⁷, S. Martin-Haugh ¹³⁶,
 G. Martinovicova ¹³⁵, V.S. Martoiu ^{28b}, A. Martone ⁸⁹, A.C. Martyniuk ⁹⁶, A. Marzin ³⁷,
 D. Mascione ^{77a,77b}, L. Masetti ¹⁰⁰, J. Masik ¹⁰¹, A.L. Maslennikov ³⁸, S.L. Mason ⁴¹,
 P. Massarotti ^{71a,71b}, P. Mastrandrea ^{73a,73b}, A. Mastroberardino ^{43b,43a}, T. Masubuchi ¹²⁶,
 T.T. Mathew ¹²⁵, J. Matousek ¹³⁵, D.M. Mattern ⁴⁸, K. Mauer ⁴⁷, J. Maurer ^{28b}, T. Maurin ⁵⁸,
 A.J. Maury ⁶⁵, B. Maček ⁹³, C. Mavungu Tsava ¹⁰², A.E. May ¹⁰¹, E. Mayer ⁴⁰, R. Mazini ^{34j},
 S.M. Mazza ¹³⁸, E. Mazzeo ³⁷, J.P. Mc Gowan ¹⁶⁸, S.P. Mc Kee ¹⁰⁶, C.C. McCracken ¹⁶⁷,
 E.F. McDonald ¹⁰⁵, L.F. Mcelhinney ⁹¹, J.A. Mcfayden ¹⁵⁰, R.P. McGovern ¹³⁰,
 R.P. Mckenzie ^{34j}, D.J. McLaughlin ⁹⁶, S.J. McMahan ¹³⁶, C.M. Mcpartland ⁹²,
 R.A. McPherson ^{168,ab}, S. Mehlhase ¹⁰⁹, A. Mehta ⁹², D. Melini ¹⁶⁶, B.R. Mellado Garcia ^{14,ah},
 A.H. Melo ⁵⁴, F. Meloni ⁴⁷, A.M. Mendes Jacques Da Costa ¹⁰¹, L. Meng ⁹¹, S. Menke ¹¹⁰,
 M. Mentink ³⁷, E. Meoni ^{43b,43a}, G. Mercado ¹¹⁷, S. Merianos ¹⁵⁶, C. Merlassino ^{68a,68c},
 C. Meroni ^{70a,70b}, J. Metcalfe ⁶, A.S. Mete ⁶, E. Meuser ¹⁰⁰, C. Meyer ⁶⁷, J-P. Meyer ¹³⁷,
 Y. Miao ^{112a}, R.P. Middleton ¹³⁶, M. Mihovilovic ⁶⁵, L. Mijović ⁵¹, G. Mikenberg ¹⁷²,
 M. Mikestikova ¹³³, M. Mikuž ⁹³, H. Mildner ¹⁰⁰, A. Milic ³⁷, D.W. Miller ³⁹, E.H. Miller ¹⁴⁷,
 A. Milov ¹⁷², D.A. Milstead ^{46a,46b}, T. Min ^{112a}, I.A. Minashvili ^{153b}, A.I. Mincer ¹¹⁹, B. Mindur ^{85a},
 M. Mineev ³⁸, Y. Mino ⁸⁷, L.M. Mir ¹³, M. Miralles Lopez ⁵⁸, M. Mironova ^{18a}, M. Missio ⁴⁰,
 A. Mitra ¹⁷⁰, V.A. Mitsou ¹⁶⁶, Y. Mitsumori ¹¹¹, P.S. Miyagawa ⁹⁴, R. Mizuhiki ⁸⁴,
 T. Mkrtchyan ³⁷, M. Mlinarevic ⁹⁶, T. Mlinarevic ⁹⁶, M. Mlynarikova ¹³⁵, L. Mlynarska ^{85a},
 C. Mo ^{142a}, S. Mobius ²⁰, M.H. Mohamed Farook ¹¹⁴, S. Mohapatra ⁴¹, M.F. Mohd Soberi ⁵¹,
 S. Mohiuddin ¹²³, G. Mokgatitswane ^{34j}, R. Mole ²¹, L. Moleri ¹⁷², U. Molinatti ¹²⁸,
 L.G. Mollier ²⁰, B. Mondal ¹³³, S. Mondal ¹³⁵, K. Mönig ⁴⁷, E. Monnier ¹⁰²,
 L. Monsonis Romero ¹⁶⁶, A. Montella ^{46a,46b}, M. Montella ¹²¹, F. Montekali ^{76a,76b},
 F. Monticelli ⁹⁰, S. Monzani ^{68a,68c}, M.E.E. Moors ²⁵, A. Morancho Tarda ⁴², N. Morange ⁶⁵,
 M. Moreno Llácer ¹⁶⁶, C. Moreno Martinez ⁵⁵, J.M. Moreno Perez ^{23b}, P. Morettini ^{56b},
 S. Morgenstern ^{62a}, M. Morii ⁶⁰, M. Morinaga ¹⁵⁷, F. Morodei ^{74a,74b}, P. Moschovakos ³⁷,
 B. Moser ⁵³, M. Mosidze ^{153b}, T. Moskalets ⁴⁴, P. Moskvitina ¹¹⁵, C.J. Mosomane ^{34b}, J. Moss ³²,
 T. Motta Quirino ^{81d}, A. Moussa ^{36d}, Y. Moyal ^{172,k}, H. Moyano Gomez ¹³, E.J.W. Moyse ¹⁰³,
 T.G. Mroz ⁸⁶, S. Muanza ¹⁰², M. Mucha ²⁵, J. Mueller ¹³¹, D. Muller ¹⁴⁵, G.A. Mullier ¹⁶⁴,
 A.J. Mullin ³³, J.J. Mullin ⁵⁰, A.C. Mullins ⁴⁴, A.E. Mulski ⁶⁰, D.P. Mungo ¹⁵⁹, D. Munoz Perez ¹²³,
 F.J. Munoz Sanchez ¹⁰¹, W.J. Murray ^{170,136}, E. Musajan ⁶¹, M. Muškinja ⁹³, C. Mwewa ⁴⁷,
 A.J. Myers ⁸, G. Myers ¹⁰⁶, M. Myska ¹³⁴, B.P. Nachman ¹⁴⁷, K. Nagai ¹²⁸, K. Nagano ⁸²,
 R. Nagasaka ¹⁵⁷, J.L. Nagle ^{30,ao}, E. Nagy ¹⁰², A.M. Nairz ³⁷, T. Nakagawa ⁸⁷, Y. Nakahama ⁸²,
 K. Nakamura ⁸², K. Nakkalil ⁵, A. Nandi ^{62b}, H. Nanjo ¹²⁶, E.A. Narayanan ⁴⁴,
 Y. Narukawa ¹⁵⁷, L. Nasella ^{70a,70b}, S. Nasri ^{118b}, C. Nass ²⁵, G. Navarro ^{23a}, A. Nayaz ¹⁹,

S. Nechaeva ^{24b,24a}, F. Nechansky ¹³³, L. Nedic ¹²⁸, A. Negri ^{72a,72b}, M. Negrini ^{24b},
 C. Nellist ¹¹⁶, C. Nelson ¹⁰⁴, K. Nelson ¹⁰⁶, S. Nemecek ¹³³, M. Nessi ^{37.g}, M.S. Neubauer ¹⁶⁵,
 J. Newell ⁹², P.R. Newman ²¹, Y.W.Y. Ng ¹⁶⁵, B. Ngair ^{118a}, H.D.N. Nguyen ¹⁰⁸,
 J.D. Nichols ¹²², R. Nicolaidou ¹³⁷, J. Nielsen ¹³⁸, M. Niemeyer ⁵⁴, J. Niermann ³⁷,
 N. Nikiforou ³⁷, I. Nikolic-Audit ¹²⁹, P. Nilsson ³⁰, G. Ninio ¹⁵⁵, A. Nisati ^{74a}, R. Nisius ¹¹⁰,
 N. Nitika ¹⁷², E.K. Nkadimeng ^{34b}, T. Nobe ¹⁵⁷, D. Noll ¹⁴⁷, T. Nommensen ¹⁵¹,
 M.B. Norfolk ¹⁴³, B.J. Norman ³⁵, L.C. Nosler ^{18a}, M. Noury ^{36a}, J. Novak ⁹³, T. Novak ⁹³,
 P. Novotny ¹⁷², R. Novotny ¹³⁴, L. Nozka ¹²⁴, K. Ntekas ³⁷, D. Ntounis ¹⁴⁷,
 N.M.J. Nunes De Moura Junior ^{81b}, J. Ocariz ¹²⁹, I. Ochoa ^{132a}, A. Odella Rodriguez ¹³,
 S. Oerdek ⁴⁷, J.T. Offermann ³⁹, A. Ogrodnik ⁸⁶, A. Oh ¹⁰¹, C.C. Ohm ¹⁴⁸, H. Oide ⁸²,
 M.L. Ojeda ³⁷, Y. Okumura ¹⁵⁷, L.F. Oleiro Seabra ^{132a}, I. Oleksiyuk ⁵⁵, G. Oliveira Correa ¹³,
 D. Oliveira Damazio ³⁰, J.L. Oliver ¹, R. Omar ⁶⁷, A.P. O'Neill ²⁰, Y. Onoda ¹⁴⁰,
 A. Onofre ^{132a,132e,e}, P.U.E. Onyisi ¹¹, M.J. Oreglia ³⁹, D. Orestano ^{76a,76b}, R. Orlandini ^{76a,76b},
 R.S. Orr ¹⁵⁹, L.M. Osojnak ⁴¹, Y. Osumi ¹¹¹, G. Otero y Garzón ³¹, H. Otono ⁸⁸,
 M. Ouchrif ^{36d}, F. Ould-Saada ¹²⁷, T. Ovsiannikova ¹⁴¹, M. Owen ⁵⁸, R.E. Owen ¹³⁶,
 S.A. Oyeniran ¹¹⁴, V.E. Ozcan ^{22a}, F. Ozturk ⁸⁶, N. Ozturk ⁸, S. Ozturk ⁸⁰, H.A. Pacey ¹²⁸,
 K. Pachal ^{160a}, A. Pacheco Pages ¹³, C. Padilla Aranda ¹³, G. Padovano ^{74a,74b},
 S. Pagan Griso ^{18a}, L. Pagani ^{75a,75b}, J. Pampel ²⁵, D.K. Panchal ¹¹, C.E. Pandini ⁵⁹,
 J.G. Panduro Vazquez ¹³⁶, H.D. Pandya ¹, H. Pang ¹³⁷, P. Pani ⁴⁷, G. Panizzo ^{68a,68c},
 L. Panwar ^{129,w}, L. Paolozzi ⁵⁵, S. Parajuli ¹⁶⁵, A. Paramonov ⁶, C. Paraskevopoulos ⁵²,
 D. Paredes Hernandez ^{63b}, S.R. Paredes Saenz ⁵¹, A. Pareti ^{72a,72b}, K.R. Park ⁴¹, T.H. Park ¹¹⁰,
 F. Parodi ^{56b,56a}, J.A. Parsons ⁴¹, U. Parzefall ⁵³, B.A. Paschen ^{18a}, B. Pascual Dias ⁴⁰,
 L. Pascual Dominguez ⁹⁹, E. Pasqualucci ^{74a}, S. Passaggio ^{56b}, F. Pastore ⁹⁵, P. Patel ⁸⁶,
 U.M. Patel ⁵⁰, J.R. Pater ¹⁰¹, T. Pauly ³⁷, A. Paunovic ¹⁶, F. Pauwels ¹³⁵, C.I. Pazos ¹⁶²,
 M. Pedersen ¹²⁷, R. Pedro ^{132a}, O. Penc ¹³³, C.C. Penelaud ¹²⁹, S. Peng ¹⁵, G.D. Penn ¹⁷⁵,
 B.S. Peralva ^{81d}, A.P. Pereira Peixoto ¹⁴¹, L. Pereira Sanchez ¹⁴⁷, D.V. Perepelitsa ^{30,ao},
 G. Perera ¹⁰³, E. Perez Codina ³⁷, M. Perganti ¹⁰, H. Pernegger ³⁷, S. Perrella ^{74a,74b},
 K. Peters ⁴⁷, R.F.Y. Peters ¹⁰¹, B.A. Petersen ³⁷, T.C. Petersen ⁴², E. Petit ¹⁰², V. Petousis ¹³⁴,
 A.R. Petri ^{70a,70b}, T. Petru ¹³⁵, M. Pettee ^{18a}, A. Petukhov ⁸⁰, K. Petukhova ³⁷, R. Pezoa ^{139g},
 L. Pezzotti ^{24b,24a}, G. Pezzullo ¹⁷⁵, L. Pfaffenbichler ³⁷, A.J. Pflieger ⁷⁸, T.M. Pham ¹⁷³,
 T. Pham ¹⁰⁵, P.W. Phillips ¹³⁶, G. Piacquadio ¹⁴⁹, E. Pianori ^{18a}, F. Piazza ¹²⁵, R. Piegai ³¹,
 D. Pietreanu ^{28b}, A.D. Pilkington ¹⁰¹, M. Pinamonti ^{68a,68c}, J.L. Pinfeld ², G. Pinheiro Matos ⁴¹,
 B.C. Pinheiro Pereira ^{132a}, J. Pinol Bel ¹³, A.E. Pinto Pinoargote ¹²⁹, L. Pintucci ^{68a,68c},
 K.M. Piper ¹⁵⁰, A. Pirttikoski ⁵⁵, D.A. Pizzi ³⁵, L. Pizzimento ^{63b}, A. Plebani ³³,
 M.-A. Pleier ³⁰, V. Pleskot ¹³⁵, E. Plotnikova ³⁸, G. Poddar ⁹⁴, R. Poettgen ⁹⁸, L. Poggioli ¹²⁹,
 S. Polacek ¹³⁵, G. Polesello ^{72a}, A. Poley ¹⁴⁶, A. Polini ^{24b}, C.S. Pollard ¹⁷⁰, Z.B. Pollock ¹²¹,
 E. Pompa Pacchi ¹²², N.I. Pond ⁹⁶, D. Ponomarenko ⁶⁷, L. Pontecorvo ³⁷, S. Popa ^{28a},
 G.A. Popeneciu ^{28d}, A. Poreba ^{62a}, D.M. Portillo Quintero ^{160a}, S. Pospisil ¹³⁴, M.A. Postill ¹⁴³,
 P. Postolache ^{28c}, K. Potamianos ¹⁷⁰, P.A. Potepa ^{85a}, I.N. Potrap ³⁸, C.J. Potter ³³, H. Potti ¹⁵¹,
 J. Poveda ¹⁶⁶, M.E. Pozo Astigarraga ³⁷, R. Pozzi ³⁷, A. Prades Ibanez ^{75a,75b}, S.R. Pradhan ¹⁴³,
 J. Pretel ¹⁶⁸, D. Price ¹⁰¹, M. Primavera ^{69a}, L. Primomo ^{68a,68c}, M.A. Principe Martin ⁹⁹,
 R. Privara ¹²⁴, T. Procter ^{85b}, M.L. Proffitt ¹⁴¹, N. Proklova ¹³⁰, K. Prokofiev ^{63c}, G. Proto ¹¹⁰,
 J. Proudfoot ⁶, M. Przybycien ^{85a}, W.W. Przygoda ^{85b}, A. Psallidas ⁴⁵, D. Pudzha ⁵², P. Puhl ⁵⁷,
 H.I. Purnell ¹, D. Pyatizbyantseva ¹¹⁵, J. Qian ¹⁰⁶, R. Qian ¹⁰⁷, D. Qichen ¹²⁸, Y. Qin ¹³,
 T. Qiu ⁵¹, A. Quadt ⁵⁴, M. Queitsch-Maitland ¹⁰¹, G. Quetant ⁵⁵, R.P. Quinn ¹⁶⁷,
 D. Rafanoharana ¹¹⁰, J.L. Rainbolt ³⁹, S. Rajagopalan ³⁰, E. Ramakoti ³⁸, L. Rambelli ^{56b,56a},
 I.A. Ramirez-Berend ³⁵, K. Ran ^{106,112c}, S.D. Randles ⁹², D.S. Rankin ¹³⁰, N.P. Rapheeha ^{34j},

H. Rasheed ^{128b}, A. Rastogi ^{18a}, S. Rave ¹⁰⁰, S. Ravera ^{56b,56a}, B. Ravina ³⁷, I. Ravinovich ¹⁷²,
 M. Raymond ³⁷, A.L. Read ¹²⁷, N.P. Readioff ¹⁴³, D.M. Rebuzzi ^{72a,72b}, A.S. Reed ⁵⁸,
 K. Reeves ²⁷, D. Reikher ³⁷, A. Rej ⁴⁸, C. Rembser ³⁷, H. Ren ⁶¹, M. Renda ^{28b}, F. Renner ⁴⁷,
 A.G. Rennie ⁵⁸, M. Repik ⁵⁵, A.L. Rescia ^{56b,56a}, S. Resconi ^{70a}, M. Ressegotti ^{56b},
 S. Rettie ¹¹⁶, W.F. Rettie ³⁵, M.M. Revering ³³, O.L. Rezanova ³⁸, P. Reznicek ¹³⁵, H. Riani ^{36d},
 N. Ribaric ⁵⁰, B. Ricci ^{68a,68c}, E. Ricci ^{77a,77b}, R. Richter ¹¹⁰, E. Richter-Was ^{85b}, M. Ridel ¹²⁹,
 S. Ridouani ^{36d}, P. Riedler ³⁷, E.M. Riefel ^{46a,46b}, J.O. Rieger ¹¹⁶, M. Rimoldi ^{34c},
 L. Rinaldi ^{24b,24a}, P. Rincke ^{164,54}, G. Ripellino ¹⁶⁴, I. Riu ¹³, J.C. Rivera Vergara ¹⁶⁸,
 F. Rizatdinova ¹²³, E. Rizvi ⁹⁴, B.R. Roberts ³⁹, S.S. Roberts ¹³⁸, D. Robinson ³³, A. Robson ⁵⁸,
 A. Rocchi ^{75a,75b}, C. Roda ^{73a,73b}, F.A. Rodriguez ¹¹⁷, S. Rodriguez Bosca ³⁷,
 Y. Rodriguez Garcia ^{23a}, A.M. Rodríguez Vera ¹¹⁷, S. Roe ³⁷, J.T. Roemer ³⁷, O. Røhne ¹²⁷,
 R.A. Rojas ³⁷, Z. Rokavec ⁹³, C.P.A. Roland ¹²⁹, A. Romaniouk ⁷⁸, E. Romano ^{72a,72b},
 M. Romano ^{24b}, N. Rompotis ⁹², L. Roos ¹²⁹, S. Rosati ^{74a}, L. Roscher ⁴⁷, B.J. Rosser ³⁹,
 E. Rossi ¹²⁸, E. Rossi ^{71a,71b}, L.P. Rossi ⁶⁰, L. Rossini ⁵³, R. Rosten ¹²¹, M. Rotaru ^{28b},
 R. Roth ³⁷, D. Rousseau ⁶⁵, D. Rousso ⁴⁷, S. Roy-Garand ¹⁵⁹, A. Rozanov ¹⁰²,
 Z.M.A. Rozario ⁵⁸, Y. Rozen ¹⁵⁴, A. Rubio Jimenez ¹⁶⁶, V.H. Ruelas Rivera ¹⁹, T.A. Ruggeri ¹,
 A. Ruggiero ¹²⁸, A. Ruiz-Martinez ¹⁶⁶, A. Rummler ³⁷, G.B. Rupnik Boero ³⁷,
 N.A. Rusakovich ³⁸, S. Rucelli ⁴⁸, H.L. Russell ¹⁶⁸, G. Russo ¹³⁸, J.P. Rutherford ⁷,
 S. Rutherford Colmenares ¹¹⁹, M. Rybar ¹³⁵, P. Rybczynski ^{85a}, A. Ryzhov ⁴⁴,
 F. Safai Tehrani ^{74a}, S. Saha ¹, B. Sahoo ¹⁷², A. Saibel ¹⁶⁶, B.T. Saifuddin ¹²², M. Saimpert ¹³⁷,
 I. Sainz Saenz Diez ^{62a}, G.T. Saito ^{81c}, M. Saito ¹⁵⁷, T. Saito ¹⁵⁷, A. Sala ^{70a,70b}, O.T. Salin ⁶⁵,
 A. Salnikov ¹⁴⁷, J. Salt ¹⁶⁶, A. Salvador Salas ¹⁵⁵, F. Salvatore ¹⁵⁰, A. Salzburger ³⁷,
 D. Sammel ⁵³, E. Sampson ⁹¹, D. Sampsonidis ^{156,d}, D. Sampsonidou ¹²⁵, M.A.A. Samy ⁵⁸,
 J. Sánchez ¹⁶⁶, V. Sanchez Sebastian ¹⁶⁶, H. Sandaker ¹²⁷, C.O. Sander ⁴⁷, J.A. Sandesara ¹⁷³,
 M. Sandhoff ¹⁷⁴, C. Sandoval ^{23b}, L. Sanfilippo ^{62a}, D.P.C. Sankey ¹³⁶, T. Sano ⁸⁷, A. Sansar ^{22c},
 A. Sansoni ⁵², M. Santana Queiroz ^{18b}, L. Santi ³⁷, C. Santoni ⁴⁰, H. Santos ^{132a,132b},
 L. Santos Pereira Trigo ⁴⁷, E. Sanzani ^{24b,24a}, K.A. Saoucha ^{83b}, J.G. Saraiva ^{132a,132d},
 J. Sardain ⁷, S. Sarkar ⁵⁰, O. Sasaki ⁸², K. Sato ¹⁶¹, C. Sauer ³⁷, E. Sauvan ⁴, P. Savard ^{159,aj},
 R. Sawada ¹⁵⁷, C. Sawyer ¹³⁶, L. Sawyer ⁹⁷, A.M. Sayed ²⁷, C. Sbarra ^{24b}, A. Sbrizzi ^{24b,24a},
 R. Scaglioni ^{72a,72b}, T. Scanlon ⁹⁶, J. Schaarschmidt ¹⁴¹, U. Schäfer ¹⁰⁰, A.C. Schaffer ^{65,44},
 D. Schaile ¹⁰⁹, R.D. Schamberger ¹⁴⁹, C. Scharf ¹⁹, M.M. Schefer ²⁰, D. Scheirich ¹³⁵,
 M. Schernau ^{139f}, C. Scheulen ⁵⁵, C. Schiavi ^{56b,56a}, M. Schioppa ^{43b,43a}, S. Schlenker ³⁷,
 T. Schlomer ⁵⁴, J. Schmeing ¹⁷⁴, E. Schmidt ¹¹⁰, M.A. Schmidt ¹⁷⁴, K. Schmieden ²⁵,
 C. Schmitt ¹⁰⁰, N. Schmitt ¹⁰⁰, S. Schmitt ⁴⁷, N.A. Schneider ¹⁰⁹, L. Schoeffel ¹³⁷,
 A. Schoening ^{62b}, P.G. Scholer ³⁵, E. Schopf ¹⁴⁵, M. Schott ²⁵, S. Schramm ⁵⁵, T. Schroer ⁵⁵,
 H-C. Schultz-Coulon ^{62a}, M. Schumacher ⁵³, B.A. Schumm ¹³⁸, Ph. Schune ¹³⁷, H.R. Schwartz ⁷,
 A. Schwartzman ¹⁴⁷, T.A. Schwarz ¹⁰⁶, Ph. Schwemling ¹³⁷, R. Schwienhorst ¹⁰⁷,
 F.G. Sciacca ²⁰, A. Sciandra ³⁰, G. Sciolla ²⁷, S.A. Scoville ¹³¹, F. Scuri ^{73a}, C.D. Sebastiani ³⁷,
 K. Sedlaczek ¹¹⁷, A. Sehrawat ^{139b}, S.C. Seidel ¹¹⁴, B.D. Seidlitz ⁴¹, C. Seitz ⁴⁷,
 J.M. Seixas ^{81b}, G. Sekhniaidze ^{71a}, L. Selem ¹²⁹, N. Semprini-Cesari ^{24b,24a}, A. Semushin ¹⁷⁶,
 V. Senthilkumar ¹¹⁶, L. Serin ⁶⁵, M. Sessa ^{71a,71b}, H. Severini ¹²², F. Sforza ^{56b,56a}, A. Sfyrla ⁵⁵,
 Q. Sha ¹⁴, H. Shaddix ¹¹⁷, A.H. Shah ³³, R. Shaheen ¹⁴⁸, J.D. Shahinian ¹³⁰, M. Shamim ³⁷,
 L.Y. Shan ¹⁴, M. Shapiro ^{18a}, A. Sharma ³⁷, A.S. Sharma ¹⁶⁷, P. Sharma ³⁰, K. Shaw ¹⁵⁰,
 S.M. Shaw ¹⁰¹, D. Shemyakin ¹⁷², Q. Shen ¹⁴, D.J. Sheppard ¹⁴⁶, P. Sherwood ⁹⁶, L. Shi ^{112b},
 X. Shi ¹⁴, S. Shimizu ⁸², S. Shirabe ⁸⁸, M. Shiyakova ^{38,z}, M.J. Shochet ³⁹, D.R. Shope ¹²⁷,
 B. Shrestha ¹²², S. Shrestha ^{121,aq}, I. Shreyber ³⁸, M.J. Shroff ¹⁰⁴, P. Sicho ¹³³, A.M. Sickles ¹⁶⁵,
 E. Sideras Haddad ^{34j}, A.C. Sidley ¹¹⁶, A. Sidoti ^{24b}, F. Siegert ⁴⁹, Dj. Sijacki ¹⁶, F. Sili ⁶¹,

J.M. Silva ⁵¹, I. Silva Ferreira ^{81b}, M.V. Silva Oliveira ³⁰, S.B. Silverstein ^{46a}, S. Simion ⁶⁵, R. Simoniello ³⁷, E.L. Simpson ¹⁰¹, H. Simpson ¹⁵⁰, L.R. Simpson ⁶, S. Simsek ⁸⁰, S. Sindhu ⁵⁴, S.N. Singh ²⁷, S. Singh ³⁰, S. Sinha ⁴⁷, S. Sinha ¹⁰¹, M. Sioli ^{24b,24a}, K. Sioulas ⁹, I. Siral ³⁷, E. Sitnikova ⁴⁷, J. Sjölin ^{46a,46b}, A. Skaf ⁵⁴, E. Skorda ²¹, P. Skubic ¹²², M. Slawinska ⁸⁶, I. Slazyk ¹⁷, I. Sliusar ¹²⁷, V. Smakhtin ¹⁷², B.H. Smart ¹³⁶, S.Yu. Smirnov ^{139b}, Y. Smirnov ^{34c}, O. Smirnova ⁹⁸, A.C. Smith ⁴¹, J.L. Smith ¹⁰¹, M.B. Smith ³⁵, R. Smith ¹⁴⁷, H. Smitmanns ¹⁰⁰, M. Smizanska ⁹¹, K. Smolek ¹³⁴, P. Smolyanskiy ¹³⁴, A.A. Snegarev ³⁸, H.L. Snoek ¹¹⁶, R.M. Snyder ⁵⁰, S. Snyder ³⁰, R. Sobie ^{168,ab}, A. Soffer ¹⁵⁵, C.A. Solans Sanchez ³⁷, E.Yu. Soldatov ³⁸, U. Soldevila ¹⁶⁶, A.A. Solodkov ^{34j}, S. Solomon ²⁷, A. Soloshenko ³⁸, O.V. Solovyanov ⁴⁰, P. Sommer ⁴⁹, A. Sopczak ¹³⁴, A.L. Sopio ⁵¹, F. Sopkova ^{29b}, J.D. Sorenson ¹¹⁴, I.R. Sotarriva Alvarez ¹⁴⁰, V. Sothilingam ^{62a}, O.J. Soto Sandoval ^{139c,139b}, S. Sottocornola ⁶⁷, R. Soualah ^{83a}, D. South ⁴⁷, N. Soybelman ¹⁷², S. Spagnolo ^{69a,69b}, A.S. Spellman ¹²⁵, D. Sperlich ⁵³, B. Spisso ^{71a,71b}, L. Splendori ¹⁰², M. Spousta ¹³⁵, E.J. Staats ³⁵, R. Stamen ^{62a}, E. Stanecka ⁸⁶, W. Stanek-Maslouska ⁴⁷, M.V. Stange ⁴⁹, B. Stanislaus ^{18a}, M.M. Stanitzki ⁴⁷, G.H. Stark ¹³⁸, J. Stark ⁸⁹, P. Staroba ¹³³, P. Starovoitov ^{83b}, R. Staszewski ⁸⁶, C. Stauch ¹⁰⁹, G. Stavropoulos ⁴⁵, A. Stefl ³⁷, A. Stein ¹⁰⁰, P. Steinberg ³⁰, B. Stelzer ^{146,160a}, H.J. Stelzer ¹³¹, O. Stelzer ^{160a}, H. Stenzel ⁵⁷, T.J. Stevenson ¹⁵⁰, G.A. Stewart ⁴⁷, G. Stoica ^{28b}, M. Stolarski ^{132a}, S. Stonjek ¹¹⁰, A. Straessner ⁴⁹, J. Strandberg ¹⁴⁸, S. Strandberg ^{46a,46b}, M. Stratmann ¹⁷⁴, M. Strauss ¹²², T. Strebler ¹⁰², P. Strizenc ^{29b}, R. Ströhmer ¹⁶⁹, D.M. Strom ¹²⁵, R. Stroynowski ⁴⁴, A. Strubig ^{46a,46b}, S.A. Stucci ³⁰, B. Stugu ¹⁷, J. Stupak ¹²², N.A. Styles ⁴⁷, D. Su ¹⁴⁷, S. Su ⁶¹, X. Su ⁶¹, D. Suchy ^{29a}, A.D. Sudhakar Ponnu ⁵⁴, L. Sudit ¹⁷², Y. Sue ⁸², K. Sugizaki ¹³⁰, D.M.S. Sultan ¹²⁸, L. Sultanaliyeva ²⁵, S. Sultansoy ^{3b}, S. Sun ¹⁷³, W. Sun ¹⁴, S. Sundar Raman ¹⁶⁷, N. Sur ⁹⁸, J.P. Surdutovich ¹²¹, N. Suri Jr ¹⁷⁵, M.R. Sutton ¹⁵⁰, M. Svatos ¹³³, P.N. Swallow ³³, S.N. Swatman ³⁷, M. Swiatlowski ^{160a}, A. Swoboda ³⁷, I. Sykora ^{29a}, M. Sykora ¹³⁵, T. Sykora ¹³⁵, D. Ta ¹⁰⁰, K. Tackmann ^{47,y}, A. Taffard ¹⁶³, R. Tafirout ^{160a}, Y. Takubo ⁸², M. Talby ¹⁰², N.M. Tamir ¹⁵⁵, A. Tanaka ¹⁵⁷, J. Tanaka ¹⁵⁷, R. Tanaka ⁶⁵, M. Tanasini ¹⁴⁹, Z. Tao ¹⁶⁷, S. Tapia Araya ^{139g}, S. Tapprogge ¹⁰⁰, A. Tarek Abouelfadl Mohamed ³⁷, S. Tarem ¹⁵⁴, K. Tariq ¹⁴, G. Tarna ³⁷, G.F. Tartarelli ^{70a}, M.J. Tartarin ^{142b}, P. Tas ¹³⁵, M. Tasevsky ¹³³, E. Tassi ^{43b,43a}, A.C. Tate ¹⁶⁵, Y. Tayalati ^{36e,aa}, G.N. Taylor ¹⁰⁵, W. Taylor ^{160b}, R.J. Taylor Vara ¹⁶⁶, A.S. Tegetmeier ⁸⁹, P. Teixeira-Dias ⁹⁵, J.J. Teoh ¹⁵⁹, K. Terashi ¹⁵⁷, J. Terron ⁹⁹, S. Terzo ¹³, M. Testa ⁵², R.J. Teuscher ^{159,ab}, A. Thaler ⁷⁸, T. Theveneaux-Pelzer ¹⁰², J.P. Thomas ²¹, E.A. Thompson ^{18a}, P.D. Thompson ²¹, E. Thomson ¹³⁰, R.E. Thornberry ³⁰, T.M. Thory-Rao ²¹, C. Tian ⁶¹, Y. Tian ⁵⁵, V. Tikhomirov ⁸⁰, Yu.A. Tikhonov ³⁸, D. Timoshyn ¹³⁵, E.X.L. Ting ¹, P. Tipton ¹⁷⁵, A. Tishelman-Charny ³⁰, K. Todome ¹⁴⁰, S. Todorova-Nova ¹³⁵, L. Toffolin ^{68a,68c}, M. Togawa ⁸², J. Tojo ⁸⁸, S. Tokár ^{29a}, O. Toldaiev ⁶⁷, G. Tolkachev ¹⁰², M. Tomoto ⁸², L. Tompkins ¹⁴⁷, E. Torrence ¹²⁵, H. Torres ⁸⁹, D.I. Torres Arza ^{139g}, E. Torres Reoyo ¹⁶⁶, E. Torró Pastor ¹⁶⁶, M. Toscani ³¹, C. Tosciri ³⁹, M. Tost ¹¹, D.R. Tovey ¹⁴³, T. Trefzger ¹⁶⁹, P.M. Tricarico ¹³, A. Tricoli ³⁰, I.M. Trigger ^{160a}, S. Trincaz-Duvoid ¹²⁹, D.A. Trischuk ¹⁶⁸, A. Tropina ³⁸, D. Truncali ^{75a,75b}, L. Truong ^{34c}, M. Trzebinski ⁸⁶, A. Trzupek ⁸⁶, F. Tsai ¹⁴⁹, A. Tsiamis ¹⁵⁶, P.V. Tsiarehka ³⁸, S. Tsigaridas ^{160a}, A. Tsirigotis ^{156,t}, V. Tsiskaridze ^{153a}, E.G. Tskhadadze ^{153a}, H.F. Tsoi ¹³⁰, Y. Tsujikawa ⁸⁷, V. Tsulaia ^{18a}, K. Tsurii ¹²⁰, D. Tsybychev ¹⁴⁹, Y. Tu ^{63b}, A. Tudorache ^{28b}, V. Tudorache ^{28b}, S.B. Tuncay ¹²⁸, S. Turchikhin ^{56b,56a}, I. Turk Cakir ^{3a}, R. Turra ^{70a}, T. Turtuvshin ^{38,ac}, P.M. Tuts ⁴¹, Y. Uematsu ⁸², F. Ukegawa ¹⁶¹, P.A. Ulloa Poblete ^{139c,139b}, G. Unal ³⁷, A. Undrus ³⁰, J. Urban ^{29b}, P. Urrejola ^{139e}, G. Usai ⁸, R. Ushioda ¹⁵⁸, M. Usman ¹⁰⁸, F. Ustuner ⁵¹, Z. Uysal ⁸⁰, V. Vacek ¹³⁴, B. Vachon ¹⁰⁴,

T. Vafeiadis ³⁷, A. Vaitkus ⁹⁶, C. Valderanis ¹⁰⁹, E. Valdes Santurio ^{46a,46b}, M. Valente ³⁷,
 S. Valentinetti ^{24b,24a}, A. Valero ¹⁶⁶, E. Valiente Moreno ¹⁶⁶, A. Vallier ⁸⁹, J.A. Valls Ferrer ¹⁶⁶,
 D.R. Van Arneman ¹¹⁶, R. Van Den Broucke ¹²⁹, A. Van Der Graaf ⁴⁸, H.Z. Van Der Schyf ^{34j},
 P. Van Gemmeren ⁶, M. Van Rijnbach ³⁷, S. Van Stroud ⁹⁶, I. Van Vulpen ¹¹⁶, P. Vana ¹³⁵,
 M. Vanadia ^{75a,75b}, U.M. Vande Voorde ¹⁴⁸, W. Vandelli ³⁷, E.R. Vandewall ¹⁴⁷, D. Vannicola ¹⁵⁵,
 R. Vari ^{74a}, M. Varma ¹⁷⁵, E.W. Varnes ⁷, C. Varni ^{85a}, D. Varouchas ⁶⁵, L. Varriale ¹⁶⁶,
 K.E. Varvell ¹⁵¹, M.E. Vasile ^{28b}, A. Vasileiadou ⁹, L. Vaslin ⁸², M.D. Vassilev ¹⁴⁷, A. Vasyukov ³⁸,
 L.M. Vaughan ¹²³, R. Vavricka ¹³⁵, T. Vazquez Schroeder ¹³, J. Veatch ³², V. Vecchio ¹⁰¹,
 M.J. Veen ¹⁰³, I. Veliscek ³⁰, I. Velkovska ⁹³, L.M. Veloce ¹⁵⁹, F. Veloso ^{132a,132c},
 A.G. Veltman ⁵¹, S.H. Venetianer ¹⁶², S. Veneziano ^{74a}, A. Ventura ^{69a,69b}, A. Verbitskyi ¹¹⁰,
 M. Verducci ^{73a,73b}, C. Vergis ⁹⁴, M. Verissimo De Araujo ^{81b}, W. Verkerke ¹¹⁶,
 J.C. Vermeulen ¹¹⁶, C. Vernieri ¹⁴⁷, M. Vessella ¹⁶³, M.C. Vetterli ^{146,aj}, A. Vgenopoulos ¹⁰⁰,
 N. Viaux Maira ^{139g,af}, L. Vicens ¹³⁴, T. Vickey ¹⁴³, O.E. Vickey Boeriu ¹⁴³,
 G.H.A. Viehhauser ¹²⁸, L. Vigani ^{62b}, M. Vigi ¹¹⁰, M. Villa ^{24b,24a}, M. Villaplana Perez ¹⁶⁶,
 E.M. Villhauer ³⁹, E. Vilucchi ⁵², M. Vincent ¹⁶⁶, M.G. Vincter ³⁵, A. Visibile ¹¹⁶, A. Visive ¹¹⁶,
 C. Vittori ¹⁶², I. Vivarelli ^{24b,24a}, M.I. Vivas Albornoz ⁴⁷, E. Voevodina ¹¹⁰, F. Vogel ¹⁰⁹,
 J.C. Voigt ⁴⁹, P. Vokac ¹³⁴, Yu. Volkotrub ^{85b}, L. Vomberg ²⁵, E. Von Toerne ²⁵,
 B. Vormwald ³⁷, K. Vorobev ⁵⁰, M. Vos ¹⁶⁶, K. Voss ¹⁴⁵, M. Vozak ³⁷, L. Vozdecky ¹²²,
 N. Vranjes ¹⁶, M. Vranjes Milosavljevic ¹⁶, M. Vreeswijk ¹¹⁶, N.K. Vu ^{112a}, R. Vuillermet ³⁷,
 O. Vujinovic ¹⁰⁰, I. Vukotic ³⁹, I.K. Vyas ³⁵, J.F. Wack ³³, A. Wada ¹¹¹, S. Wada ¹⁶¹,
 C. Wagner ¹⁴⁷, J.M. Wagner ^{18a}, W. Wagner ¹⁷⁴, S. Wahdan ¹⁷⁴, H. Wahlberg ⁹⁰, C.H. Waits ¹²²,
 J. Walder ¹³⁶, R. Walker ¹⁰⁹, K. Walkingshaw Pass ⁵⁸, W. Walkowiak ¹⁴⁵, A. Wall ¹³⁰,
 E.J. Wallin ⁹⁸, T. Wamorkar ¹⁴⁷, K. Wandall-Christensen ¹⁶⁶, A. Wang ⁶¹, A.Z. Wang ¹³⁸,
 C. Wang ⁴⁷, C. Wang ¹¹, H. Wang ^{18a}, J. Wang ^{63c}, P. Wang ¹⁰¹, P. Wang ⁹⁶, R. Wang ⁶⁰,
 R. Wang ¹⁰⁶, R. Wang ⁶, S.M. Wang ¹⁵², S. Wang ¹⁴, T. Wang ¹¹⁵, T. Wang ⁶¹, W.T. Wang ¹²⁸,
 X. Wang ¹⁶⁵, X. Wang ^{142a}, X. Wang ⁴⁷, Y. Wang ¹⁴⁹, Y. Wang ¹¹⁴, Z. Wang ¹⁰⁶, Z. Wang ¹⁴,
 Z. Wang ^{63b}, C. Wanotayaroj ⁸², A. Warburton ¹⁰⁴, A.L. Warnerbring ¹⁴⁵, S. Waterhouse ⁹⁶,
 A.T. Watson ²¹, H. Watson ⁵¹, M.F. Watson ²¹, E. Watton ³⁷, G. Watts ¹⁴¹, B.M. Waugh ⁹⁶,
 J.M. Webb ⁵³, C. Weber ³⁰, M.S. Weber ²⁰, C. Wei ⁶¹, Y. Wei ⁵³, A.R. Weidberg ¹²⁸,
 E.J. Weik ¹¹⁹, J. Weingarten ⁴⁸, C. Weiser ⁵³, C.J. Wells ⁴⁷, T. Wenaus ³⁰, T. Wengler ³⁷,
 N.S. Wenke ¹¹⁰, N. Wermes ²⁵, M. Wessels ^{62a}, A.M. Wharton ⁹¹, A.S. White ³⁷, A. White ⁸,
 M.J. White ¹, D. Whiteson ¹⁶³, L. Wickremasinghe ¹²⁶, W. Wiedenmann ¹⁷³, M. Wielers ¹³⁶,
 R. Wierda ¹⁴⁸, C. Wiglesworth ⁴², H.G. Wilkens ³⁷, J.J.H. Wilkinson ³³, S. Williams ³³,
 S. Willocq ¹⁰³, D.J. Wilson ¹⁰¹, P.J. Windischhofer ³⁹, F.I. Winkel ³¹, F. Winklmeier ¹²⁵,
 B.T. Winter ⁵³, M. Wittgen ¹⁴⁷, M. Wobisch ⁹⁷, T. Wojtkowski ⁵⁹, Z. Wolfs ¹¹⁶, J. Wollrath ³⁷,
 M.W. Wolter ⁸⁶, H. Wolters ^{132a,132c}, M.C. Wong ¹³⁸, E.L. Woodward ⁴¹, S.D. Worm ⁴⁷,
 B.K. Wosiek ⁸⁶, K.A. Wozniak ⁵⁵, K.W. Woźniak ⁸⁶, S. Wozniowski ⁵⁴, K. Wraight ⁵⁸,
 C. Wu ¹⁵⁹, C. Wu ²¹, J. Wu ¹⁵⁷, M. Wu ^{112b}, M. Wu ¹¹⁵, S.L. Wu ¹⁷³, S. Wu ^{14,an}, X. Wu ⁶¹,
 Y.Q. Wu ¹⁵⁹, Y. Wu ⁶¹, Z. Wu ¹⁰², Z. Wu ^{112a}, J. Wuerzinger ¹¹⁰, T.R. Wyatt ¹⁰¹,
 B.M. Wynne ⁵¹, S. Xella ⁴², L. Xia ^{112a}, M. Xie ⁶¹, A. Xiong ¹²⁵, I. Xiotidis ³⁷, D. Xu ¹⁴,
 H. Xu ⁶¹, L. Xu ⁶¹, R. Xu ¹³⁰, T. Xu ¹⁰⁶, W. Xu ^{112a}, Y. Xu ¹⁴¹, Z. Xu ⁵¹, R. Xue ¹³¹,
 B. Yabsley ¹⁵¹, S. Yacoub ¹¹, Y. Yamaguchi ⁸², E. Yamashita ¹⁵⁷, H. Yamauchi ¹⁶¹,
 T. Yamazaki ^{18a}, Y. Yamazaki ⁸⁴, S. Yan ⁵⁸, Z. Yan ¹⁰³, C. Yang ^{18a}, H.J. Yang ^{142a},
 H.T. Yang ⁶¹, S. Yang ⁶¹, X. Yang ³⁷, X. Yang ¹⁴, Y. Yang ¹⁵⁷, Y. Yang ⁶¹, W-M. Yao ^{18a},
 C.L. Yardley ¹⁵⁰, J. Ye ¹⁴, S. Ye ³⁰, X. Ye ⁶¹, I. Yeletsikh ³⁸, B. Yeo ^{18b}, M.R. Yexley ⁹⁶,
 T.P. Yildirim ¹²⁸, K. Yorita ¹⁷¹, C.J.S. Young ³⁷, C. Young ¹⁴⁷, I.N.L. Young ⁵⁸, N.D. Young ¹²⁵,
 Y. Yu ⁶¹, J. Yuan ^{14,112c,an}, M. Yuan ¹⁰⁶, R. Yuan ^{142b}, L. Yue ⁹⁶, M. Zaazoua ⁶¹,

B. Zabinski ⁸⁶, I. Zahir ^{36a}, Q.U.A. Zahoor ⁵¹, A. Zaio^{56b,56a}, Z.K. Zak ⁸⁶, T. Zakareishvili ¹⁶⁶, S. Zambito ⁵⁵, J. Zang ¹⁵⁷, R. Zanzottera ^{70a,70b}, O. Zaplatilek ¹³⁴, E. Zaya ¹⁴⁸, C. Zeitnitz ¹⁷⁴, H. Zeng ¹⁴, D.T. Zenger Jr ²⁷, T. Ženiš ^{29a}, S. Zenz ⁹⁴, D. Zerwas ⁶⁵, B. Zhang ¹⁷⁰, D.F. Zhang ¹⁴³, G. Zhang ^{14,an}, J. Zhang ^{113b}, J. Zhang ⁶, L. Zhang ⁶¹, L. Zhang ^{112a}, P. Zhang ^{14,112c}, R. Zhang ^{112a}, S. Zhang ⁸⁹, Y. Zhang ¹⁴¹, Y. Zhang ⁹⁶, Y. Zhang ⁶¹, Y. Zhang ^{112a}, Z. Zhang ^{18a}, Z. Zhang ^{113b}, Z. Zhang ⁶⁵, H. Zhao ¹⁴¹, T. Zhao ^{113b}, Y. Zhao ³⁵, Z. Zhao ⁶¹, Z. Zhao ⁶¹, A. Zhemchugov ³⁸, J. Zheng ^{112a}, K. Zheng ¹⁶⁵, L. Zheng ^{113b}, X. Zheng ⁶¹, Z. Zheng ¹⁴⁷, D. Zhong ¹⁶⁵, B. Zhou ¹⁰⁶, B. Zhou ^{142b,142a}, N. Zhou ^{142a}, Y. Zhou ¹⁵, Y. Zhou ^{112a}, Y. Zhou⁷, Z. Zhou ⁶¹, J. Zhu ¹⁰⁶, X. Zhu^{142b}, Y. Zhu ^{142a}, X. Zhuang ¹⁴, K. Zhukov ⁶⁷, N.I. Zimine ³⁸, J. Zinsser ^{62b}, M. Ziolkowski ¹⁴⁵, L. Živković ¹⁶, A. Zoccoli ^{24b,24a}, K. Zoch ³⁷, A. Zografos ³⁷, T.G. Zorbas ¹⁴³, L. Zwalinski ³⁷.

¹Department of Physics, University of Adelaide, Adelaide; Australia.

²Department of Physics, University of Alberta, Edmonton AB; Canada.

^{3(a)}Department of Physics, Ankara University, Ankara;^(b)Division of Physics, TOBB University of Economics and Technology, Ankara; Türkiye.

⁴LAPP, Université Savoie Mont Blanc, CNRS/IN2P3, Annecy; France.

⁵APC, Université Paris Cité, CNRS/IN2P3, Paris; France.

⁶High Energy Physics Division, Argonne National Laboratory, Argonne IL; United States of America.

⁷Department of Physics, University of Arizona, Tucson AZ; United States of America.

⁸Department of Physics, University of Texas at Arlington, Arlington TX; United States of America.

⁹Physics Department, National and Kapodistrian University of Athens, Athens; Greece.

¹⁰Physics Department, National Technical University of Athens, Zografou; Greece.

¹¹Department of Physics, University of Texas at Austin, Austin TX; United States of America.

¹²Institute of Physics, Azerbaijan Academy of Sciences, Baku; Azerbaijan.

¹³Institut de Física d'Altes Energies (IFAE), Barcelona Institute of Science and Technology, Barcelona; Spain.

¹⁴Institute of High Energy Physics, Chinese Academy of Sciences, Beijing; China.

¹⁵Physics Department, Tsinghua University, Beijing; China.

¹⁶Institute of Physics, University of Belgrade, Belgrade; Serbia.

¹⁷Department for Physics and Technology, University of Bergen, Bergen; Norway.

^{18(a)}Physics Division, Lawrence Berkeley National Laboratory, Berkeley CA;^(b)University of California, Berkeley CA; United States of America.

¹⁹Institut für Physik, Humboldt Universität zu Berlin, Berlin; Germany.

²⁰Albert Einstein Center for Fundamental Physics and Laboratory for High Energy Physics, University of Bern, Bern; Switzerland.

²¹School of Physics and Astronomy, University of Birmingham, Birmingham; United Kingdom.

^{22(a)}Department of Physics, Bogazici University, Istanbul;^(b)Department of Physics Engineering, Gaziantep University, Gaziantep;^(c)Department of Physics, Istanbul University, Istanbul; Türkiye.

^{23(a)}Facultad de Ciencias y Centro de Investigaciones, Universidad Antonio Nariño, Bogotá;^(b)Departamento de Física, Universidad Nacional de Colombia, Bogotá; Colombia.

^{24(a)}Dipartimento di Fisica e Astronomia A. Righi, Università di Bologna, Bologna;^(b)INFN Sezione di Bologna; Italy.

²⁵Physikalisches Institut, Universität Bonn, Bonn; Germany.

²⁶Department of Physics, Boston University, Boston MA; United States of America.

²⁷Department of Physics, Brandeis University, Waltham MA; United States of America.

^{28(a)}Transilvania University of Brasov, Brasov;^(b)Horia Hulubei National Institute of Physics and Nuclear

- Engineering, Bucharest;^(c)Department of Physics, Alexandru Ioan Cuza University of Iasi, Iasi;^(d)National Institute for Research and Development of Isotopic and Molecular Technologies, Physics Department, Cluj-Napoca;^(e)National University of Science and Technology Politehnica, Bucharest;^(f)West University in Timisoara, Timisoara;^(g)Faculty of Physics, University of Bucharest, Bucharest; Romania.
- ^{29(a)}Faculty of Mathematics, Physics and Informatics, Comenius University, Bratislava;^(b)Department of Subnuclear Physics, Institute of Experimental Physics of the Slovak Academy of Sciences, Kosice; Slovak Republic.
- ³⁰Physics Department, Brookhaven National Laboratory, Upton NY; United States of America.
- ³¹Universidad de Buenos Aires, Facultad de Ciencias Exactas y Naturales, Departamento de Física, y CONICET, Instituto de Física de Buenos Aires (IFIBA), Buenos Aires; Argentina.
- ³²California State University, CA; United States of America.
- ³³Cavendish Laboratory, University of Cambridge, Cambridge; United Kingdom.
- ^{34(a)}Department of Physics, University of Cape Town, Cape Town;^(b)iThemba Labs, Western Cape;^(c)Department of Mechanical Engineering Science, University of Johannesburg, Johannesburg;^(d)National Institute of Physics, University of the Philippines Diliman (Philippines);^(e)Department of Physics, Stellenbosch University, Matieland;^(f)University of KwaZulu-Natal, School of Agriculture and Science, Mathematics, Westville;^(g)University of South Africa, Department of Physics, Pretoria;^(h)University of Pretoria, Department of Mechanical and Aeronautical Engineering, Pretoria;⁽ⁱ⁾University of Zululand, KwaDlangezwa;^(j)School of Physics, University of the Witwatersrand, Johannesburg; South Africa.
- ³⁵Department of Physics, Carleton University, Ottawa ON; Canada.
- ^{36(a)}Faculté des Sciences Ain Chock, Université Hassan II de Casablanca;^(b)Faculté des Sciences, Université Ibn-Tofail, Kénitra;^(c)Faculté des Sciences Semlalia, Université Cadi Ayyad, LPHEA-Marrakech;^(d)LPMR, Faculté des Sciences, Université Mohamed Premier, Oujda;^(e)Faculté des sciences, Université Mohammed V, Rabat;^(f)Institute of Applied Physics, Mohammed VI Polytechnic University, Ben Guerir; Morocco.
- ³⁷CERN, Geneva; Switzerland.
- ³⁸Affiliated with an international laboratory covered by a cooperation agreement with CERN.
- ³⁹Enrico Fermi Institute, University of Chicago, Chicago IL; United States of America.
- ⁴⁰LPC, Université Clermont Auvergne, CNRS/IN2P3, Clermont-Ferrand; France.
- ⁴¹Nevis Laboratory, Columbia University, Irvington NY; United States of America.
- ⁴²Niels Bohr Institute, University of Copenhagen, Copenhagen; Denmark.
- ^{43(a)}Dipartimento di Fisica, Università della Calabria, Rende;^(b)INFN Gruppo Collegato di Cosenza, Laboratori Nazionali di Frascati; Italy.
- ⁴⁴Physics Department, Southern Methodist University, Dallas TX; United States of America.
- ⁴⁵National Centre for Scientific Research "Demokritos", Agia Paraskevi; Greece.
- ^{46(a)}Department of Physics, Stockholm University;^(b)Oskar Klein Centre, Stockholm; Sweden.
- ⁴⁷Deutsches Elektronen-Synchrotron DESY, Hamburg and Zeuthen; Germany.
- ⁴⁸Fakultät Physik, Technische Universität Dortmund, Dortmund; Germany.
- ⁴⁹Institut für Kern- und Teilchenphysik, Technische Universität Dresden, Dresden; Germany.
- ⁵⁰Department of Physics, Duke University, Durham NC; United States of America.
- ⁵¹SUPA - School of Physics and Astronomy, University of Edinburgh, Edinburgh; United Kingdom.
- ⁵²INFN e Laboratori Nazionali di Frascati, Frascati; Italy.
- ⁵³Physikalisches Institut, Albert-Ludwigs-Universität Freiburg, Freiburg; Germany.
- ⁵⁴II. Physikalisches Institut, Georg-August-Universität Göttingen, Göttingen; Germany.
- ⁵⁵Département de Physique Nucléaire et Corpusculaire, Université de Genève, Genève; Switzerland.
- ^{56(a)}Dipartimento di Fisica, Università di Genova, Genova;^(b)INFN Sezione di Genova; Italy.

- ⁵⁷II. Physikalisches Institut, Justus-Liebig-Universität Giessen, Giessen; Germany.
- ⁵⁸SUPA - School of Physics and Astronomy, University of Glasgow, Glasgow; United Kingdom.
- ⁵⁹LPSC, Université Grenoble Alpes, CNRS/IN2P3, Grenoble INP, Grenoble; France.
- ⁶⁰Laboratory for Particle Physics and Cosmology, Harvard University, Cambridge MA; United States of America.
- ⁶¹Department of Modern Physics and State Key Laboratory of Particle Detection and Electronics, University of Science and Technology of China, Hefei; China.
- ⁶²(^a) Kirchhoff-Institut für Physik, Ruprecht-Karls-Universität Heidelberg, Heidelberg; (^b) Physikalisches Institut, Ruprecht-Karls-Universität Heidelberg, Heidelberg; Germany.
- ⁶³(^a) Department of Physics, Chinese University of Hong Kong, Shatin, N.T., Hong Kong; (^b) Department of Physics, University of Hong Kong, Hong Kong; (^c) Department of Physics and Institute for Advanced Study, Hong Kong University of Science and Technology, Clear Water Bay, Kowloon, Hong Kong; China.
- ⁶⁴Department of Physics, National Tsing Hua University, Hsinchu; Taiwan.
- ⁶⁵IJCLab, Université Paris-Saclay, CNRS/IN2P3, 91405, Orsay; France.
- ⁶⁶Centro Nacional de Microelectrónica (IMB-CNM-CSIC), Barcelona; Spain.
- ⁶⁷Department of Physics, Indiana University, Bloomington IN; United States of America.
- ⁶⁸(^a) INFN Gruppo Collegato di Udine, Sezione di Trieste, Udine; (^b) ICTP, Trieste; (^c) Dipartimento Politecnico di Ingegneria e Architettura, Università di Udine, Udine; Italy.
- ⁶⁹(^a) INFN Sezione di Lecce; (^b) Dipartimento di Matematica e Fisica, Università del Salento, Lecce; Italy.
- ⁷⁰(^a) INFN Sezione di Milano; (^b) Dipartimento di Fisica, Università di Milano, Milano; Italy.
- ⁷¹(^a) INFN Sezione di Napoli; (^b) Dipartimento di Fisica, Università di Napoli, Napoli; Italy.
- ⁷²(^a) INFN Sezione di Pavia; (^b) Dipartimento di Fisica, Università di Pavia, Pavia; Italy.
- ⁷³(^a) INFN Sezione di Pisa; (^b) Dipartimento di Fisica E. Fermi, Università di Pisa, Pisa; Italy.
- ⁷⁴(^a) INFN Sezione di Roma; (^b) Dipartimento di Fisica, Sapienza Università di Roma, Roma; Italy.
- ⁷⁵(^a) INFN Sezione di Roma Tor Vergata; (^b) Dipartimento di Fisica, Università di Roma Tor Vergata, Roma; Italy.
- ⁷⁶(^a) INFN Sezione di Roma Tre; (^b) Dipartimento di Matematica e Fisica, Università Roma Tre, Roma; Italy.
- ⁷⁷(^a) INFN-TIFPA; (^b) Università degli Studi di Trento, Trento; Italy.
- ⁷⁸Universität Innsbruck, Department of Astro and Particle Physics, Innsbruck; Austria.
- ⁷⁹Department of Physics and Astronomy, Iowa State University, Ames IA; United States of America.
- ⁸⁰Istinye University, Sariyer, Istanbul; Türkiye.
- ⁸¹(^a) Departamento de Engenharia Elétrica, Universidade Federal de Juiz de Fora (UFJF), Juiz de Fora; (^b) Universidade Federal do Rio De Janeiro COPPE/EE/IF, Rio de Janeiro; (^c) Instituto de Física, Universidade de São Paulo, São Paulo; (^d) Rio de Janeiro State University, Rio de Janeiro; (^e) Federal University of Bahia, Bahia; Brazil.
- ⁸²KEK, High Energy Accelerator Research Organization, Tsukuba; Japan.
- ⁸³(^a) Khalifa University of Science and Technology, Abu Dhabi; (^b) University of Sharjah, Sharjah; United Arab Emirates.
- ⁸⁴Graduate School of Science, Kobe University, Kobe; Japan.
- ⁸⁵(^a) AGH University of Krakow, Faculty of Physics and Applied Computer Science, Krakow; (^b) Marian Smoluchowski Institute of Physics, Jagiellonian University, Krakow; Poland.
- ⁸⁶Institute of Nuclear Physics Polish Academy of Sciences, Krakow; Poland.
- ⁸⁷Faculty of Science, Kyoto University, Kyoto; Japan.
- ⁸⁸Research Center for Advanced Particle Physics and Department of Physics, Kyushu University, Fukuoka ; Japan.
- ⁸⁹L2IT, Université de Toulouse, CNRS/IN2P3, UPS, Toulouse; France.

- ⁹⁰Instituto de Física La Plata, Universidad Nacional de La Plata and CONICET, La Plata; Argentina.
- ⁹¹Physics Department, Lancaster University, Lancaster; United Kingdom.
- ⁹²Oliver Lodge Laboratory, University of Liverpool, Liverpool; United Kingdom.
- ⁹³Department of Experimental Particle Physics, Jožef Stefan Institute and Department of Physics, University of Ljubljana, Ljubljana; Slovenia.
- ⁹⁴Department of Physics and Astronomy, Queen Mary University of London, London; United Kingdom.
- ⁹⁵Department of Physics, Royal Holloway University of London, Egham; United Kingdom.
- ⁹⁶Department of Physics and Astronomy, University College London, London; United Kingdom.
- ⁹⁷Louisiana Tech University, Ruston LA; United States of America.
- ⁹⁸Fysiska institutionen, Lunds universitet, Lund; Sweden.
- ⁹⁹Departamento de Física Teórica C-15 and CIAFF, Universidad Autónoma de Madrid, Madrid; Spain.
- ¹⁰⁰Institut für Physik, Universität Mainz, Mainz; Germany.
- ¹⁰¹School of Physics and Astronomy, University of Manchester, Manchester; United Kingdom.
- ¹⁰²CPPM, Aix-Marseille Université, CNRS/IN2P3, Marseille; France.
- ¹⁰³Department of Physics, University of Massachusetts, Amherst MA; United States of America.
- ¹⁰⁴Department of Physics, McGill University, Montreal QC; Canada.
- ¹⁰⁵School of Physics, University of Melbourne, Victoria; Australia.
- ¹⁰⁶Department of Physics, University of Michigan, Ann Arbor MI; United States of America.
- ¹⁰⁷Department of Physics and Astronomy, Michigan State University, East Lansing MI; United States of America.
- ¹⁰⁸Group of Particle Physics, University of Montreal, Montreal QC; Canada.
- ¹⁰⁹Fakultät für Physik, Ludwig-Maximilians-Universität München, München; Germany.
- ¹¹⁰Max-Planck-Institut für Physik (Werner-Heisenberg-Institut), München; Germany.
- ¹¹¹Graduate School of Science and Kobayashi-Maskawa Institute, Nagoya University, Nagoya; Japan.
- ¹¹²(^a) Department of Physics, Nanjing University, Nanjing; (^b) School of Science, Shenzhen Campus of Sun Yat-sen University; (^c) University of Chinese Academy of Science (UCAS), Beijing; China.
- ¹¹³(^a) School of Physics, Nankai University, Tianjin; (^b) Institute of Frontier and Interdisciplinary Science and Key Laboratory of Particle Physics and Particle Irradiation (MOE), Shandong University, Qingdao; (^c) School of Physics, Zhengzhou University; China.
- ¹¹⁴Department of Physics and Astronomy, University of New Mexico, Albuquerque NM; United States of America.
- ¹¹⁵Institute for Mathematics, Astrophysics and Particle Physics, Radboud University/Nikhef, Nijmegen; Netherlands.
- ¹¹⁶Nikhef National Institute for Subatomic Physics and University of Amsterdam, Amsterdam; Netherlands.
- ¹¹⁷Department of Physics, Northern Illinois University, DeKalb IL; United States of America.
- ¹¹⁸(^a) New York University Abu Dhabi, Abu Dhabi; (^b) United Arab Emirates University, Al Ain; United Arab Emirates.
- ¹¹⁹Department of Physics, New York University, New York NY; United States of America.
- ¹²⁰Ochanomizu University, Otsuka, Bunkyo-ku, Tokyo; Japan.
- ¹²¹Ohio State University, Columbus OH; United States of America.
- ¹²²Homer L. Dodge Department of Physics and Astronomy, University of Oklahoma, Norman OK; United States of America.
- ¹²³Department of Physics, Oklahoma State University, Stillwater OK; United States of America.
- ¹²⁴Palacký University, Joint Laboratory of Optics, Olomouc; Czech Republic.
- ¹²⁵Institute for Fundamental Science, University of Oregon, Eugene, OR; United States of America.
- ¹²⁶Graduate School of Science, University of Osaka, Osaka; Japan.

- ¹²⁷Department of Physics, University of Oslo, Oslo; Norway.
- ¹²⁸Department of Physics, Oxford University, Oxford; United Kingdom.
- ¹²⁹LPNHE, Sorbonne Université, Université Paris Cité, CNRS/IN2P3, Paris; France.
- ¹³⁰Department of Physics, University of Pennsylvania, Philadelphia PA; United States of America.
- ¹³¹Department of Physics and Astronomy, University of Pittsburgh, Pittsburgh PA; United States of America.
- ¹³²(^a) Laboratório de Instrumentação e Física Experimental de Partículas - LIP, Lisboa; (^b) Departamento de Física, Faculdade de Ciências, Universidade de Lisboa, Lisboa; (^c) Departamento de Física, Universidade de Coimbra, Coimbra; (^d) Centro de Física Nuclear da Universidade de Lisboa, Lisboa; (^e) Departamento de Física, Escola de Ciências, Universidade do Minho, Braga; (^f) Departamento de Física Teórica y del Cosmos, Universidad de Granada, Granada (Spain); (^g) Departamento de Física, Instituto Superior Técnico, Universidade de Lisboa, Lisboa; Portugal.
- ¹³³Institute of Physics of the Czech Academy of Sciences, Prague; Czech Republic.
- ¹³⁴Czech Technical University in Prague, Prague; Czech Republic.
- ¹³⁵Charles University, Faculty of Mathematics and Physics, Prague; Czech Republic.
- ¹³⁶Particle Physics Department, Rutherford Appleton Laboratory, Didcot; United Kingdom.
- ¹³⁷IRFU, CEA, Université Paris-Saclay, Gif-sur-Yvette; France.
- ¹³⁸Santa Cruz Institute for Particle Physics, University of California Santa Cruz, Santa Cruz CA; United States of America.
- ¹³⁹(^a) Departamento de Física, Pontificia Universidad Católica de Chile, Santiago; (^b) Millennium Institute for Subatomic physics at high energy frontier (SAPHIR), Santiago; (^c) Instituto de Investigación Multidisciplinario en Ciencia y Tecnología, y Departamento de Física, Universidad de La Serena; (^d) Universidad Andres Bello, Department of Physics, Santiago; (^e) Universidad San Sebastian, Recoleta; (^f) Instituto de Alta Investigación, Universidad de Tarapacá, Arica; (^g) Departamento de Física, Universidad Técnica Federico Santa María, Valparaíso; Chile.
- ¹⁴⁰Department of Physics, Institute of Science, Tokyo; Japan.
- ¹⁴¹Department of Physics, University of Washington, Seattle WA; United States of America.
- ¹⁴²(^a) State Key Laboratory of Dark Matter Physics, School of Physics and Astronomy, Shanghai Jiao Tong University, Key Laboratory for Particle Astrophysics and Cosmology (MOE), SKLPPC, Shanghai; (^b) State Key Laboratory of Dark Matter Physics, Tsung-Dao Lee Institute, Shanghai Jiao Tong University, Shanghai; China.
- ¹⁴³Department of Physics and Astronomy, University of Sheffield, Sheffield; United Kingdom.
- ¹⁴⁴Department of Physics, Shinshu University, Nagano; Japan.
- ¹⁴⁵Department Physik, Universität Siegen, Siegen; Germany.
- ¹⁴⁶Department of Physics, Simon Fraser University, Burnaby BC; Canada.
- ¹⁴⁷SLAC National Accelerator Laboratory, Stanford CA; United States of America.
- ¹⁴⁸Department of Physics, Royal Institute of Technology, Stockholm; Sweden.
- ¹⁴⁹Departments of Physics and Astronomy, Stony Brook University, Stony Brook NY; United States of America.
- ¹⁵⁰Department of Physics and Astronomy, University of Sussex, Brighton; United Kingdom.
- ¹⁵¹School of Physics, University of Sydney, Sydney; Australia.
- ¹⁵²Institute of Physics, Academia Sinica, Taipei; Taiwan.
- ¹⁵³(^a) E. Andronikashvili Institute of Physics, Iv. Javakhishvili Tbilisi State University, Tbilisi; (^b) High Energy Physics Institute, Tbilisi State University, Tbilisi; (^c) University of Georgia, Tbilisi; Georgia.
- ¹⁵⁴Department of Physics, Technion, Israel Institute of Technology, Haifa; Israel.
- ¹⁵⁵Raymond and Beverly Sackler School of Physics and Astronomy, Tel Aviv University, Tel Aviv; Israel.
- ¹⁵⁶Department of Physics, Aristotle University of Thessaloniki, Thessaloniki; Greece.

- ¹⁵⁷International Center for Elementary Particle Physics and Department of Physics, University of Tokyo, Tokyo; Japan.
- ¹⁵⁸Graduate School of Science and Technology, Tokyo Metropolitan University, Tokyo; Japan.
- ¹⁵⁹Department of Physics, University of Toronto, Toronto ON; Canada.
- ¹⁶⁰(^a)TRIUMF, Vancouver BC; (^b)Department of Physics and Astronomy, York University, Toronto ON; Canada.
- ¹⁶¹Division of Physics and Tomonaga Center for the History of the Universe, Faculty of Pure and Applied Sciences, University of Tsukuba, Tsukuba; Japan.
- ¹⁶²Department of Physics and Astronomy, Tufts University, Medford MA; United States of America.
- ¹⁶³Department of Physics and Astronomy, University of California Irvine, Irvine CA; United States of America.
- ¹⁶⁴Department of Physics and Astronomy, University of Uppsala, Uppsala; Sweden.
- ¹⁶⁵Department of Physics, University of Illinois, Urbana IL; United States of America.
- ¹⁶⁶Instituto de Física Corpuscular (IFIC), Centro Mixto Universidad de Valencia - CSIC, Valencia; Spain.
- ¹⁶⁷Department of Physics, University of British Columbia, Vancouver BC; Canada.
- ¹⁶⁸Department of Physics and Astronomy, University of Victoria, Victoria BC; Canada.
- ¹⁶⁹Fakultät für Physik und Astronomie, Julius-Maximilians-Universität Würzburg, Würzburg; Germany.
- ¹⁷⁰Department of Physics, University of Warwick, Coventry; United Kingdom.
- ¹⁷¹Waseda University, Tokyo; Japan.
- ¹⁷²Department of Particle Physics and Astrophysics, Weizmann Institute of Science, Rehovot; Israel.
- ¹⁷³Department of Physics, University of Wisconsin, Madison WI; United States of America.
- ¹⁷⁴Fakultät für Mathematik und Naturwissenschaften, Fachgruppe Physik, Bergische Universität Wuppertal, Wuppertal; Germany.
- ¹⁷⁵Department of Physics, Yale University, New Haven CT; United States of America.
- ¹⁷⁶Yerevan Physics Institute, Yerevan; Armenia.
- ^a Also at Affiliated with an institute formerly covered by a cooperation agreement with CERN.
- ^b Also at An-Najah National University, Nablus; Palestine.
- ^c Also at Borough of Manhattan Community College, City University of New York, New York NY; United States of America.
- ^d Also at Center for Interdisciplinary Research and Innovation (CIRI-AUTH), Thessaloniki; Greece.
- ^e Also at Centre of Physics of the Universities of Minho and Porto (CF-UM-UP); Portugal.
- ^f Also at CERN, Geneva; Switzerland.
- ^g Also at Département de Physique Nucléaire et Corpusculaire, Université de Genève, Genève; Switzerland.
- ^h Also at Departament de Física de la Universitat Autònoma de Barcelona, Barcelona; Spain.
- ⁱ Also at Department of Financial and Management Engineering, University of the Aegean, Chios; Greece.
- ^j Also at Department of Modern Physics and State Key Laboratory of Particle Detection and Electronics, University of Science and Technology of China, Hefei; China.
- ^k Also at Department of Physics, Ben Gurion University of the Negev, Beer Sheva; Israel.
- ^l Also at Department of Physics, Bolu Abant İzzet Baysal University, Bolu; Türkiye.
- ^m Also at Department of Physics, King's College London, London; United Kingdom.
- ⁿ Also at Department of Physics, Stellenbosch University; South Africa.
- ^o Also at Department of Physics, University of Fribourg, Fribourg; Switzerland.
- ^p Also at Department of Physics, University of Thessaly; Greece.
- ^q Also at Department of Physics, Westmont College, Santa Barbara; United States of America.
- ^r Also at Faculty of Physics, Sofia University, 'St. Kliment Ohridski', Sofia; Bulgaria.
- ^s Also at Faculty of Physics, University of Bucharest; Romania.

- ^t Also at Hellenic Open University, Patras; Greece.
- ^u Also at Henan University; China.
- ^v Also at Imam Mohammad Ibn Saud Islamic University; Saudi Arabia.
- ^w Also at Indian Institute of Technology (IIT), Jodhpur; India.
- ^x Also at Institutio Catalana de Recerca i Estudis Avancats, ICREA, Barcelona; Spain.
- ^y Also at Institut für Experimentalphysik, Universität Hamburg, Hamburg; Germany.
- ^z Also at Institute for Nuclear Research and Nuclear Energy (INRNE) of the Bulgarian Academy of Sciences, Sofia; Bulgaria.
- ^{aa} Also at Institute of Applied Physics, Mohammed VI Polytechnic University, Ben Guerir; Morocco.
- ^{ab} Also at Institute of Particle Physics (IPP); Canada.
- ^{ac} Also at Institute of Physics and Technology, Mongolian Academy of Sciences, Ulaanbaatar; Mongolia.
- ^{ad} Also at Institute of Physics, Azerbaijan Academy of Sciences, Baku; Azerbaijan.
- ^{ae} Also at Institute of Theoretical Physics, Ilia State University, Tbilisi; Georgia.
- ^{af} Also at Millennium Institute for Subatomic physics at high energy frontier (SAPHIR), Santiago; Chile.
- ^{ag} Also at National Institute of Physics, University of the Philippines Diliman (Philippines); Philippines.
- ^{ah} Also at School of Physics, University of the Witwatersrand, Johannesburg; South Africa.
- ^{ai} Also at The Collaborative Innovation Center of Quantum Matter (CICQM), Beijing; China.
- ^{aj} Also at TRIUMF, Vancouver BC; Canada.
- ^{ak} Also at Università di Napoli Parthenope, Napoli; Italy.
- ^{al} Also at Università degli Studi Link; Italy.
- ^{am} Also at University and INFN Torino, Torino; Italy.
- ^{an} Also at University of Chinese Academy of Sciences (UCAS), Beijing; China.
- ^{ao} Also at University of Colorado Boulder, Department of Physics, Colorado; United States of America.
- ^{ap} Also at University of Siena; Italy.
- ^{aq} Also at Washington College, Chestertown, MD; United States of America.
- ^{ar} Also at Yeditepe University, Physics Department, Istanbul; Türkiye.
- * Deceased